TECHNISCHE UNIVERSITÄT MÜNCHEN

Fakultät für Medizin

Novel polypharmacotherapies for the treatment of obesity and diabetes

Stephan Jakob Sachs

Vollständiger Abdruck der von der Fakultät für Medizin der Technischen Universität München zur Erlangung des akademischen Grades eines

Doktors der Naturwissenschaften (Dr. rer. nat.)

genehmigten Dissertation.

Vorsitzender:	Prof. Dr. Dr. Stefan Engelhardt
Prüfer der Dissertation:	1. Prof. Dr. Heiko Lickert
	2. apl. Prof. Dr. Johannes Beckers
	3. Prof. Dr. Carolin Daniel

Die Dissertation wurde am 28.11.2019 bei der Technischen Universität München eingereicht und durch die Fakultät für Medizin am 06.10.2020 angenommen.

Abstract

Insulin-secreting β-cells and glucagon-secreting α-cells in pancreatic islets of Langerhans cooperate to regulate blood glucose. Dysfunction or destruction of β-cells leads to type 1 and type 2 diabetes. Currently, no pharmacological treatment can prevent or reverse diabetes progression and its devastating micro- and macrovascular complications leading to exogenous insulin supplementation for survival. Islet transplantation can substitute for insulin deficiency and prevent secondary complications, but donors are scare. Bariatric surgeries recover dysfunction of insulin producing β-cells leading to type 2 diabetes remission in obese patients. However, these surgeries are not broadly applicable. Hence, novel pharmacological approaches are urgently needed that prevent, halt, or even revert diabetes progression.

Aim 1: Determine new treatment options that restore β-cell mass and function in diabetes. β-cell dedifferentiation has been proposed as a major mechanism of functional β-cell mass loss in type 1 and type 2 diabetes. It is unclear whether dedifferentiated β-cells can redifferentiate through pharmacological treatment to obtain disease remission. This thesis establishes the murine model of multiple low dose of streptozotocin (mSTZ) induced diabetes as adequate model for the analysis of β-cell de- and redifferentiation without genetic lesions and autoimmunity. Single cell RNA sequencing of insulin positive cells in this diabetes model not only revealed novel markers and pathways of β-cell dedifferentiation, but also sets forth β-cell redifferentiation induced by a novel polyagonist treatment approach as a viable diabetes treatment option. Daily treatment with insulin or a stable Glucagon-like peptide-1 (GLP-1)/estrogen conjugate for over 100 days directly targeted β-cells to restore β-cell maturity and functionality. Combining both treatments reduced daily insulin requirements by 60%, enhanced estrogen delivery and activity in β-cells, and increased β-cell survival and functionality in the mSTZ model. Importantly, GLP-1/estrogen protected human β-cells against cytokine-induced dysfunction. GLP-1 and estrogen alone had no disease modifying effects in these models. Altogether, this study describes previously unknown processes of β-cell dedifferentiation and reveals the potential and mechanisms of single and poly-pharmacological approaches to halt and reverse diabetes progression by targeting dedifferentiated β-cells.

Aim 2: Unveil shared benefits of incretin dual agonism in mice and bariatric surgery in humans. Roux-En-Y gastric bypass (RYGB) is unmatched in correcting obesity and normalizing glucose metabolism in type 2 diabetes by reverting β-cell dysfunction. However, these surgeries are risky, highly invasive, not reversible and thus not broadly applicable. Novel pharmacology is urgently needed that mimics the metabolic benefits of RYGB. Recently, plasma proteome profiling (PPP) captured systemic benefits of RYGB in humans. The aim of

this work was to test whether polypharmacological targeting of receptors for GLP-1 and glucose-dependent insulinotropic polypeptide (GIP) (GLP-1/GIP co-agonist) in diet-induced obese male and female mice mimics RYGB-induced systemic metabolic changes in humans. GLP-1/GIP improved diet-induced obesity, glucose metabolism, and hepatic steatosis with superior potency relative to GLP-1 and GIP mono-agonists in male and female mice. Compared to either mono-agonist, GLP-1/GIP reduced hypercholesterolemia in both sexes by decreasing protein components of low-density lipoprotein particles similarly to RYGB in humans. GLP-1/GIP more efficiently reduced systemic inflammatory protein levels, which are known to be modulated by RYGB in humans. Hence, these results suggest that a GLP-1/GIP co-agonist more closely mimics metabolic benefits of bariatric surgery, thereby outperforming currently best in class anti-obesity and -diabetes GLP-1 mono-agonists.

The results of this thesis show that novel GLP-1-based polypharmacotherapy has the potential to improve the disease state in obese and diabetic patients in order to prevent the loss of and regenerate functional β-cell mass.

Zusammenfassung

Die Langerhansschen Inseln des Pankreas beinhalten insulinproduzierende β-Zellen und glukagonproduziernde α-Zellen - beide Zelltypen kontrollieren zusammen den Blutzucker. Die Dysfunktion oder Zerstörung insulinproduzierender β-Zellen führt zu Typ 1 und Typ 2 Diabetes, welches die Zufuhr von exogenem Insulin notwendig macht um zu überleben. Derzeit gibt es kein Medikament, welches das Fortschreiten der Krankheit und deren verheerenden mikro- und makrovaskulären Komplikationen verhindern oder umkehren könnte. Die Transplantation von Langerhans-Inseln kann zwar dem Insulindefizit entgegenwirken und damit sekundäre Komplikationen verhindern, allerdings gibt es nicht genügend Organspender. Die Adipositaschirurgie führt zur Remission des Typ 2 Diabetes in übergewichtigen Patienten indem sie die Funktionalität der β-Zellen wiederherstellt. Diese Operationen sind allerdings riskant und können nicht bei allen Patienten angewandt werden. Aus diesen Gründen werden dringend neue pharmakologische Ansätze benötigt, die den Diabetes verhindern, aufhalten, oder sogar rückgängig machen können.

Ein Ziel dieser Dissertation war es, neue Medikamente zur Wiederherstellung der β-Zellmasse und -funktion zu finden. Die Dedifferenzierung von β-Zellen ist ein grundlegender Mechanismus, der zum Verlust der funktionellen β-Zellmasse bei Typ 1 und Typ 2 Diabetes beiträgt. Es ist jedoch bisher unklar, ob Medikamente die β-Zell-Redifferenzierung induzieren und somit zu einer Remission des Diabetes führen können. Die Ergebnisse dieser Arbeit etablieren das durch die Verabreichung von mehreren niedrigen, nicht diabetogenen Dosen von Streptozotozin (mSTZ) induzierte Maus Diabetes-Modell, als Modell, das die Untersuchung von β-Zell-De- und -redifferenzierung in Abwesenheit von genetischen Veränderungen oder Autoimmunität ermöglicht. Dabei zeigte die Einzelzell-RNA-Sequenzierung von β-Zellen in diesem Diabetes-Modell neue Mechanismen der β-Zell-Dedifferenzierung. Zusätzlich konnte eine intensive medikamentöse Behandlung dieser Tiere über 100 Tagen zeigen, dass die pharmakologische β-Zell-Redifferenzierung eine potentielle Behandlungsoption für Diabetes darstellt. Die tägliche Behandlung mit Insulin oder einem stabilen Konjugat aus dem Glukagonähnlichen Peptid 1 (GLP-1) und Östrogen (GLP-1/Östrogen-Konjugat) hatte einen direkten Einfluss auf β-Zellen, um deren Zellreife und Funktionalität wiederherzustellen. Die Kombination beider Behandlungen reduzierte den täglichen Insulinbedarf um 60%, erhöhte den Transport von Östrogen in β-Zellen und verbesserte dadurch das Überleben und die Funktionalität der β-Zellen im mSTZ Maus Diabetes-Modell. Außerdem schützte GLP-1/Östrogen menschliche β-Zellen vor einer Zytokin-induzierten Dysfunktion. Die Behandlung mit GLP-1 und Östrogen als Einzelpräparat hatte in

diesen Modellen keine positiven Effekte. Demnach beschreibt diese Studie Prozesse der β-Zell-Dedifferenzierung und zeigt das Potenzial und die Mechanismen einzelner und polypharmakologischer Ansätze, um das Voranschreiten von Diabetes zu stoppen.

Ein weiteres Ziel der Dissertation war es, metabolische Veränderungen einer Behandlung mit einem neuartigen, dualen Inkretin-Koagonisten in der Maus, mit der Adipositaschirurgie am Menschen zu vergleichen. Der Roux-en-Y-Magenbypass (RYGB) ist bisher für Körpergewichtsreduktion und Normalisierung des Glukosemetabolismus in Typ 2 Diabetikern die effektivste Behandlungsmethode. Der Eingriff ist jedoch riskant, maximal invasiv, nicht reversibel und damit keine Option für alle übergewichtigen und Typ 2 diabetischen Patienten. Es werden demnach neue Medikamente benötigt, die den Behandlungserfolg eines RYGB bestmöglich nachahmen. Mit Hilfe des sogenannten Plasma Proteom Profiling (PPP) konnte vor Kurzem das gesamte Plasma Proteom nach einem RYGB im Menschen erfasst werden. Ziel dieser Arbeit war es nun, zu testen, ob die Behandlung von männlichen und weiblichen diätinduzierten adipösen Mäusen mit einem neuartigen GLP-1/Glukoseabhängigen insulinotropen Polypeptid (GIP)-Koagonisten (GLP-1/GIP-Koagonist) ähnliche Veränderungen im Plasma Proteom induziert, wie die eines RYGB im Menschen. Dabei zeigte sich, dass die Behandlung mit dem GLP-1/GIP-Koagonisten die diätetisch bedingte Adipositas verringerte, den Glukosestoffwechsel verbesserte und die Leberverfettung reduzierte. Diese positiven Auswirkungen waren stärker als die alleinige Gabe der einzelnen Hormone. Außerdem senkte insbesondere der GLP-1/GIP-Koagonist die Cholesterinspiegel in beiden Geschlechtern. Dabei reduzierte der GLP-1/GIP-Koagonist Proteinkomponenten des LDL (low density lipoproteins) und ähnelte der Wirkung des RYGB im Menschen. Zusätzlich waren inflammatorische Plasmaproteine nach Behandlung mit dem GLP-1/GIP-Koagonisten stärker verringert, als nach der alleinigen Gabe von GLP-1 oder GIP. Eine ähnliche Reduktion von inflammatorischen Proteinen konnte im Plasma nach einer RYGB-Operation gefunden werden. Demnach deuten die Ergebnisse dieser Arbeit darauf hin, dass die metabolischen Vorteile der Adipositaschirurgie durch die Gabe des GLP-1/GIP-Koagonisten besser erzielt werden, als durch die Gabe der beiden Einzelkomponenten.

Die Ergebnisse dieser Arbeit zeigen, dass neuartige, auf GLP-1 basierende polypharmakologische Medikamente, das Potential haben, den Gesundheitszustand von übergewichtigen und diabetischen Patienten zu verbessern, indem sie den Verlust der β-Zellen verhindern oder sogar neue β-Zellen regenerieren.

Table of contents

Abbreviations

AGB	Adjustable Gastric Banding
Aib	Aminoisobuturic Acid
Aldh1a3	Aldehyde Dehydrogenase 1 Family Member A3
Aldob	Aldolase B
Angptl3	Angiopoietin-Related Protein 3
Apcs	Serum Amyloid P-Component
Apoa1	Apolipoprotein A1
Apoc1	Apolipoprotein C1
Apoc3	Apolipoprotein C3
Apoc4	Apolipoprotein C4
Apod	Apolipoprotein D
BMI	Body Mass Index
C1qc	Complement C1Q C Chain
Cd5l	Cd5 Molecule Like
Cgref1	Cell Growth Regulator With Ef Hand Domain Protein 1
Col18a1	Collagen Type Xviii Alpha 1 Chain
Cpb2	Carboxypeptidase B2
Cpn1	Carboxypeptidase N
Cxcl4	C-X-C Motif Chemokine 4
DIO	Diet-Inuced Obesity
Dpep2	Dipeptidase 2
DPP-IV	Dipeptidyl Peptidase-4
DYRK1A	Dual specificity tyrosine phosphorylation-regulated kinase 1A
Enpep	Glutamyl Aminopeptidase
ER	Endoplasmic Reticulum
ERAD	ER-associated degradation
F11	Plasma Blood Coagulation Factor Xi
F13a1	Coagulation Factor Xiii A Chain
F13b	Coagulation Factor Xiii B Chain
F2	Plasma Blood Coagulation Factor Ii
FoxO1	Forkhead Box Protein O1
GABA	Gamma-Aminobutyric Acid
Gcg	Glucagon
GIP	Glucose-Dependent Insulinotropic Polypeptide
GIPR	Glucose-Dependent Insulinotropic Polypeptide Receptor
GLP-1	Glucagon Like Peptide 1
GLP-1R	Glucagon Like Peptide 1 Receptor
Got1	Glutamic-Oxaloacetic Transaminase
Gpld1	Phosphatidylinositol-Glycan-Specific Phospholipase D
GSIS	Glucose Stimulated Insulin Secretion
HbA1c	Glycated Hemoglobin

Hbb1	Hemoglobin Subunit Beta-1
Hc	Protein Hc
hESC	Human Ebryonic Stem Cells
HFD	High-fat, high-sugar diet
Hgfac	Hepatocyte Growth Factor Activator
IGF	Insulin Growth Factor
Ins	Insulin
iPSC	Induced Pluripotent Stem Cells
Isl1	Islet 1
Lap3	Leucine Aminopeptidase 3
Ldha	Lactate Dehydrogenase A
LDL	Low-Density-Lipoprotein Cholesterol
Lrg1	Leucine-Rich Alpha-2-Glycoprotein
MafA	V-Maf Avian Musculoaponeurotic Oncogene Homolog A
MafB	V-Maf Avian Musculoaponeurotic Oncogene Homolog B
Masp2	Mannan-Binding Lectin-Associated Serine Proteases
Mcam	Melanoma Cell Adhesion Molecule
Me1	Nadp-Dependent Malic Enzyme
mSTZ	Multiple Low Dose Of Streptocotozin
MUP	Major Urinary Proteins
NAFL	Nonalcoholic Fatty Liver
NAFLD	Nonalcoholic Fatty Liver Disease
Nanog	Nanog Homeobox
NASH	Nonalcoholic Steatohepatitis
NeuroD1	Neuronal differentiation 1
Ngn3	Neurogenin 3
Nkx2.2	Homeobox Protein Nkx-2.2
Nkx6.1	Nk6 Homeobox1
Oct4	Octamer-Binding Transcription Factor 4
Orm1	Alpha-1-Acid Glycoprotein 1
Orm2	Alpha-1-Acid Glycoprotein 2
PAGA	Partition-Based Graph Abstraction
Pax4	Paired Box 4
Pax6	Paired Box Protein Pax-6
PCA	Principal-Component Analysis
Pdx1	Pancreatic Duodenal Homeobox 1
PEG-insulin	Pegylated Insulin Analog
Pf4	Platelet Factor 4
Pglyrp2	Peptidoglycan Recognition Protein 2
Pkm	Pyruvate Kinase
Pltp	Phospholipid Transfer Protein
PP	Pancreatic Polypeptide
PPP	Plasma Proteome Profiling
Prg4	Proteoglycan 4

RNA	Ribonucleic Acid
Saa1	Serum Amyloid A1
Saa4	Serum Amyloid A4
Serpin10	Serpin Family A Member 10
SerpinB1	Leukocyte elastase inhibitor
Serping1	Plasma Protease C1 Inhibitor
Sord	Sorbitol Dehydrogenase
Sox9	SRY-Box 9
Sptlc2	Serine Palmitoyltransferase, Long Chain Base Subunit 2
Sst	Somatostatin
STZ	Streptocotozin
T1D	Type 1 Diabetes
T2D	Type 2 Diabetes
TF	Transcription Factor
Thbs1	Thrombospondin 1
VSG	Vertical Sleeve Gastrectomy

Index of Figures

Index of Tables

1. Introduction

The exocrine (acinar cells and ductal cells) and endocrine pancreas (islets of Langerhans) are the two morphologically distinct compartments of the pancreas. Both are central in the control of energy consumption and metabolism. Acinar cells of the exocrine pancreas produce and secrete a range of digestive enzymes into the duodenum that facilitates the break down and thus the absorption of fats, proteins, and carbohydrates. In humans, endocrine islets only make up 5% of the total pancreatic mass, but they number more than a billion cells (Zhou and Melton 2018). Each of the five different endocrine cell types secrete one major hormone: glucagon (α-cells), insulin (β-cells), somatostatin (δ-cells), pancreatic polypeptide (PP cells), and ghrelin (ε-cells). α-and β-cells are the most prominent ones due to their integral role in whole body glucose homeostasis.

Diabetes is the most common disease that afflicts the endocrine pancreas. Thereby, the progressive loss or dysfunction of insulin-producing β-cells leads to systemic hyperglycemia, which when insufficiently treated, causes micro- and macrovascular tissue damages including kidney failure, peripheral vascular disease, stroke, and coronary artery disease (Zhou and Melton 2018). Diabetes afflicts more than 400 million people worldwide and has become a major and growing health burden. More than 90% of people with diabetes suffer from type 2 diabetes (T2D). T2D mostly results from obesity-induced peripheral insulin resistance by peripheral organs including liver, fat, and muscle (Zheng et al., 2018). The resulting increase in insulin demand initially induces compensatory β-cell expansion and hyperinsulinemia to maintain euglycemia (~80-100 mg/dl in humans) (Weir and Bonner-Weir, 2013). With a progressive worsening of insulin resistance, β-cell insulin secretion cannot cope with the increasing insulin demand (Ahrén, 2005). Consequently, glucose levels increase, which is accompanied by progressive worsening of β-cell function, reduction of glucose-stimulated insulin secretion (GSIS), and ultimately a reduction of total β-cell numbers (Butler et al., 2003; Prentki, 2006; Weir and Bonner-Weir, 2013). Type 1 diabetes (T1D), which makes up about 5–10% of all diabetes cases, is a consequence of autoimmune destruction of β-cells leading to absolute insulin deficiency (Bluestone et al., 2010). Hence, ultimately T1D and T2D patients need exogenous insulin supplementation for survival. Currently, no treatment option can revert or stop disease progression, except for islet transplantation in T1D and bariatric surgery in T2D (Hering et al., 2016; Schauer et al., 2017). The transplantation of cadaveric islets has been shown to reverse diabetes (Hering et al., 2016; Shapiro et al., 2000), but graft function progressively declines leading to return of insulin dependency of up to ~75% of transplant recipients within two years (Potter et al., 2014; Shapiro et al., 2006). Moreover, insufficient exogenous material and the need to fight against the life-long auto- and alloimmunity limits its widespread application (Zhou and Melton 2018). Bariatric surgery is the most effective therapy for long-term T2D remission and recovers functional β-cell mass (Buchwald and Buchwald, 2019; Mingrone et al., 2015). However, these operations are not without risk, mostly

irreversible, and not applicable to all patients in need of such surgeries. Hence, new ways to prevent diabetes progression, enhance or induce the intrinsic regenerative ability that preserve or expand pancreatic β-cell mass, or strategies to produce insulin-secreting β-cells are urgently needed as they will have profound implications for an effective therapeutic approach.

1.1 Targeting endogenous β-cell regeneration for diabetes therapy

Cells of e.g. the gut, skin, or blood are constantly replaced within days (gut, skin) or a few weeks (blood). In contrast, cells from the endocrine pancreas have a very slow turnover (Teta et al., 2005). In fact, it remains elusive whether β-cells are regenerated in any physiologically meaningful way from the adult human pancreas (Zhou and Melton, 2018). Hence, lost β-cell mass leads to irreversible diabetes and medical approaches to regenerate functional β-cells are urgently needed. Currently, two main strategies to replace lost and/or dysfunctional β-cell mass are extensively explored: stem cell derived β-cell differentiation *in vitro* and endogenous β-cell regeneration *in vivo*. The former holds the potential to replace cadaveric islet transplantations, which cures diabetes (Hering et al., 2016; Shapiro et al., 2000), but organ donors are scare and alternative sources of islet cells are urgently needed. In this respect, stem-cell-derived cells are promising. Successful cultivation of human embryonic stem cells (hESC) and the discovery that induced pluripotent stem cells (iPSC) can be derived from somatic cells (Takahashi et al., 2007; Thomson, 1998) has led to the development of step-wise protocols that induce the differentiation of these cells (D'Amour et al., 2006; Pagliuca et al., 2014). Thereby, the cells undergo a successive development form the definitive endoderm to β-like cells (D'Amour et al., 2006; Pagliuca et al., 2014). After transplantation, stem-cell derived β-like cells secrete insulin and ameliorate hyperglycemia in diabetic mice (Kroon et al., 2008; Pagliuca et al., 2014; Rezania et al., 2014). Despite substantial advances in differentiating β-like cells from stem cells, important challenges remain prior human application. These include improvements in the efficacy of β-like cell differentiation to prevent uncontrolled progenitor cell proliferation and teratoma formation, eliminating unwanted cells, and, in case of T1D, transplants must provide autoimmune protection. To bypass some of these obstacles, recent research efforts aim to induce the regeneration of functional, glucose responding insulin-producing cells from endogenous cell sources (Figure 1) (Zhou and Melton, 2018). Thereby, new β-cells might be generated by differentiation of progenitor cells into β-cells (neogenesis), transdifferentiation (that is the direct conversion of a terminally differentiated cell type into another cell type) of extra- and pancreatic cells into β-cells, replication of remaining β-cells, and/or redifferentiation of dedifferentiated β-cells. These concepts of endogenous β-cell regeneration are summarized in the following.

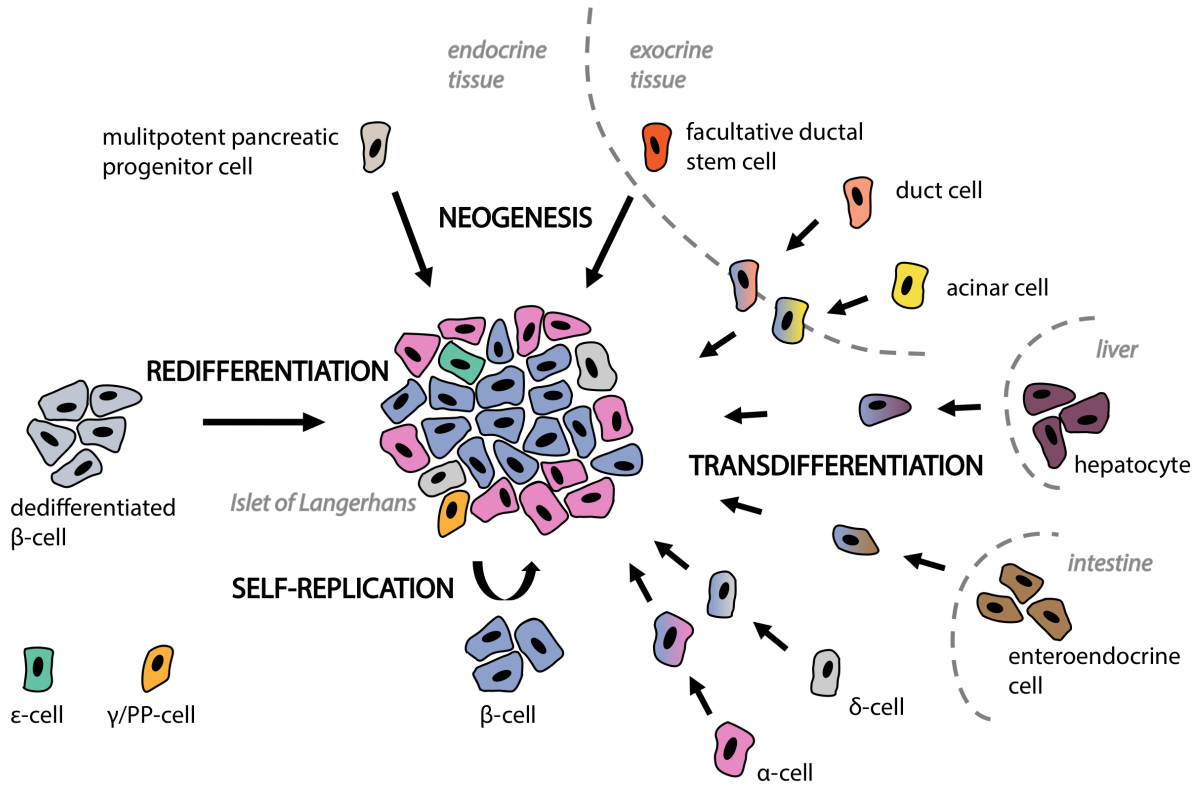

Figure 1: Main routes for endogenous β-cell mass regeneration in diabetes.

Summary of possible ways of β-cell regeneration that are discussed in the text (adopted from Tritschler et al., 2017).

1.1.1 Stimulating β-cell proliferation

β-cell replication is the major model of β-cell renewal in adult mice (Dor et al., 2004). Hence, enhancing β-cell proliferation is a simple and intuitive solution to increase total β-cell mass (Zhou and Melton, 2018). Substantial human β-cell proliferation only occurs in early childhood and declines during ageing (Gregg et al., 2012; Kassem et al., 2000; Köhler et al., 2011; Meier et al., 2008; Reers et al., 2009). Also in mice, the proliferative capacity of β-cells declines with age (Tschen et al., 2009). But in contrast to humans, physiological conditions such as pregnancy and obesity can induce β-cell replication in adult mice to compensate for increased insulin demand (Butler et al., 2010; Parsons et al., 1992; Rieck and Kaestner, 2010; Saisho et al., 2013; Sorenson and Brelje, 1997; Tschen et al., 2009). It is still unclear why human adult β-cells proliferate at such low rates. They possess all crucial components to reenter the cell cycle, but for unknown reasons these cycling factors reside in the cytoplasm of mature β-cells (Fiaschi-Taesch et al., 2013a, 2013b). This might contribute to the refractory nature of human β-cells to proliferate. Recently, high-throughput screens have identified small molecules that have the potential to manipulate human β-cell replication. Inhibitors of the dual specificity tyrosine phosphorylation-regulated kinase 1A (DYRK1A) potently stimulated proliferation of cultured human β-cells *in vitro* and transplanted human β-cells *in vivo* (Dirice et al., 2016; Shen et al., 2015; Wang et al., 2015, 2019). Similarly, SerpinB1, a liver secreted proteinase inhibitor

(also known as leukocyte elastase inhibitor (LEI)), and small molecules mimicking SerinB1's activity, were found to increase human β-cell proliferation (El Ouaamari et al., 2016). Despite these encouraging findings, influencing the cell cycle concurrently raises the problem of uncontrolled cell growth and increased cancer risk. This makes a cell type-specific delivery necessary before advancing into clinics. Moreover, whether increasing the proliferation of declining β-cells can enhance functional β-cells mass in diabetes and thus ameliorate the disease state is ill defined.

1.1.2 Induction of neogenesis for β-cell regeneration

Neogenesis refers to the differentiation of new endocrine islet cells from pancreatic progenitor or stem cells. The contribution of neogenesis to the initial formation of the endocrine pancreas during embryogenesis is generally accepted (Bonner-Weir et al., 2004; Jo et al., 2011; Peng et al., 2009). Thereby, endocrine progenitor-precursor cells are derived from SRY-Box 9 (Sox9) positive bipotent ductal/endocrine progenitors cells and characterized by temporary expression of the master regulatory transcription factor (TF) Neurogenin 3 (Neurog 3, hereafter called Ngn3) (Jørgensen et al., 2007; Pan and Wright, 2011). Ngn3 is necessary for endocrine neogenesis and Ngn3 positive cells give rise to all endocrine cells in the pancreas (Gradwohl et al., 2000). Thus, Ngn3 expression is used as neogenesis marker in the pancreas. The contribution of neogenesis to endocrine islets regeneration in adulthood was historically studied in two rodent injury models of the pancreas: partial pancreatectomy and partial duct ligation (Bonner-Weir et al., 1993; Wang et al., 1995). Partial duct ligation causes major acinar cell death, but endocrine islets are spared with no sign of β-cell neogenesis (Rankin et al., 2013). The capacity of pancreas regeneration after partial pancreatectomy declines with age (Menge et al., 2008; Téllez et al., 2016; Watanabe et al., 2005) and conflicting results exist whether partial pancreatectomy induces neogenesis in mice (Ackermann Misfeldt et al., 2008; Peshavaria et al., 2006) or not (Dor et al., 2004; Lee et al., 2006; Teta et al., 2007). Pioneer work by Dor et al. using lineage tracing of insulin positive cells revealed β-cell replication of pre-existing β-cells and not neogenesis as main mechanism of β-cell expansion in adult mice (Dor et al., 2004). Together, these results indicated a minor role of β-cell neogenesis in health or disease state for β-cell regeneration in mice.

However, caveats like promotor leakage (i.e., the tissue-specific promotors used for cell tagging might be dynamically and unevenly expressed also in other cells) and labeling efficiency bias findings from genetic lineage studies (Domínguez-Bendala et al., 2019). For example, using a similar genetic approach as described by Dor et al., Smukler et al. described progenitor-like cells that express insulin (Smukler et al., 2011). Hence, 'pre-existing β-cells' potentially contributed to β-cell regeneration in adult mice (Smukler et al., 2011). While the underlining mechanism of physiological increased β-cell mass in human remains unclear, the histological examination of pancreata from pregnant and obese and/or T2D subjects revealed increased proportion of small islets and scattered insulin positive cells as well as an increased number of insulin positive cells within the duct (Butler et al., 2010; Hanley et al., 2010; Mezza

et al., 2014; Yoneda et al., 2013). These results might suggest a contribution of neogenesis to human β-cell mass expansion under such conditions, although the source of these cells is unknown. Insulin positive cells in ductal regions suggest slow rate of neogenesis from tissue resident ductal progenitors in humans (Bouwens and Pipeleers, 1998; Butler et al., 2003). On-going research tries to identify pancreatic stem or progenitor cells in the adult pancreas (Bonner-Weir et al., 2008; Klein et al., 2015; Qadir et al., 2018). However, how these progenitor cells could be targeted to induce new β-cell differentiation for diabetes therapy is unclear.

1.1.3 β-like cells from non-β-cell transdifferentiation

The differentiation of mature β-cells is regulated via timed regulation of expression levels of essential TFs including Ngn3, Pancreatic duodenal homeobox 1 (Pdx1), Islet-1 (Isl1), Paired box 6 (Pax6), v-Maf avian musculoaponeurotic oncogene homolog A and B (MafA and MafB), NK2 Homeobox 2 (Nkx2.2), NK6 Homeobox1 (Nkx6.1), and Neuronal differentiation 1 (NeuroD1) (Bastidas-Ponce et al., 2017; Pan and Wright, 2011). Genetic overexpression of β-cell essential TFs reprogrammed extra-pancreatic cells such as liver and gastrointestinal cells as well as pancreatic non-endocrine acinar and ductal cells into insulin producing cells that ameliorate hyperglycemia in rodent models of diabetes (Al-Hasani et al., 2013; Ariyachet et al., 2016; Chen et al., 2014; Collombat et al., 2009; Ferber et al., 2000; Kaneto et al., 2005; Li et al., 2014; Zhou et al., 2008). These results demonstrated that non-endocrine cells can be reprogrammed into β-like cells by forced expression of β-cell lineage determent TFs.

Lineage tracing studies performed in the Herrera lab were the first to show that endocrine cells can spontaneously convert into β-cells after extreme β-cell loss of > 95% (Chera et al., 2014; Thorel et al., 2010). Interestingly, while in adult mice predominantly α-cells converted to β-cells, it was δ-to-β-cell transdifferentiation that occurred after near complete β-cell ablation in juvenile mice (Chera et al., 2014; Thorel et al., 2010). Intrudingly, two studies reported α-to-β-cell transdifferentiation by pharmacological treatment with gamma-Aminobutyric acid (GABA) or artemisinins (Ben-Othman et al., 2017; Li et al., 2017). These new β-cells were functional and reversed diabetes in mice (Ben-Othman et al., 2017; Li et al., 2017). However, these initial findings were challenged by contradicting results of no on-going α-to-β-cell fate switch after treatment with the same compounds in two other labs (Ackermann et al., 2018; van der Meulen et al., 2018). In a recent proof-of-concept study, Furuyama et al. showed that human endocrine non-β-cells (α-, δ- and PP-cells) can be converted into insulin producing cells via *in vitro* over expression of PDX1 and MAFA, demonstrating that also human endocrine cells have the ability of cell-fate conversions (Furuyama et al., 2019). After transplantation, human α-cell derived insulin producers reversed diabetes in mice despite maintaining an α-cell gene and protein signature (Furuyama et al., 2019).

Currently, it is unknown whether endocrine or other cells can be pharmacologically re-programmed into insulin-producers *in vivo*. Moreover, it remains challenging to translate the reprograming approach into the clinic as this requires more efficient and reliable protocols to

produce human β-like cells, which develop into transplants that are functional and stable (Zhou and Melton, 2018).

1.1.4 Trigger redifferentiation of dedifferentiated β-cells

In a series of studies, Weir and colleagues showed that pancreatic islets lose the expression of β-cell specific key TFs and maturity markers in experimentally induced rodent models of hyperglycemia (Jonas et al., 1999; Laybutt et al., 2002, 2003). In 2012, genetic lineage tracing proved the β-cell specific loss of maturation markers (Talchai et al., 2012). In this genetic model of hyperglycemia, the Forkhead box protein O1 (FoxO1; known regulator of β-cell maturity and stress response) TF was specifically deleted in β-cells (Talchai et al., 2012). As a consequence, expression levels of β-cell TFs such as MafA, Nkx6.1, and Pdx1 were reduced in β-cells from these genetic modified mice, while TFs that mark pluripotency or endocrine progenitors were increased (e.g. Ngn3, Octamer-binding transcription factor 4 (Oct4), Nanog homeobox (Nanog)) (Talchai et al., 2012). Moreover, some of these β-cells converted to glucagon producing cells (Talchai et al., 2012). Similarly, β-cell specific genetic deletion of β-cell identity TFs such as Isl1, Pdx1, NeuroD1, Pax6, Nkx2.2, and Nkx6.1 caused hyperglycemia as well as a loss of β-cell maturation markers and partial β-cell transdifferentiation (Ediger et al., 2014; Gao et al., 2014; Gu et al., 2010; Gutiérrez et al., 2016; Swisa et al., 2016; Taylor et al., 2013). Hence, β-cell dedifferentiation refers to a process of β-cell specific loss of key terminal differentiation and maturation markers contributing to β-cell dysfunction and worsening of glycemia in diabetes (Figure 2). Due to the genetic lesions of these mice, it was unclear whether high glucose levels *per se* or the genetic modifications caused β-cell dedifferentiation.

K_{ATP} channels regulate GSIS from β-cells (Ashcroft et al., 1984). A rise in blood glucose increases intracellular ATP, which closes K_{ATP} channels. Positively charged potassium ions are restrained within cells leading to cell membrane depolarization and opening of voltage-dependent Ca^{2+} channels. The intracellular influx of Ca^{2+} ultimately triggers insulin secretion from β-cells. Genetic mutations in the β-cell K_{ATP} channel lead to β-cell dysfunction and hyperglycemia (Gloyn et al., 2004). Lineage tracing in mice with genetic modifications of the K_{ATP} channel demonstrated β-cell dedifferentiation accompanied by reduced expression of MafA, Nkx6.1, Pdx1, and insulin (Brereton et al., 2014; Wang et al., 2014). β-cell dedifferentiation could be reversed by glycemia normalization using exogenous insulin administration in these genetic models (Brereton et al., 2014; Wang et al., 2014). Although these results provided evidence that hyperglycemia alone can cause β-cell dedifferentiation, it remains unclear whether redifferentiated β-cells upon glycemia normalization were functional due to the genetic modifications in these mice. Thereby, it remains unclear whether β-cells dedifferentiate to a state of pluripotency, which is characterized by Ngn3 upregulation.

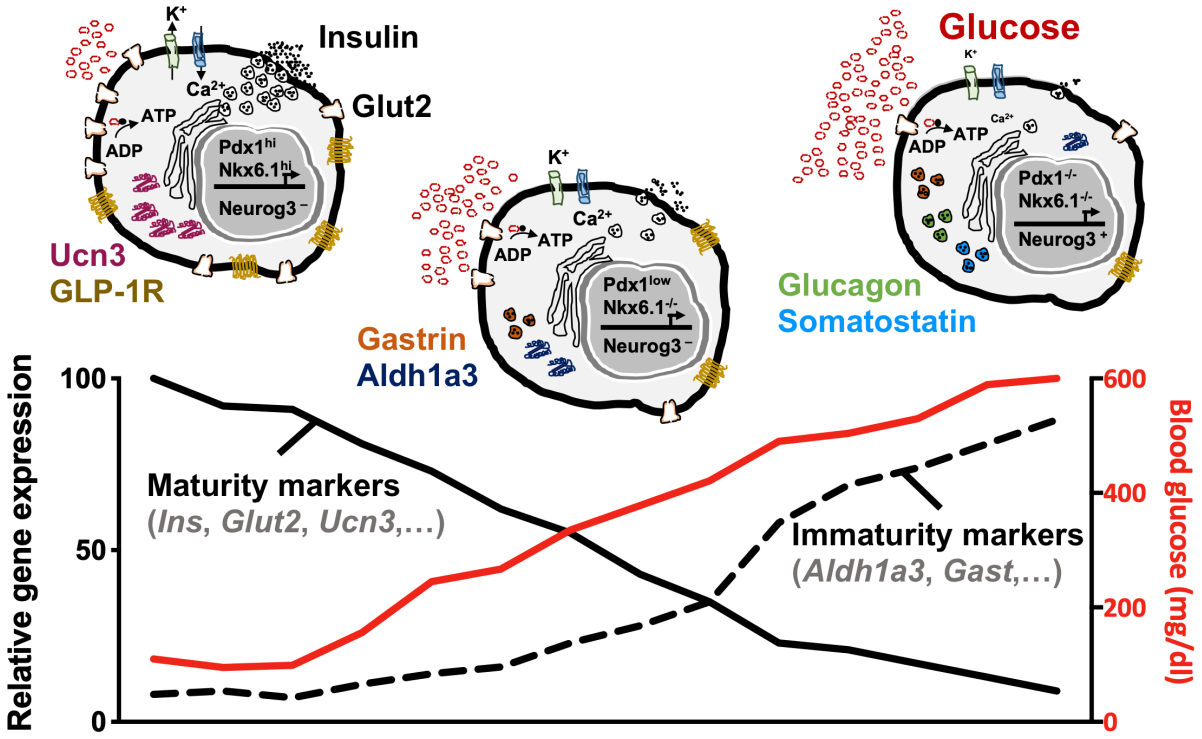

Figure 2: Process of β-cell dedifferentiation.

Upon hyperglycemia, β-cells dedifferentiate and loose the expression of key maturations markers such as *Insulin*, *Glut2*, or *Ucn3*. Some dedifferentiated β-cells express the only known dedifferentiation markers *Gastrin* and/or *Aldh1a3*. If hyperglycemia further deteriorates, β-cells may dedifferentiate into a progenitor-like state marked by Ngn3 upregulation. Some dedifferentiated β-cells might acquire other endocrine hormones such as *Glucagon* and/or *Somatostatin*.

Importantly, there is now cumulating evidence that β-cell dedifferentiation occurs in human T1D and T2D. β-cell identity TFs MAFA, NKX6.1, and PDX1 were reduced in islets from T2D cadaveric donors (Cinti et al., 2016; Guo et al., 2013). Aldehyde Dehydrogenase 1 Family Member A3 (ALDH1A3) is the only validated marker of dedifferentiated islet endocrine cells (Kim-Muller et al., 2016). In T2D pancreata, ALDH1A3 expression co-localized with the β-cell specific TF NKX6.1 suggesting that some of the ALDH1A3 positive cells were in fact dedifferentiated β-cells (Cinti et al., 2016). Recently, Dahan et al. showed that dedifferentiated β-cells may turn on the expression of the fetal islet hormone Gastrin in T2D (Dahan et al., 2017). Gastrin is usually only expressed during pancreas development (Suissa et al., 2013). The role of Gastrin in T2D islets is unclear.

First evidence of β-cell dedifferentiation in T1D came from the non-obese diabetic (NOD) mouse model. Similar to pathogenesis of human T1D, β-cells of NOD mice are destroyed by autoimmune killing (Pearson et al., 2016). However, Rui et al. showed that upon immune stress a population of β-cells dedifferentiate leading to protection from autoimmune destruction and long-term survival of dysfunctional and progenitor-like β-cells (Rui et al., 2017). Using imaging mass cytometry, Damond et al. could show that human β-cells in T1D loose the expression of key β-cell makers prior immune cell recruitment and β-cell destruction (Damond et al., 2019). Remaining insulin in the blood stream of long-term T1D patients (Keenan et al., 2010) might

originate from dedifferentiated β-cells, but also polyhormonal non-β-cells that function as "insulin microsecretors" (Lam et al., 2018). Recently, Seiron et al. identified endocrine cells that express glucagon and the β-cell specific TF PDX1 in recent onset T1D patients (Seiron et al., 2019). Hence, glucagon and PDX1 double positive cells might either be dedifferentiated β-cells that acquired glucagon expression or transdifferentiated α-cells (Seiron et al., 2019). Altogether, β-cell dysfunction and dedifferentiation are common features of functional β-cell mass loss in T1D and T2D. It is still undefined whether the progressive decline of β-cell function and mass can be stopped and reversed by pharmacological intervention. Redifferentiation of remaining dedifferentiated β-cells along developmental trajectories seems a logical route, but dedifferentiation paths, mechanisms, and marker need to be understood for clinical translation and pharmacological intervention.

1.2 The obesity and T2D epidemic

While T1D is an autoimmune disease, T2D is predominately a consequence of long-term obesity, which can be prevented by maintaining a healthy body weight (Schellenberg et al., 2013). The increasing prevalence of T2D parallels the world-wide obesity epidemic (Zheng et al., 2018). Obesity prevalence (defined as BMI >= 30 kg/m^2) has doubled since 1980 and more than 600 million adults were obese in 2015 with an increasing threat for developing countries and, strikingly, adolescents (The GBD 2015 Obesity Collaborators, 2017). Obesity is a major risk factor for metabolic complications such as T2D and nonalcoholic fatty liver disease (NAFLD), both of which are main risk factors for cardiovascular disease (CVD), which is the leading cause of death worldwide (The Emerging Risk Factors Collaboration, 2011; Younossi et al., 2016). Accordingly, there is an urgent need to further prevent obesity epidemic expansion and related co-morbidities, which will ultimately reduce the risk of T2D and thus functional β-cell mass loss.

1.2.1 Obesity treatment

Life style intervention is still the first treatment option for obesity. A combination of dietary-, exercise-, behavioral-, and if indicated also psychotherapy can result in an initial weight loss of ~7% in obese patients, which has been shown to reduce the incidence of T2D in obese patients at high risk (Unick et al., 2013). However, adherence to a continuous life style change is poor and thus long-term effectiveness of such interventions is disappointing (Middleton et al., 2013). As of today, bariatric surgery is the most effective treatment option to reduce body weight, improve co-morbidities, and reduce cardiovascular risk in obese patients (Aguilar-Olivos et al., 2016; Beamish et al., 2016; Buchwald et al., 2009). RYGB, vertical sleeve gastrectomy (VSG), and adjustable gastric banding (AGB) are the most commonly performed surgeries and cause a 20-35% total body weight loss and maintenance (Angrisani et al., 2015; Buchwald et al., 2004; O'Brien et al., 2006).

In obese patients with T2D (glycated hemoglobin A1c (HbA1c) > 7%), bariatric surgery is more effective than intensive medical therapy to induce diabetes remission (HbA1c < 6%) (Schauer et al., 2017). Moreover, bariatric surgery is more efficient than usual care (intensive life style intervention) to prevent T2D development in obese patients (Carlsson et al., 2012). Thereby, surgeries rapidly reduce blood glucose levels accompanied by improved β-cell function, even before body weight decreases (Camastra et al., 2007; Jørgensen et al., 2012; Mullally et al., 2019; Polyzogopoulou et al., 2003). These results might suggest rapid reversal/redifferentiation of dysfunctional/dedifferentiated β-cells upon glucose normalization in T2D after bariatric surgery, but this has not been formally proven yet.

The underlying mechanism of acute- and long-term metabolic benefits after bariatric surgery are still incompletely understood. The physical restriction of food intake alone does not explain the weight-lowering effects of bariatric surgery (Miras and le Roux, 2013; Seeley et al., 2015). Instead, gastrointestinal-derived endocrine signals affecting appetite, food reward, and food preference change after surgery, likely contributing to sustained weight loss (Faria et al., 2014; Karamanakos et al., 2008; Roux et al., 2006; Scholtz et al., 2014; Sumithran et al., 2011).

However, most studies have been restricted to few molecules or hormones and thus systemic metabolic changes after surgery remain uncertain. Recently, Wewer Albrechtsen et al. applied plasma proteome profiling (PPP), which uses unbiased and system-wide mass spectrometry (MS), to obese patients undergoing RYGB surgery and found systemic resolution of inflammation as well as alterations in lipid metabolism (Geyer et al., 2016a, 2017; Wewer Albrechtsen et al., 2018). The contribution of systemic inflammation to obesity, T2D, and other metabolic diseases has been investigated extensively on the molecular and cellular level (Brestoff and Artis, 2015). Hence, these systemic changes might contribute to long-term metabolic benefits of RYGB. Bariatric surgeries are highly invasive, expensive, not without risk, mostly irreversible, and thus not applicable to all patients that are in need to reduce body weight. Hence, novel pharmacological means that can safely mimic the multi-beneficial metabolic outcomes of such surgical procedures are urgently needed.

1.2.2 Long acting glucagon-like peptide 1 agonists for obesity and diabetes therapy

GLP-1 is a peptide hormone secreted by entero-endocrine L-cells in the distal ileum and colon upon food ingestion (Müller et al., 2019). After secretion, GLP-1 is immediately degraded by dipeptidylpeptidase IV (DDP-IV) and GLP-1 is further inactivated in the liver (Holst, 2007). Thus, only a small percentage of approximately 10-15% of active GLP-1 reaches the systemic circulation with a half-life of 1-2 minutes in plasma (Holst, 2007). GLP-1 exerts its metabolic effects solely through the G-protein coupled GLP-1 receptor (GLP-1R), which is primarily expressed in the brain, pancreatic β-cells, and the gastrointestinal tract (Campbell and Drucker, 2015; Göke et al., 1995). As incretin, GLP-1 stimulates β-cell insulin secretion in a glucose-dependent manner (Kreymann et al., 1987; Nauck and Meier, 2016). In addition, GLP-1 potentiates β-cell insulin synthesis (Holst, 2007). GLP-1 delivers a satiety signal to the brain, which in turn reduces appetite, increases satiety, delays gastric emptying, and thus reduces

body weight in rodents and humans (Müller et al., 2019). Of note, plasma GLP-1 levels are increased immediately after but also after years of bariatric surgeries (Jørgensen et al., 2012). Increased GLP-1 levels might thus contribute to the immediate and long-term beneficial effects of such surgeries to improve glucose metabolism and reduce body weight (Jørgensen et al., 2012). This makes GLP-1 to an interesting candidate for the treatment of obesity and T2D (Müller et al. 2019).

Due to its rapid degradation, biochemical modifications to improve the pharmacokinetics of native GLP-1 have led to the development of long acting GLP-1 analogs with enhanced therapeutic benefits (Müller et al., 2019). They include Exenatide (Byetta®, short-acting; and Bydureon®, long-acting, AstraZeneca), Lixisenatide (Lyxumia®, Sanofi), Liraglutide (Victoza®; Novo Nordisk), Dulaglutide (Trulicity®; Eli Lilly & Co), Albiglutide (Tanzeum®, GlaskoSmithKline), and Semaglutide (Ozempic®, Novo Nordisk) (Müller et al., 2019).

In 2005, Exenatide (Byetta® and Bydureon®, AstraZeneca) was the first approved GLP-1 analog for the treatment of T2D (Figure 3). In T2D patients, Exenatide improves glucose metabolism, reduces cardiovascular risk factors, and decreases body weight (up to 5% compared to placebo) (Ratner et al., 2006; Toft-Nielsen et al., 1999). In 2009, Liraglutide was the second GLP-1 analog approved for T2D treatment at a dose of 1.2 and 1.8mg (Figure 3). Liraglutide was also the first approved GLP-1 analog for treatment of obesity at a dose of 3mg (Saxenda®) and yields a typical weight loss in the range of 5-10% after 52 weeks of treatment in non-diabetic obese subjects (O'Neil et al., 2018). Semaglutide is currently the most potent long-acting GLP-1R agonist to reduce body weight and improve glucose metabolism in obese patients with or without T2D (Figure 3) (Aroda et al., 2017; O'Neil et al., 2018). At the highest dose, injected Semaglutide (0.4mg/day) reduced body weight by 13.8% in obese patients after 52 weeks of treatment (O'Neil et al., 2018). Recently, an oral formulation of Semaglutide was approved for T2D treatment and is thus the first GLP-1 analog that is not injected (Davies et al., 2017; Granhall et al., 2019; Husain et al., 2019).

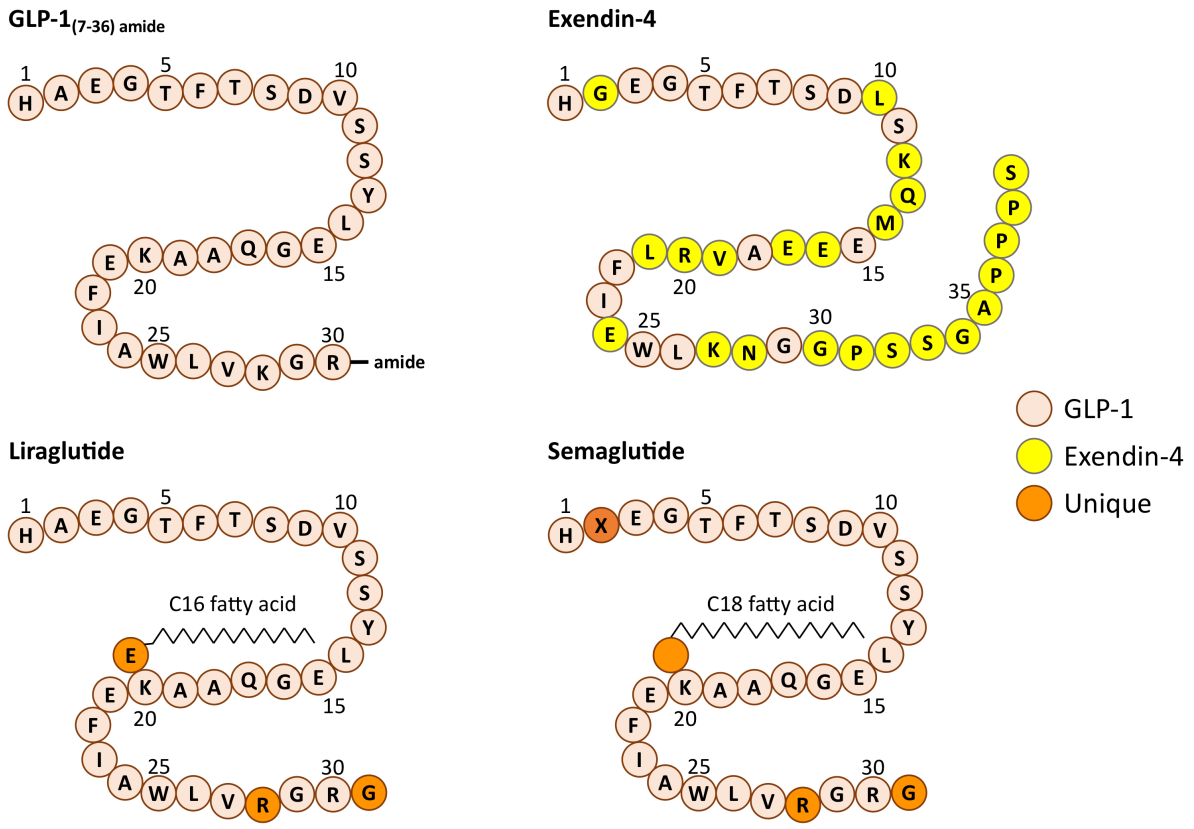

Figure 3: Schematic of major GLP-1 derivatives approved by the FDA for the treatment of T2D.

Exenatide is a synthetic 39-amino acid peptide based on exendin-4, which was discovered in the saliva of the glia monster (Eng, 1992). Glycine at position two protects exendin-4 against DPP-IV degradation. Liraglutide is based on the native GLP-1 peptide. Lysine at residue 28 is replaced with arginine. Alanine at position two is preserved. A palmitic acid (C16:0) extension at position 20 protects against DPP-IV degradation and leads to non-covalent binding to albumin, which delays renal clearance (Agersø et al., 2002). Semaglutide is a chemically optimized liraglutide analog. Substitution of alanine with Aminoisobutyric acid (Aib) at position two protects against DPP-IV inactivation. A dicarboxylic-stearic acid (C18:0) acylation at position 20 (lysine) enhances noncovalent binding to albumin and decelerates renal clearance (Gotfredsen et al., 2014; Lau et al., 2015).

Despite these intriguing results of long-acting GLP-1 analogs for obesity and T2D treatment, intestinal side effects such as nausea and vomiting limit higher dosage, which would be required to reach a meaningful decrease in body weight as currently only achieved by bariatric surgery. Furthermore, despite promising preclinical results of GLP-1R agonists to improve β-cell function, proliferation, and viability in rodent models of diabetes (Dai et al., 2017; Farilla et al., 2002; Li et al., 2005; Tourrel et al., 2001; Xu et al., 1999), GLP-1 analogs have not been proven to be similar effective in obese and diabetic humans (Chon and Gautier, 2016; Drucker, 2018; The RISE Consortium, 2019). Hence, optimization of GLP-1 based pharmacology is an important clinical goal to further enhance efficacy and safety for the treatment of obesity and diabetes.

1.3 GLP-1 based polypharmacy

One way to enhance the metabolic effects of GLP-1R agonists is to combine them with other hormones in order to simultaneously activate redundant or additive pathways. Ideally, the individual components could then be used at lower doses, which potentially reduces the risk of side effects, while enhancing metabolic benefits (Clemmensen et al., 2019).

1.3.1 GLP-1/GIP co-agonist

The Glucose-dependent insulinotropic polypeptide (GIP) is a 42-amino-acid peptide. GIP is secreted from K-cells in the duodenum and jejunum stimulated by dietary nutrients, especially lipids (Inagaki et al., 1989; Lardinois et al., 1988; Takeda et al., 1987). GIP complements GLP-1 to stimulate GSIS (i.e. incretin effect) supporting the combination of both hormones to synergize glycemic benefit (Elrick et al., 1964; Holst et al., 1987; Kreymann et al., 1987). However, the insulionotropic effect of GIP is blunted upon hyperglycemia in T2D (Nauck et al., 1993). By combining GLP-1R with GIP receptor (GIPR) agonism, the body weight and glucose lowering effects of GLP-1 could prime GIP activity. Indeed, co-administration of GLP-1 and GIP in humans additively increased the insulinotropic effect compared to the effect of either incretin alone. In DIO rodents, co-treatment with GLP-1 and GIP synergistically decreased body weight and improved glucose metabolism relative to mono-therapies (Finan et al., 2013). A more recent polypharmacological approach integrates sequences of structurally related hormones into a single entity to generate unimolecular multi-agonists of enhanced potency and sustained action (Day et al., 2009; Finan et al., 2013, 2015). Based on the similarities of the GLP-1 and GIP peptides, Finan et al. developed and preclinically tested unimolecular GLP-1/GIP co-agonists with balanced potency at both receptors that was either slightly enhanced (fatty-acylated GLP-1/GIP co-agonist) or slightly diminished (pegylated GLP-1/GIP co-agonist) relative to the native hormones (Figure 4) (Finan et al., 2013). Both co-agonists outperformed best-in-class, pharmacokinetically-matched GLP-1R mono-agonists to reduce body weight, enhance insulin sensitivity, and improve glucose control in preclinical models of diet- and genetic-induced obesity and diabetes (Finan et al., 2013). Glycemic improvements of the GLP-1/GIP co-agonists translated from rodents to nonhuman primates and humans (Finan et al., 2013; Frias et al., 2017; Schmitt et al., 2017).

More recently, a novel GLP-1/GIP co-agonist (Tirzepatide® or LY3298176, Eli Lilly) was shown to dose-dependently reduce HbA1c and body weight in a 26-week study in patients with T2D without reaching a plateau (Frias et al., 2018). Interestingly, Tirzepatide® is a biased GIPR agonist with a relative potency at the GIPR which is ~4-5 higher compared to native GIP (Coskun et al., 2018). The potency of Tirzepatide® at the GLP-1R is similar to that of native GLP-1 (Figure 4) (Coskun et al., 2018).

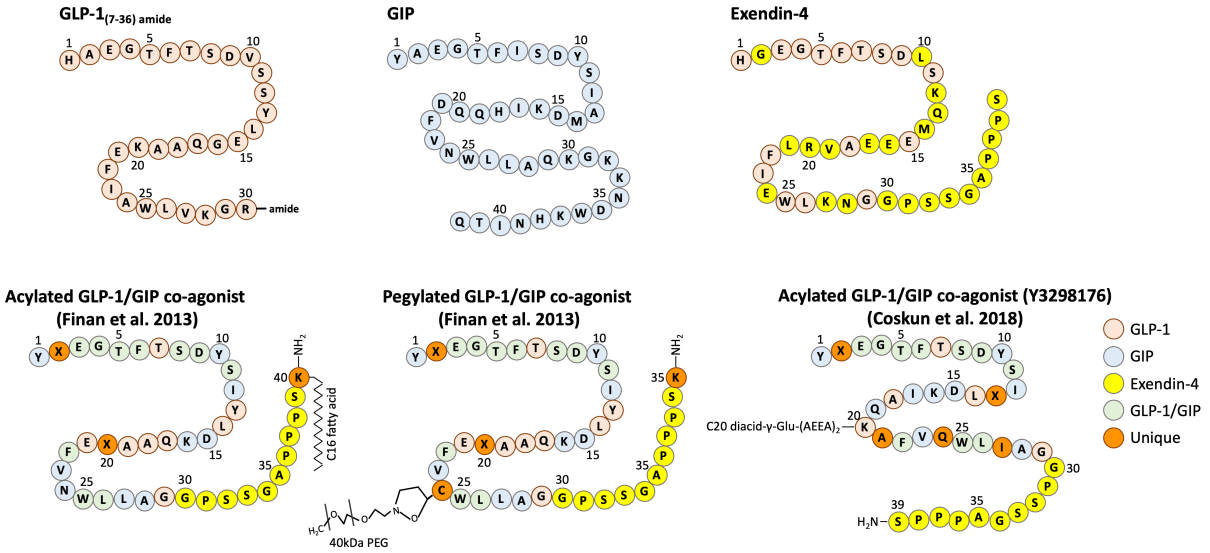

Figure 4: Schematic of the major peptides as blueprint for development of clinically advancing GLP-1/GIP co-agonists.

Finan et al. introduced GIP residues in the GLP-1 peptide sequence (Finan et al., 2013). A nine-amino-acid extension (also found in exendin-4) prolongs the C terminus. The introduction of Aib at position 2 protects against DPP-IV inactivation. GLP-1/GIP peptides were either fatty-acylated at the Lys40 with palmitic acid or site-specifically modified with a 40-kDa PEG at Cys-24. These modifications extend the *in vivo* time action of the peptides. Both dual-agonists equally activate the GLP-1R and GIPR. Recently, the development of a GIP-based GLP-1/GIP co-agonist was described (LY3298176) (Coskun et al., 2018). Amino acids at positions two and 13 are substituted by Aib. A C20 fatty diacid moiety is connected to the lysine residue at position 20 via a linker, which enables albumin binding and half-life extension. The exendin-4 derived C-terminus is amidated.

GLP-1/GIP co-agonists are currently one of the most promising approaches for obesity and T2D treatment. However, more studies are needed to show whether these multi-agonists can close the gap to the metabolic improvements of bariatric surgery, thereby being more effective than best-in-class GLP-1R mono-agonists without worsening the safety profile.

1.3.2 GLP-1/estrogen conjugate

Based on pioneering work of antibody-drug conjugates for tissue targeting in the oncology research field (Dugger et al., 2018), a similar approach in metabolism research has emerged recently (Clemmensen et al. 2019). The rationale was to use peptides with a distinct tissue receptor expression profile as carrier to safely deliver the biological effects of nuclear hormones into target cells (Finan et al., 2012, 2016; Quarta et al., 2017). Thereby, the use of GLP-1 analogs as carrier peptide is attractive due to the relative selective expression of the GLP-1R in obesity and diabetes relevant organs such as pancreatic islets and the central nervous system.

Estrogens, the female reproductive hormones, have been repeatedly implicated in the treatment of metabolic disease. The gonadal steroid hormone 17β-estradiol (here referred to as estrogen) acts in the hypothalamus to regulate thermogenesis and as a leptinomimetic to reduce food intake and adiposity in diet-induced obese (DIO) mice (Dubuc, 1985; Gao et al.,

2007; Martínez de Morentin et al., 2014). Moreover, estrogen has been proposed as a potential drug to preserve or restore functional β-cell mass in diabetes (Mauvais-Jarvis, 2016; Tiano and Mauvais-Jarvis, 2012). Estrogen increases insulin biosynthesis, prevents β-cell apoptosis, and promotes β-cell survival and proliferation in rodent models of diabetes by enhancing the action at both nuclear estrogen receptors (ER) alpha and beta, respectively (Alonso-Magdalena et al., 2008; Le May et al., 2006; Puah and Bailey, 1985; Tiano et al., 2011; Wong et al., 2010). There is also evidence from randomized controlled trials and observational studies in which estrogen replacement therapy (ERT) reduces T2D risk in postmenopausal women (Godsland, 2005; Mauvais-Jarvis et al., 2017). Seven out of eleven clinical studies showed that ERT restored insulin secretion capacity in women after menopause suggesting a direct effect of estrogens on pancreatic β-cells (Mauvais-Jarvis et al., 2017). However, systemic estrogen therapy is limited due to gynecological and tumor-promoting detrimental actions.

A single-molecule GLP1–estrogen conjugate with specific estrogen targeting to GLP-1R-positve tissues enhanced the weight-lowering and anorectic effects in DIO mice in comparison to GLP-1 or estrogen alone (Finan et al., 2012). Importantly, stable GLP-1/estrogen targeting was devoid of adverse estrogen effects on uterus and breast tissue growth, which do not express the GLP-1R (Finan et al., 2012). In addition, GLP-1-estrogen demonstrated profound ability to prevent islet destruction in polygenetic diabetes-prone New Zealand Obese (NZO) mice (Schwenk et al., 2015). It is not clear whether the islet protective effect resulted from direct action of GLP-1/estrogen in islets or mostly indirect through other mechanisms such as reduced food intake (Schwenk et al., 2015). Hence, the therapeutic efficacy of GLP-1/estrogen on β-cell biology in diabetes has not been thoroughly explored yet.

1.3.3 GLP-1 and insulin co-therapy

Currently, the progressive loss of β-cell function and number cannot be stopped by pharmacological approaches, which leads to exogenous insulin necessity in T1D and T2D (Zhou and Melton, 2018). Current insulin therapies unsatisfactorily sustain stable normoglycemia and cannot prevent the development of micro- and macrovascular complications (Lipska et al., 2017; Stark Casagrande et al., 2013). The risk of life-threatening hypoglycemia and undesirable weight gain (especially in T2D) of insulin treatment, further highlight the necessity of novel treatment options for diabetes therapy (Brown et al., 2004, 2010; Davies, 2004; Matthews et al., 1998; Zaykov et al., 2016). Interestingly, intensive insulin therapy and glycemia normalization directly at disease onset transiently reverses β-cell dysfunction in preclinical as well as clinical findings from type 1 and 2 diabetic patients (Harrison et al., 2012; Kramer et al., 2013, 1998; Wang et al., 2014). In T2D, insulin therapy better preserved β-cell function compared to oral anti-diabetic drugs, while glycemia control was similar between both treatments (Alvarsson et al., 2003; Weng et al., 2008). This suggests additional glucose-independent beneficial effects of insulin therapy on β-cell function.

The insulin/insulin growth factor (IGF) signaling pathway has been implicated in β-cell protection, function, and compensatory proliferation (Kubota et al., 2000; Kulkarni et al., 1999a, 1999b, 2002; Ueki et al., 2006; Withers et al., 1998). The direct effect of insulin on β-cells is still controversially discussed (Leibiger et al., 2008; Rhodes et al., 2013). Notably, total insulin and IGF signaling resistance of β-cells causes diabetes and it was proposed that therapeutic improvement of insulin/IGF signaling might protect from diabetes (Ueki et al., 2006). It remains elusive if the glucose lowering effect of insulin itself or direct actions on remaining β-cells could regenerate functional β-cell mass.

Long acting GLP-1R agonists potentiate glucose-dependent insulin secretion of β-cells while minimizing hypoglycemia and limiting weight gain, making them an attractive treatment option for T2D to counteract undesirable side effects of insulin therapy (Chon and Gautier, 2016; Drucker, 2018). Indeed, clinical studies have demonstrated that the combination of basal insulin and GLP-1R agonists improve glycemic control with low risk of hypoglycemia and weight gain in type 2 diabetic patients (Anderson and Trujillo, 2016). Also in T1D, the co-treatment achieved superior results to decrease HbA1c levels while reducing weight gain and insulin dosage (Wang et al., 2017). However, it is unclear whether such co-therapies rescue declining functional β-cell mass.

2. Scope of this thesis

Loss or dysfunction of β-cells leading to systemic hyperglycemia are the hallmark of T1D and T2D, placing β-cells in the center of disease initiation and progression. Understanding the molecular underpinnings of β-cell loss in diabetes is important to develop new therapeutics that can prevent the loss or regenerate dysfunctional β-cell mass. In this PhD thesis multiple pharmacological approaches were tested with the overarching goal to improve obesity and diabetes treatment. The specific aims of this thesis were:

(1) To find new treatment options that restore β-cell mass and function in diabetes.

The overarching objective of the first part of this thesis was to get insights in diabetic β-cell failure and to find mechanisms and entry points of β-cell regeneration. Genetic mouse models suggest β-cell dedifferentiation as major mechanism of functional β-cell mass loss in T1D and T2D. However, due the genetic pressure of these models, β-cell dedifferentiation is ill defined and pharmacological β-cell regeneration is limited.

Streptozotocin (STZ) is a chemical toxin, which specifically destroys β-cells (Rakieten et al. 1963), but when injected in multiple low doses (mSTZ), some β-cells survive (Like and Rossini 1976). Hence, we used the mSTZ model to investigate the fate of remaining β-cells upon long-term hyperglycemia and change of the islet cell niche. By combining cell biology and single cell RNA sequencing (scRNA-seq), we wanted to extensively characterize diabetic β-cells in the absence of genetic lesions. On this basis, we further wanted to investigate whether we can use pharmacological treatments to regenerate functional β-cell mass in mSTZ-diabetic mice and, if so, we sought to describe the origin (neogenesis, proliferation, transdifferentiation, redifferentiation) of these new β-cells. Specifically, we tested whether a stable GLP-1/estrogen conjugate with or without daily insulin substitution can directly deliver estrogen into GLP-1R expressing β-cells in mSTZ-diabetic mice for diabetes remission.

(2) To unveil shared benefits of GLP-1R/GIPR agonism in mice and human bariatric surgery.

Bariatric surgery is unmatched in correcting obesity and inducing T2D remission by increasing β-cell function. The objective of the second part of this thesis was to compare the metabolic benefits of GLP-1/GIP co-agonist treatment in male and female DIO obese mice with bariatric surgery in humans. Therefore, we combined rodent pharmacology with plasma proteomic profiling (PPP) to test whether GLP-1/GIP-induced plasma proteome changes in mice mimic RYGB-induced changes in humans.

3. Material and Methods

Table 1: Primary antibodies.

Protein	Generated in	Company	Item number
Aldh1a3	Rabbit	Novus	NBP2-15339
Caspase-3	Rabbit	Cell Signaling	9661
Cck	Rabbit	ENZO Life Sciences	BML-CA1124
Gast	Rabbit	Abcam	Ab16035
GLP-1R	Rabbit	Novo Nordisk	–
Glucagon	Guinea pig	Takara	M182
Glut2 (Slc2a2)	Goat	Abcam	ab111117
Insulin	Guinea pig	Thermo Scientific	PA1-26938
Insulin	Rabbit	Cell Signaling	3014
Insulin	Guinea pig	ABD Serotec	5330-0104G
Ngn3	Rabbit	Donated by H. Edlund	–
Nkx6.1	Goat	R&D systems	AF5857
Slc5a10	Rabbit	Abcam	ab167156
Somatostatin	Goat	Santa Cruz	sc-7819
Somatostatin	Rat	Invitrogen	MA5-16987
Ucn3	Rabbit	Phoenix Pharmaceuticals	H-019-29

Table 2: Secondary antibodies.

Protein	Conjugated	Company	Item number
Donkey anti-Goat IgG	Alexa Fluor 633	Invitrogen	A-21082
Donkey anti-Rabbit IgG	Alexa Fluor 555	Invitrogen	A-31572
Donkey anti-Rabbit IgG	Alexa Fluor 488	Invitrogen	A-21206
Donkey anti-Guinea pig IgG	DyLight 649	Dianova	706-495-148
Donkey anti-Rat IgG	DyLight 647	Dianova	711-605-152
Donkey anti-Rat IgG	Cy3	Dianova	712-165-153
Donkey anti-Guinea pig	Alexa Fluor 488	Dianova	706-545-148

3.1 Mouse studies

3.1.1 Generating mSTZ-diabetic mice

8-week old male C57BLJ/6 mice (n=125; Janvier Labs) were injected intraperitoneally with STZ (Sigma) dissolved in ice-cold citrate buffer (pH 4.5): 0.1M citric acid monohydrate (Roth) + 0.1M trisodium citrate, dihydrate (Fisher Scientific) at a dose of 50 mg/kg/day for five consecutive days, as described in the mSTZ mouse model to induce diabetes (Like and

Rossini 1976). Age-matched control animals (n=20) were injected with ice-cold citrate buffer (pH 4.5). To assess the diabetic status of mice, fasting blood glucose, insulin, and C-peptide levels were measured ten days after the last STZ or citrate buffer injection. Functional β-cells mass after mSTZ treatment was estimated by combining fasting blood glucose levels, the homeostatic model assessment of β-cell function (HOMA-β; as HOMA-β = (fasting insulin (ng/ml)/ 0.0347 * 360) / (fasting glucose (mg/dl) – 63)), and the ratio of fasting C-peptide to blood glucose levels (Sachs et al. 2020a). Nine mice with fasting blood glucose levels < 190 mg/dl were excluded. Furthermore, mSTZ treated mice with fasting glucose levels > 25th percentile, a HOMA-β-score < 25th percentile, and a C-peptide/blood glucose ratio < 25th percentile were excluded from the study (n=9) (Sachs et al. 2020a). Mice were housed up to four per cage on a 12:12-h light-dark cycle at 22+/-2°C and 55 +/- 10% relative humidity with free access to normal chow diet and water.

3.1.2 Generating age- and body weight-matched male and female DIO mice

To induce DIO in female mice, eight-week old C57BL/6J females (Charles River Laboratories) were fed a high-fat, high-sugar diet (HFD) comprising 58% kcal from fat (Research Diets). As male mice more rapidly gain body weight on HFD relative to female mice on HFD (Jall et al., 2017), eight-week old male C57BL/6J mice (Charles River Laboratories) were maintained on regular chow diet and switched to HFD at the age of 33 weeks. This diet regime generated 37-week old male and female DIO mice that were body weight-matched. All mice were double-housed and maintained at 22+/-2°C, 55 +/- 10% relative humidity, and a 12-h light/dark cycle with free access to food and water.

3.1.3 Pharmacological studies

mSTZ-diabetic mice were randomized and evenly distributed to different treatments according to fasting blood glucose levels. Treatment groups were vehicle (PBS; n=17, not mSTZ-treated), vehicle (PBS; n=17, mSTZ-treated), a GLP-1 analog (n=16, mSTZ-treated), estrogen (n=14, mSTZ-treated), GLP-1/estrogen (n=28, mSTZ-treated of which n=11 mice were switched to vehicle (PBS) treatment after 12 weeks of GLP-1/estrogen treatment), PEG-insulin (n=13, mSTZ-treated), or GLP-1/estrogen and PEG-insulin (n=16, mSTZ-treated). Mice were treated with daily subcutaneous injections at the indicated doses for 100 consecutive days.

Age- and body weight-matched DIO male (n=30) and female (n=28) mice were randomly assigned to treatment groups matched for body weight and fat mass. Treatment groups were vehicle (n (female)=7, n (male)=7), acyl-GIP (n (female)=7, n (male)=8), acyl-GLP-1 (n (female)=7), n (male)=7), or acyl-GLP1/GIP (n (female)=7, n (male)=8). Obese mice were treated with daily subcutaneous injections at the indicated doses for 21 consecutive days. Compounds were injected in a vehicle of PBS and were given at a volume of 5 µl per g body weight. All procedures were approved by the local Animal Use and Care Committee and the local authorities of Upper Bavaria, Germany in accordance with European and German animal welfare regulations.

3.1.4 Compound formulations

Study in mSTZ-diabetic mice. The synthesis, purification, and characterization of the GLP-1/estrogen conjugate and the pharmacokinetic-matched GLP-1 peptide was described previously and used without chemical modification or change in formulation (Finan et al., 2012). Pegylated insulin (PEG-insulin) was synthesized by the insulin N-terminal amine reductive amination with 20K Methoxy PEG Propionaldehyde (JenKem Technology) (Sachs et al. 2020a). Therefore, human insulin was dissolved in 50mM Sodium Acetate buffer (pH 5.0) and 50% acetonitrile (Sachs et al. 2020a). To this buffer containing insulin, a 30-fold excess of sodium cyanoborohydride and a 1.5-fold excess of methoxy PEG propionaldehyde (M-ALD-20K, JenKem Technology USA Inc., Plano, TX) was added and stirred at room temperature for 3h (Sachs et al. 2020a). PEG-insulin was purified by reverse phase chromatography on a C-8 column in 0.1%TFA acetonitrile solvents, which yielded a final product of greater than 95% purity (Sachs et al. 2020a). Estrogen (17β-Estradiol, Sigma) was dissolved in 100% ethanol (Sigma) at a concentration of 1 mg/ml. Dissolved estrogen was diluted with PBS to the concentration needed.

Study in obese male and female mice. The synthesis, purification, and characterization of the fatty-acylated GLP-1/GIP co-agonist as well as the pharmacokinetic-matched fatty-acylated GLP-1 and GIP mono-agonists was described previously (Finan et al., 2013). Peptides were used without chemical modification or change in formulation.

All compound synthesis was performed and supervised by Brian Finan (Novo Nordisk, Indianapolis, USA).

3.1.5 Body composition measurements

Whole-body composition (fat and lean mass) was measured via nuclear magnetic resonance technology (EchoMRI).

3.1.6 Intraperitoneally glucose tolerance test

For the determination of glucose tolerance, mice were subjected to 6 h of fasting and intraperitoneally injected with either 0.5g (mSTZ-study) or 2g (study in obese mice) glucose per kg body weight (20% (wt/v) D-glucose (Sigma) in 0.9% (wt/v)). Glucose was administered at a volume of 5 µl per g body weight. Tail blood glucose concentrations were measured before (0 min) and at 15, 30, 60, 90 and 120 min after injection using a handheld glucometer (Freestyle).

3.1.7 Administration of EdU

To assess cell proliferation, we used the modified Uracil analog 5´ethynyl-2´-desoxyuridine (EdU; Life Technologies). EdU (50µg/kg body weight) was intraperitoneally injected prior to mouse sacrifice.

3.2 Molecular biological analyses

3.2.1 Blood parameters

For the mSTZ-study, blood from non-diabetic and mSTZ-diabetic lean mice was collected bi-weekly from tail veins after a 4-h fast, using EDTA-coated microvette tubes (Sarstedt). 4-h fasting blood glucose levels were determined using a handheld glucometer (Freestyle). To assess fasting blood glucose and insulin levels in male and female DIO obese mice, mice were fasted for 6h prior to tail vein blood collection (EDTA-coated microvette tubes) and glucose measurements (handheld glucometer). Collected blood was directly put on ice. Plasma was separated by centrifugation at 5000g at 4°C for 10min using a micro centrifuge and stored at -20°C until further usage. Levels of mouse insulin (Crystal Chem), C-peptide (Crystal Chem), and total plasma cholesterol (Thermo Fisher Scientific) were measured following the manufactures' instructions. The homeostatic model assessment of insulin resistance (HOMA-IR) was calculated using the formula: HOMA-IR = [((fasting insulin (ng/ml) * 172.5 /6.945) * fasting glucose (mg/dl)) / 405]. For lipoprotein separation, samples from the different treatment groups were pooled and analyzed in a fast-performance liquid chromatography gel filtration on two Superose 6 columns connected in series as described previously (Hofmann et al., 2008). The FPLC analyses were performed together with Sebastian Cucuruz and Prof. Dr. Susanna Hofmann from the Institute of Diabetes and Regeneration Research at the Helmholtz Zentrum München.

3.2.2 Liver histopathology

Mice were euthanized using CO_2 and dissected liver was immediately fixed in 4% (w/v) neutrally buffered formalin (Sigma). For evaluation of hepatic lipid content, formalin fixed liver samples were embedded in paraffin. Tissue was cut in 4mm sections and stained with hematoxylin and eosin (H&E staining). Stained tissue sections were scanned with an AxioScan. Z1 digital slide scanner (Zeiss, Jena, Germany) using a 20X magnification objective. Following a previously published procedure (Feuchtinger et al., 2015), liver sections were evaluated using the commercially available image analysis software Definiens Developer XD 2 (Definiens AG, Munich, Germany). Hepatic lipid vacuoles were clearly distinguishable from the stained tissue and a specific rule set was defined to detect and quantify the lipid positive area. Histological evaluations were performed together with Dr. Annette Feuchtinger from the Research Unit Analytical Pathology at the Helmholtz Zentrum München.

3.2.3 Pancreas immunohistochemistry

Mice were euthanized using CO_2 and dissected pancreata were immediately fixed in 4% (w/v) neutrally buffered formalin for 24h at 4°C. Tissue-cryoprotection was performed in sequential gradients of 7.5, 15, and 30% sucrose (Appli Chem)-PBS solutions at room temperature (2h incubation for each solution). Thereafter, pancreata were incubated in 30% sucrose and tissue-

embedding medium (Leica) (1:1) at 4°C overnight and subsequently embedded using tissue-freezing medium (Leica). Embedded pancreata were frozen on dry ice and stored at -80°C until further usage. Pancreata were cut in 20µm sections, mounted on a glass slide and dried for 10min at RT and stored at -20°C until further usage.

Pancreatic tissue sections were rehydrated with PBS and then permeabilized with 0.15-0.2% Triton X-100 (Sigma) in PBS for 30 min. Permeabilization was not performed in case of GLP-1R staining.

Sections were blocked (blocking solution: PBS, 0.1% Tween-20 (Sigma), 1% donkey serum (Millipore), 5% FCS (Gibco)) for 1h at room temperature prior administration of first antibodies. The following primary antibodies were used: guinea pig polyclonal anti-insulin (1:300, Thermo Scientific), goat polyclonal anti-Glut2 (1:500, Abcam), goat polyclonal anti-Nkx6.1 (1:200, R&D systems), goat polyclonal anti-somatostatin (1:500, Santa Cruz), rat monoclonal anti-somatostatin (1:300, Invitrogen), rabbit polyclonal anti-urocortin 3 (1:300, Phoenix Pharmaceuticals), rabbit monoclonal anti-insulin (1:300, Cell Signaling), guinea pig polyclonal anti-glucagon (1:500, Takara), guinea pig polyclonal anti-insulin (1:300, ABD Serotec), rabbit polyclonal cleaved caspase-3 (Asp 175) (1:300, Cell Signaling), rabbit monoclonal anti-ki67 (1:300, Abcam), rabbit polyclonal anti-Aldh1a3 (1:300, Abcam), rabbit monoclonal anti-GLP-1R (1 µg/ml, Novo Nordisk), rabbit polyclonal anti-gastrin (1:100, Abcam), rabbit polyclonal anti-cholecystokinin (1:100, ENZO life sciences) and rabbit anti-Ngn3 (1:800, donated by H. Edlund). Antibody dilutions were prepared in blocking solution and sections were incubated at 4°C overnight. Slides were rigorously washed with PBS prior incubation with secondary antibodies diluted in blocking solution. The following secondary antibodies were used: donkey anti-Goat IgG (H+L) secondary antibody (Alexa Fluor 633 Invitrogen A-2108), donkey anti-Rabbit IgG (H+L) secondary antibody (Alexa Fluor 555 Invitrogen A-31572); donkey anti-Rabbit IgG (H+L) secondary antibody (Alexa Fluor 488 Invitrogen A-21206); donkey anti-Guinea pig IgG (H+L) secondary antibody (DyLight 649 Dianova 706-495-148); donkey anti-Rat IgG (H+L) secondary antibody (DyLight 647 Dianova 711-605-152); donkey anti-Rat IgG (H+L) secondary antibody (Cy3 Dianova 712-165-153); donkey anti-Guinea pig (H+L) secondary antibody (Alexa Fluor 488 Dianova 706-545-148). Dilution for all secondary antibodies was 1:800 and incubated for 4-5h at room temperature. Slides were rigorously washed with PBS and stained with DAPI (1:500 in PBS) for 30 min. Images were taken by confocal microscopy (Leica DMI 6000) and the LAS AF software (Leica). Final pictures were produced with ImageJ.

3.2.4 Automatic pancreatic tissue analysis

Pancreatic insulin, glucagon, and somatostatin positive area of stained tissue sections was determined using an AxioScan. Z1 digital slide scanner (Zeiss, Jena, Germany) equipped with a 20X magnification objective. Three slides with three tissue sections each were analyzed per animal unless noted otherwise. Tissue sections were separated by at least 100 µm. Images were evaluated using the commercially available image analysis software Definiens Developer

XD 2 (Definiens AG, Munich, Germany) following a previously published procedure (Feuchtinger et al., 2015). For endocrine islet cell compositions, islets of Langerhans were manually annotated and a specific rule set based on the fluorescence intensity of DAPI and cell morphology, size and neighborhood was defined to detect and quantify islet cells. Fluorescence intensity of insulin, glucagon, and somatostatin was used to automatically classify β-, α-, and δ-cells. Automatic cell annotations were performed together with Dr. Annette Feuchtinger from the Research Unit Analytical Pathology at the Helmholtz Zentrum München.

3.2.5 EdU detection protocol

EdU staining was performed following the manufactures' instructions (EdU imaging kit manual; Life Technologies) after staining with secondary antibodies. DAPI staining and mounting was done as mentioned above.

3.2.6 Pancreatic insulin content

Dissected pancreata were washed in PBS and homogenized using a tissue homogenizer in an acid-ethanol solution (1.5% HCl (Merck) in 70% ethanol (Merck): 5ml/pancreas) and incubated at -20°C for 24h. After 2 rounds of acid-ethanol precipitation, homogenized tissue was centrifuged (2000rpm, 15min, 4°C) and the supernatant neutralized with 1M Tris pH 7.5. Mouse insulin (Crystal Chem) was measured following the manufactures' instructions and normalized to total protein content, which was determined by the bicinchoninic acid (BCA) method (Pierce Biotechnology; BCA).

3.2.7 Islet isolation and single cell suspension

Islet isolation was performed by collagenase P digestion, islet purification, and hand picking of individual islets. Therefore, collagenase P (Roche) (1mg/ml in G-solution (HBSS (Lonza) + 1% BSA (Sigma)) was injected into the bile duct and the perfused pancreas was dissected and transferred to 3ml collagenase P solution (1mg/ml in G-solution) for pancreas digestion. After 15min at 37°C, the digested pancreas was placed on ice and 10 ml of G-solution was added. After centrifugation (1600rpm, 3min, 4°C), the pallet was washed with 2x 20ml of G-solution and re-suspended in 5.5ml of gradient medium (5mL 10% RPMI (Lonza) + 3mL 40% Optiprep (Sigma) per sample) and the suspension was placed on top of 2.5ml gradient medium. 6ml of G-solution were added on top to form a 3-layer gradient. After 10min incubation at room temperature, the gradient was centrifuged (1700rpm, 10min, room temperature, acceleration stage 3, brake stage 0) resulting in an islet-enriched interphase, which was harvested on a 70 µm Nylon filter. Restrained islets were washed with G-solution (2x 10ml). For purification, islets were handpicked under the microscope. Handpicked islets were transferred to a 1.5ml Eppendorf tube, pelleted (800rpm, 1min), washed with Mg^{2+}/Ca^{2+}-free PBS (Gibco), and digested with 0.25% Trypsin in EDTA (Gibco) at 37°C for 8min to obtain single cell suspensions. Mechanical disaggregation was required every 2-3 min.

3.2.8 Single cell sequencing

Single cell libraries were obtained using the ChromiumTM Single cell 3`library and gel bead kit v2 (10x Genomics). Islets and single cell suspensions of n=3/treatment group were pooled to reach a target cell number of 10.000 cells per sample. Therefore, 16.000 cells per sample were loaded onto one channel of the 10X chip to produce Gel Bead-in-Emulsions (GEMs). This underwent reverse transcription to barcode RNA before cleanup and cDNA amplification followed by enzymatic fragmentation and 5´adaptor and sample index attachment. Libraries were sequenced on the HiSeq4000 (Illumina) with 150bp paired-end sequencing of read2.

3.2.9 Compound treatment of reaggregated human micro-islets

Primary human islets were obtained from Prodo Laboratories Inc. Irvine, CA with no information on donor identity due to ethical and privacy reasons (donor 1: male, BMI 32.38, age 48, HbA1c 5.6%; donor 2: male, BMI 33.2, age 46, HbA1c 5.4%; donor 3: male, BMI 28.65, age 34, HbA1c 5.2%). Consent was obtained from next of kin. For production of InSphero 3D InSight™ human islet microtissues, 10000 - 20000 islet equivalents were dispersed in dissociation solution (1X TrypLE™ Express solution (Thermo Fisher Scientific), with 40 µg/ml DNase I (Sigma)) by gentle pipetting at 37°C. A cell strainer (70 µm pore size) removed remaining cell clumps from the cell suspension. Islet microtissues were obtained by hanging-drop based scaffold-free reaggregation of 2500 cells in each well of the InSphero's 96-well Hanging Drop System for five days. Primary aggregates were transferred to Akura™ 96 well-plates for islet maturation for at least eight days prior to start of experiments. Experiments were conducted within 30 days after initiation of islet aggregations. Islet microtissues were maintained in 3D InSight™ Human Islet Maintenance Medium (InSphero AG).

Compound dilutions were done in 3D InSight™ Human Islet Maintenance Medium. Compounds were added to the culture medium at the indicated concentrations one day prior cytokine exposure. The cytokine cocktail containing tumor necrosis factor alpha (TNFα, 10ng/ml (Thermo Fisher Scientific)), interferon gamma (IFNϒ, 10ng/ml (Sigma)) and interleukin-1β (IL-1β, 2ng/ml (Sigma)) was made in PBS containing 0.1% BSA (Sigma). Islet Maintenance Medium, cytokines, and compounds were changed every 2-3 days.

For GSIS, culture medium was removed and islet microtissues were washed twice with Krebs Ringer Hepes Buffer (KRHB: 131mM NaCl, 4.8mM KCl, 1.3mM $CaCl_2$, 25mM Hepes, 1.2mMm Kh_2PO_4, 1.2mM $MgSO_4$, 0.5% BSA) containing 2.8mM glucose and equilibrated for 1 hour in KRHB. GSIS was performed in KRHB containing indicated glucose concentrations for 2 hours. Insulin in the supernatant was measured using the Stellux® Chemi Human Insulin ELISA following the manufactures' instructions. Experiments with reaggregated human micro-islets were performed in collaboration with Dr. Burcak Yesildag and Aparna Neelakandhan from InsPhero AG, Schlieren, Switzerland.

3.3 Statistical analysis not including plasma proteome profiling and scRNA-seq data

Preliminary data processing and calculations during ongoing studies was done using Microsoft Excel 2016. Further statistical analyses were performed using GraphPad Prism 8. Kolmogorov-Smirnov test to assess for normality of residuals was used. Brown-Forsythe test to assess for the equality of group variances was used. To determine significance among different treatment groups, one-way analysis of variances (ANOVA) followed by Tukey's post hoc analysis was used. Two-way ANOVA was used when the influence of time and treatment was examined. When normality of residuals was not given, a Kruskal-Wallis test followed by Dunn's multiple comparison test to test for statistical significance was used. For two group comparisons, an unpaired Student two-tailed t-test was used. To account for natural variation of GSIS from human micro-islets, one-way ANOVA with donor as random effect followed by Tukey's post hoc analysis was used. This analysis was performed in R. Significant outliers were detected by a Grubbs test ($\alpha < 0.05$) and subsequently excluded from statistical testing and figure drawing. $P < 0.05$ was considered statistically significant. All data are mean ± SEM unless otherwise noted.

3.4 Plasma proteome profiling

3.4.1 Sample preparation

At study end blood was collected from mice after a 4h-fast and at least 16h after the last vehicle or compound injection in EDTA containing Eppendorf tubes. Plasma preparation, subsequent measurement with high pressure liquid chromatography and MS, and analysis of mass spectrometric raw files was done as reported previously (Geyer et al., 2016a; Niu et al., 2019). Sample preparation and MS-analysis was performed together with Lili Niu from the Novo Nordisk Foundation Center for Protein Research, Faculty of Health Sciences, University of Copenhagen, in Copenhagen, Denmark.

3.4.2 Biostatistical analysis

We excluded proteins with <30% data completeness in at least one experimental group. Missing values of the remaining 591 proteins were replaced by drawing random samples. Protein matrix preparation was performed together with Lili Niu from the Novo Nordisk Foundation Center for Protein Research, Faculty of Health Sciences, University of Copenhagen, in Copenhagen, Denmark using the Perseus platform (Tyanova et al., 2016). We removed 28 identified peptides as there was no known annotated gene name. Hence, we used a protein matrix of 563 proteins, which were identified in male and female DIO mice for further downstream analyses. Protein signal intensities were log2-transformed. Limma (Ritchie et al., 2015) with voom (Liu et al., 2015) for linear modelling was used to identify differentially regulated proteins between treatment groups. A P-value cutoff of $P < 0.01$ was used for downstream analyses unless otherwise noted. Molecular function and pathway allocations of differentially regulated proteins were identified using Enrichr (Chen et al., 2013; Kuleshov et

al., 2016) and manual search. Differentially regulated proteins were identified with R scripts. Plasma contamination biases in group comparisons were assessed according to a recently published guideline (Geyer et al., 2019). Specifically, Geyer et al. defined three panels of about 30 proteins each to identify plasma contamination derived from erythrocyte, platelet, or coagulation proteins (Geyer et al., 2019). Here, we tested whether differentially regulated proteins between treatment groups belong to one of these contamination panels to verify the likelihood of novel biomarkers to be contamination artifacts.

3.5 Analysis of scRNA-seq data

3.5.1 Preprocessing of droplet-based scRNA-seq data

The CellRanger analysis pipeline (Version 2.0.0) provided by 10X Genomics was used for demultiplexing of raw base call (BCL) files, alignment, read filtering, barcode and UMI counting. The overall distribution of total UMI counts per cell was used to select high quality barcodes using the standard CellRanger cell detection algorithm. All further analyses were done with python3 using the scanpy package (Wolf et al., 2018) (v1.0.4+92.g9a754bb, https://github.com/theislab/scanpy) except noted otherwise.

Genes which were expressed in less than 10 cells were excluded. As suggested by scanpy tutorials, cells with poor quality or outlier cells were removed if cells (i) had a high fraction of counts from mitochondrial genes (>=40%), (ii) expressed more than 7000 genes, or (iii) had more than 100000 UMI counts. Cell by gene count matrices of all samples were linked to a single matrix. To account for variances in sequencing depth, UMI counts of each cell were normalized to total cell counts (pp.normalize_per_cell with mean=TRUE). Values were log-transformed. 1625 highly variable genes were selected based on normalized dispersion (cutoff lower mean =0.0125 and dispersion=0.5). This matrix was used for all downstream analyses unless noted differently.

3.5.2 Embedding, clustering and cell type annotation

To reduce systematic biases (e.g. batch effects), cell clustering was performed on the full data set (Büttner et al., 2019). Therefore, a single cell neighborhood graph (kNN-graph) was computed based on the 50 first principal components (PCA) using 15 neighbors. To facilitate clustering while minimizing condition effects, the kNN-graph was recomputed by integrating the first 15 diffusion components of the PCA-based graph (Wolf et al., 2019). Cell type clustering and annotation was done with louvain-based clustering (Blondel et al., 2008) as implemented in louvain-igraph (v0.6.1 https://github.com/vtraag/louvain-igraph) and adopted by scanpy (tl.louvain). Due to strong changes in resolution, the resolution parameter was adjusted in different parts of the data manifold. Endocrine cells were annotated based on the mRNA expression of the four main hormones *Ins1*/*Ins2*, *Gcg*, *Sst*, and *Ppy*.

Non-endocrine cells such as stellate cells (expressing *Col1a2*), endothelial cells (expressing *Plvap*), ductal cells (expressing *Krt19*), acinar cells (expressing *Prss2*), and cells that

expressed endocrine and non-endocrine markers (potential doublet cells) were removed from further analyses. Ambient mRNA results from lysed cells that is incorporated into all droplets. Such free-floating mRNA can be found as background expression in all cells. For cell type annotations, high expression of *Ins1*/*Ins2*, *Gcg*, *Sst*, and *Ppy* that was above background levels, such in non-endocrine cells, was considered as ambient mRNA contamination.
To identify β-cell sub-states, we included insulin mono-hormonal and the closely connected Ins-PP bi-hormonal cells. We calculated a new kNN-graph based on the first 50 principal components, which was put into louvain-based clustering. Similarly, recalculating the kNN-graph on the first 50 principal components revealed an Ins-Sst cell sub-cluster, which was distinct from Ins-Sst-PP expressing cells. Ins-Gcg-Sst triple positive cells were annotated using a manual threshold for all three hormones, which was well above ambient mRNA levels. For visualization, Uniform Manifold Approximation and Projection (UMAP) (Becht et al., 2018) was used and newly calculated by recomputing the kNN-graph for each UMAP-plot using the first 50 principal components.

3.5.3 Identification of polyhormonal singlets and doublet-like endocrine cell clusters

The existence of single cells expressing more than one hormone (polyhormonal cell) in pancreatic islets have been reported before (Alpert et al., 1988; Chiang and Melton, 2003; Katsuta et al., 2010). However, in scRNA-seq analysis the presence of cells expressing multiple hormones may also be an indicator for doublets, which result when multiple hormones are expressed within the same droplet. Previous studies using the 10X technology reported a doublet rate of ~8-10% (Zheng et al., 2017). Thus, it can be difficult to discriminate between polyhormonal singlets and doublets. Polyhormonal and monohormonal doublets describe the inclusion of two different or the same cell type, respectively. Monohormonal doublets do not affect downstream analyses as they reassemble monohormonal singlets (Wolock et al., 2019). By assuming that doublets are generated by randomly sampling singlet cells and taking the frequency of monohormonal cells that potentially contribute to a doublet, we calculated the expected doublet frequency of polyhormonal doublets for a doublet rate of 10% (Wolock et al., 2019). The proportion of observed polyhormonal cells clearly exceeded the expected polyhormonal doublet frequency in every sample. Also, doublet cell detection tools such as Scrublet (Wolock et al., 2019) (v0.1, https://github.com/AllonKleinLab/scrublet) and DoubletDetection (https://github.com/JonathanShor/DoubletDetection) could not clearly distinguish doublets from polyhormonal singlets. Both tools disagreed and consistently overestimated doublets and thus it is unlikely that all detected polyhormonal cells in this study are doublets. Hence, we used the following criteria to find polyhormonal doublets: (i) Doublets should not express unique genes. At least one doublet contributor should express all genes. (ii) Doublets should express lineage-determining transcription factors and marker genes of the doublet contributors. Downregulation of these genes may indicate singlets. (iii) Reported polyhormonal singlet cells in literature. (iv) If the frequency of a polyhormonal cell cluster exceeds the doublet simulation, this indicate polyhormonal singlet clusters. (v) Clusters with a

Scrublet doublet score distribution that is comparable to monohormonal singlet clusters indicate polyhormonal singlets.
Accordingly, Ins-PP, Ins-Sst-PP, Gcg-PP (low) and Gcg-PP (high) cells could be true polyhormonal singlets. Cells expressing Ins-PP-Gcg, Ins-Gcg, Ins-Gcg-Sst, Gcg-Sst-PP and Sst-PP (high) were likely doublets.

3.5.4 Cell cycle classification

A set S and G2/M phase genes (Kowalczyk et al., 2015; Tirosh et al., 2016) was used to assign a specific score for each cell (Satija et al., 2015) and implemented in scanpy (tl.score_genes_cell_cycle). Cells with a S-score or a G2/M-score > 0.25 were classified as cycling (Sachs et al. 2020a).

3.5.5 Marker genes of main endocrine cell types

To identify specific marker genes for the four main endocrine cell types, each of the endocrine cell type was compared to the three other endocrine cell types. This was done by an implemented test in scanpy (tl.rank_genes_groups). A gene that ranked within the top 300 genes, had a test score >8, and was unique for one of the endocrine cell types was defined as marker gene (Sachs et al. 2020a).

3.5.6 Differential expression testing to describe subpopulations and treatment responses

Gene expression data was quantile-normalized (quantile threshold=0.95) and log-transformed to account for extremely high expressed genes. Using quantile normalization, highly expressed genes were not used for normalization as this can wrongly alleviate the expression of other genes. As previously recommended (Soneson and Robinson, 2018), differentially regulated genes between cell types were determined by a limma-trend (Law et al., 2014; Ritchie et al., 2015) using the Bioconductor package limma (v3.28.10) via rpy2 (v2.9.1). Genes expressed in >1% of cells in any of two cell subsets were considered for differential expression testing. Genes with a FDR < 0.01 and an estimated logFC (output from limma model not the actual logFC as log-transformed data was the input) > 0.25 | < -0.25 were used for gene and pathway enrichment analyses in EnrichR (Kuleshov et al., 2016) via its web interface. As the background expression (free-floating mRNA) of main endocrine hormones (*Ins1*/*Ins2*, *Gcg*, *Sst*, and *Ppy*) as well as other marker genes (*Pyy*, *Iapp*, *Ttr*, *Gpx3*, *Ctrb1*, *Try5*) was differentially regulated between cells, these genes were excluded from figure drawing.

3.5.6 Identification of specific β-cell dedifferentiation markers

In order to identify marker genes of β-cell dedifferentiation we took genes that were upregulated in mSTZ β-cells compared to healthy β-cells (FDR < 0.05, estimated logFC > 0.25). Furthermore, genes that were differentially expressed in other endocrine cells were

excluded. Lastly, β-cell dedifferentiation markers must be expressed in > 25% of mSTZ β-cells and in < 5% of healthy β-cells. The location of identified genes was extracted from the GeneCards database (https://www.genecards.org).

3.5.7 Inference of β-cell maturation, dedifferentiation and regeneration trajectories

A pseudotime for mature β-cells in health state and dedifferentiated β-cells in mSTZ diabetes was calculated using diffusion pseudotime (dpt) (Haghverdi et al., 2016) as implemented in scanpy (tl.dpt). Therefore, a randomly selected cell within the starting cell population was defined as root cell. Dpt as a cell-to-cell distance metric across samples was used, to estimate the location of β-cells from compound treated mice along the path from dedifferentiated to healthy β-cells. β-cell subpopulations and cycling cells were excluded from visualization as they had very high pseudotime values and were not part of the linear trajectory.

3.5.8 Inference of cluster-to-cluster distances, lineage relations and cell movement

Cluster and lineage relations were inferred by partition-based graph abstraction (PAGA, Wolf et al., 2019) using the tl.paga function (scanpy, edge significance of 0.05). In PAGA, lines indicate cluster connections or relations suggesting potential routes of cell transitions. Edge weights symbolize confidence of connections (Wolf et al., 2019).

RNA velocity was used to infer direction of possible transitions (La Manno et al., 2018) using a stochastic version implemented in the scVelo python package (v0.1.16.dev13+c1a6dad). Splicing information was extracted using velocyto (v0.17.7, http://velocyto.org) and used in the scVelo pipeline, which estimates RNA velocities and RNA velocity force fields. For this specific study, we used the workflow described in Sachs et al. (Sachs et al., 2020). First, for data preprocessing genes with less than 30 spliced or 30 unspliced counts were excluded. Spliced and unspliced counts were normalized by total counts. These genes were used to calculate the first- and second order-moments across its 15 nearest neighbors of the kNN graph in PC space (50 PCs). RNA velocities were estimated using a stochastic model of transcriptional dynamics (95% quantile fit). All potential cell transitions on the kNN graph were combined to predict a mean direction. This direction was then projected into the UMAP embedding as a velocity vector. Each potential cell transition is assigned a certain probability derived from a velocity vector. A high probability corresponds to a high correlation with the velocity vector. This projection results in a low dimensional map of RNA velocity, which indicates predicted cell state transitions (La Manno et al., 2018). Genes with a r2 > 0.1 of the velocity fit were considered for computation of the velocity graph and embedding (Sachs et al. 2020a).

The different treatments and cell from diabetic mice were used to calculate the velocities of each gene. For healthy β-cells only the healthy cells were used. We assumed that a treatment can be considered as a state where cells move from diseased cells towards healthy cells (Sachs et al. 2020a) as described for pseudotime inference. During this movement a gene can be induced and/or inhibited. To account for these intermediate gene states, all treatments were included for model fitting and velocity estimation and both PAGA and the RNA velocity

graphand projection were then computed on the represented cell subset. Therefore, the kNN-graph was recalculated for this cell subset using the first 50 principal components and the initially defined highly variable genes.
ScRNA-seq data analysis was performed by Sophie Tritschler from the Institute of Computational Biology, Helmholtz Zentrum München, 85764 Neuherberg, Germany. Data interpretation and integration was done together with Sophie Tritschler from the Institute of Computational Biology, Helmholtz Zentrum München, 85764 Neuherberg, Germany.

3.6 Contributions from Collaborations

Science has become increasingly interdisciplinary. Global collaborations contribute to scientific discoveries that would not have been achieved without the expertise and usage of cutting-edge technologies from numerous institutions. Hence, parts of the data presented in this thesis are the result of close collaborations and they have to rightfully be acknowledged. If not stated otherwise, experiments and analyses was conducted by myself (S. J. Sachs).

(1) Targeted pharmacological therapy restores β-cell function for diabetes remission.
- ScRNA-seq data analysis was performed by Sophie Tritschler (PhD student Institute of Computational Biology, Helmholtz Zentrum München).
- Automated histological analysis was performed in close collaboration with Dr. Annette Feuchtinger (Research Unit Analytical Pathology at the Helmholtz Zentrum München).
- Compound studies on human micro-islets were performed in collaboration with Dr. Burcak Yesildag (InsPhero, Zürich, Switzerland).

(2) Shared benefits of GLP-1/GIP dual-agonism in mice and bariatric surgery in humans
- MS-analysis for PPP was performed by Lili Niu (University of Copenhagen, Copenhagen, Denmark).
- Automated histological analysis was performed in close collaboration with Dr. Annette Feuchtinger (Research Unit Analytical Pathology at the Helmholtz Zentrum München).

4. Results

Part I

4.1 Targeted pharmacological therapy restores β-cell function for diabetes remission

If and how functional β-cells can be pharmacologically regenerated for diabetes treatment is still unclear. Therefore, it is of utmost importance to better understand β-cell failure in diabetes in order to find mechanisms and entry points for β-cell regeneration. In this thesis, multiple single- and polypharmacological approaches were tested to increase functional β-cell mass in the mSTZ mouse model of diabetes.

4.1.1 Paths and mechanisms of β-cell dedifferentiation on single cell level

First, we performed a scRNA-seq survey of healthy and diabetic islets after 100 days of persistent hyperglycemia to get insights into transcriptional changes of endocrine cells after STZ-induced beta cell killing. We used the mSTZ treatment (50 mg/kg on five consecutive days; Figure 5a) to generate hyperglycemic mice. Systematic blood glucose measurements over 100 days showed a severe but viable, overt diabetes (300-450 mg/dl; Figure 5b) accompanied by reduced fasting insulin (Figure 5c) and C-peptide levels (Figure 5d) as well as an almost complete loss of islet architecture due to β-cell ablation (Figure 5e).

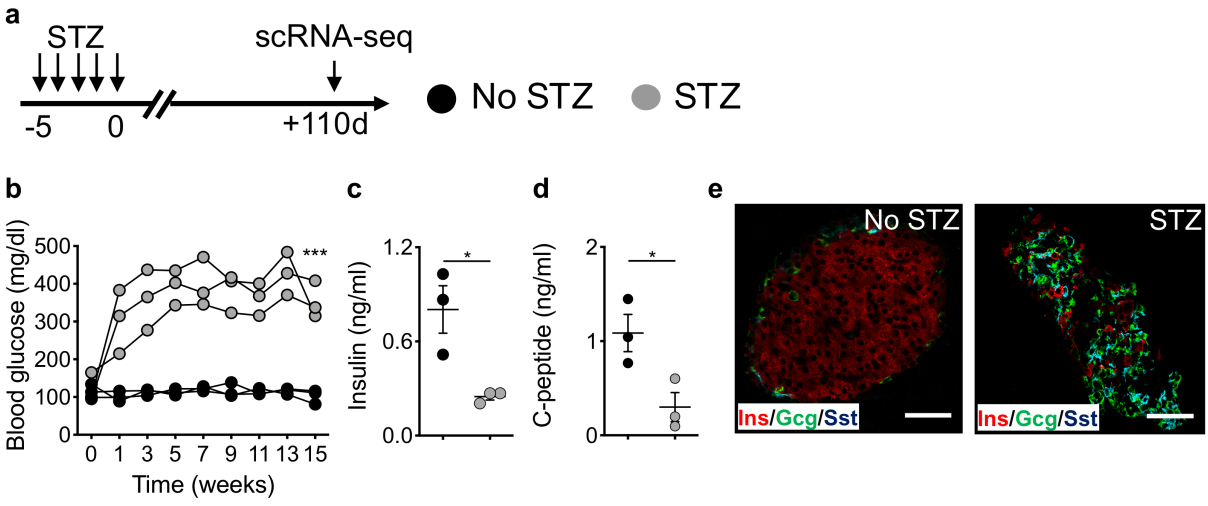

Figure 5: Viable hyperglycemia in the mSTZ-mouse model.

(a) Scheme of mSTZ treatment (mSTZ; 50 mg/kg on five consecutive days), islet isolation, and scRNA-seq. Effect of mSTZ treatment on **(b)** fasting blood glucose, **(c)** fasting insulin, and **(d)** fasting C-peptide levels of mice used for scRNA-seq analysis (n = 3 for healthy and mSTZ treated mice). Data are mean ± SEM. *P < 0.05, ***P < 0.001 determined by Student's two tailed t-test. **(e)** Immunohistochemical analysis in the end of the study indicates disrupted islet architecture in mSTZ-treated mice compared to vehicle treated mice.

β-cell heterogeneity in healthy islets

To understand endocrine cell type composition and heterogeneity in islet homeostasis, we first analyzed single cell expression profiles of healthy islets. Unbiased graph-based clustering revealed the four main endocrine subtypes: α-, β-, δ-, and PP-cells (Figures 6a, b). Endocrine cells were annotated based on predominant endocrine hormone expression of glucagon (*Gcg*), insulin (*Ins*), somatostatin (*Sst*), and pancreatic polypeptide (*PP*) (Figures 6a, b). Refined clustering focused on insulin-positive cells identified two main β-cell subpopulations: β1 and β2 (Figure 6c). Single cell trajectory inference (Haghverdi et al., 2016; Tritschler et al., 2019) revealed a continuum of transcriptional states of β1- and β2-cells (Figure 6d). This suggests a continuous transition between β1- and β2-cells rather than discrete and final β-cell phenotypes. β-cell maturity markers (e.g. *Ins1*, *Ins2*, *Ucn3* (Blum et al., 2012)) and genes of the secretion machinery (e.g. *G6pc2*, *Sytl4*, and *Slc2a2 (Glut2)*) were progressively decreased, while β-cell immaturity (e.g. *Mafb* (Nishimura et al., 2006)) as well as pan-endocrine lineage markers (e.g. *Chga* and *Chgb*) were concomitantly increased along cell trajectory inference from β1- to β2-cells (Figure 6d). β-cell identity TFs (e.g. *Pdx1*, *Nkx6.1*, and *NeuroD1*) were unaffected (Figure 6d). Gene enrichment analyses revealed that metabolic processes such as insulin secretion, oxidative phosphorylation, and cell-cycle inhibition were down- and cAMP and WNT signaling were upregulated in β2-cells (Figure 6e). Expression of cell cycle-associated genes, such as e.g. *Ki67* and *Cdk1*, was higher in immature β2-cells and accordingly, 16/403 of the β2-cells, while only 2/5319 of the mature β1-cells were classified as cycling (Figure 6f). In addition, we found subpopulations of cells expressing more than one hormone (polyhormonal cells), which could be distinguished from doublets and ambient RNA contamination - common problems of scRNA-seq (Figures 6g, h).

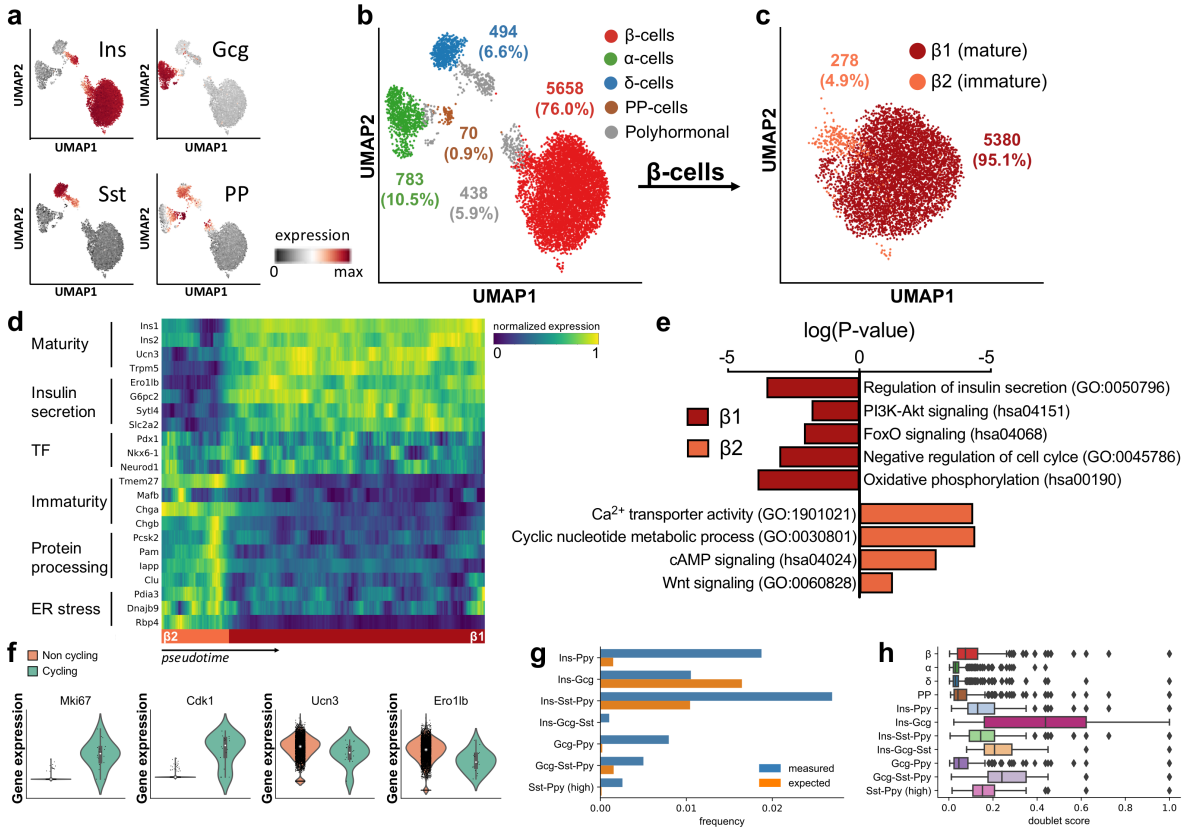

Figure 6: β-cell heterogeneity in healthy mice.

(a) *Ins*, *Gcg*, *Sst*, and *PP* expression depicted in a UMAP of healthy endocrine cells. **(b)** All endocrine cells (7578 cells) in a UMAP with total numbers and relative proportions. **(c)** The two main β-cell subpopulations identified within the insulin expressing cells. **(d)** Selected pathways and gene expression along the inferred pseudotime in which the overrepresented β1-cells were downsampled to 1000 cells. This was done for better visualization of gene expression changes. **(e)** Genes that were up- and downregulated in β2-cells compared to β1-cells were used for gene ontology and KEGG pathway enrichment analyses. The cutoff for regulated gene ontologies and KEGG pathways was log fold change>0.25 for upregulation and log fold change<-0.25 for downregulation. **(f)** The gene expression of the proliferation markers *Mki67* and *Cdk1* as well as the expression of the β-cell maturation genes *Ucn3* and *Erol1b* suggest an immature phenotype of cycling β-cells. **(g)** The expected and measured doublet frequencies of cells clusters that were classified as polyhormonal. **(h)** Doublet score distribution of mono- and polyhormonal cells. A high score implies a high doublet probability. ScRNA-seq analysis and data interpretation in collaboration with Sophie Tritschler from the Institute of Computational Biology, Helmholtz Zentrum München. Figures 6a-h with permission from Sachs et al. 2020a.

β-cell dedifferentiation on the single cell level

Next, we analyzed diabetic islets after 100 days of persistent hyperglycemia. Endocrine subtype composition and cell-intrinsic gene expression profiles were altered in mSTZ mice compared to healthy mice with a predominant effect on β-cells (Figures 7a, b). Specifically, there was a 3-fold decrease of the proportion of β-cells in mSTZ-diabetic mice and mSTZ β-cells formed a distinct cluster separated from healthy β-cells (Figure 7a). This suggests substantial changes in molecular programs, islet cell identity, and islet composition under long-standing hyperglycemia and hypoinsulinemia in mSTZ-diabetic mice. Compared to β-cells,

only very few genes were differentially regulated in other endocrine cells in mSTZ-diabetic compared to healthy mice (Figures 7b-e).

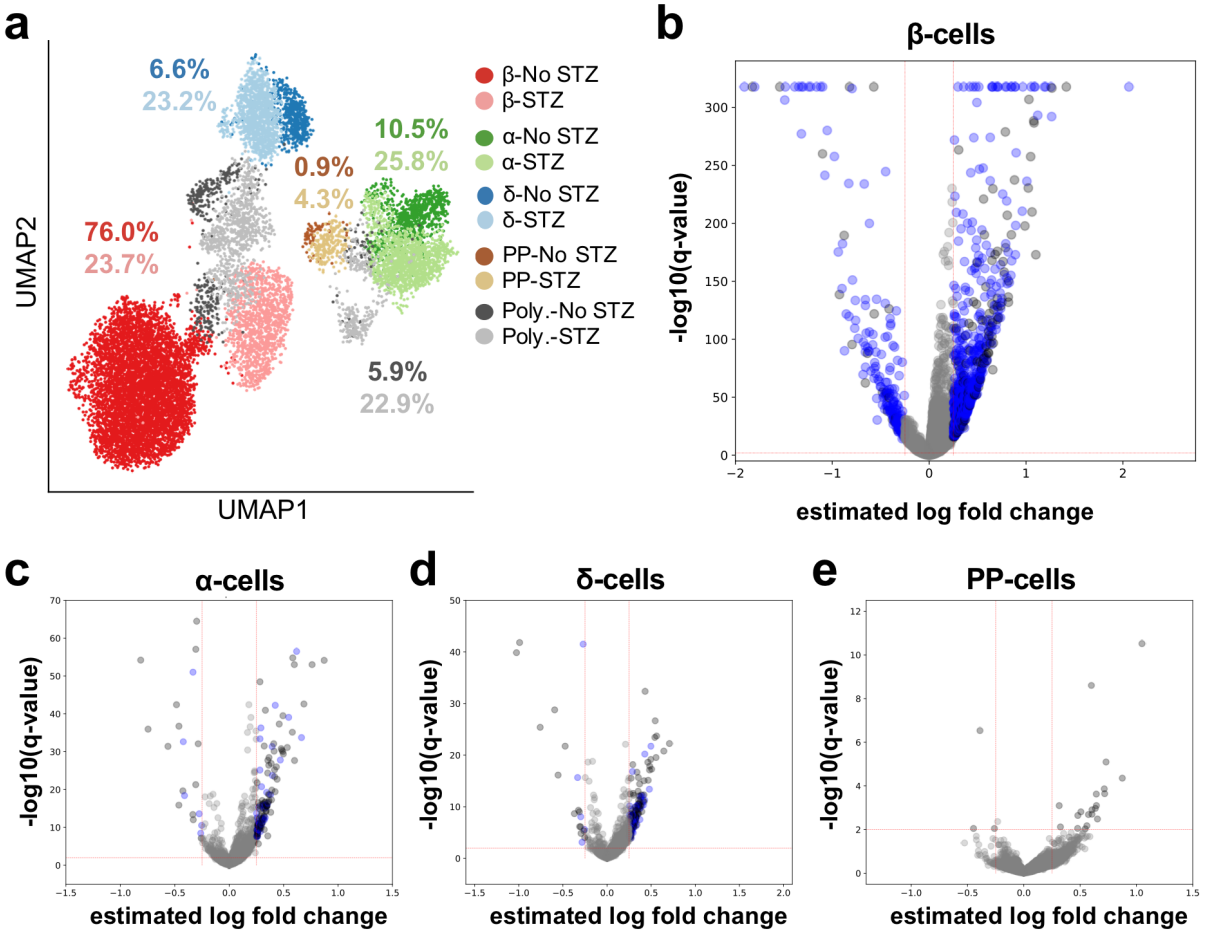

Figure 7: Altered endocrine subtype populations in mSTZ diabetes.

(a) 12430 endocrine cells from healthy and mSTZ-treated mice depicted in a UMAP. Percentage of each cell cluster in each condition is indicated. Differential expressed genes and its significance (-log10(adjusted p-Value), limma) of **(b)** β-cells, **(c)** α-cells, **(d)** δ-cells, **(e)** PP-cells between healthy and mSTZ-diabetic mice depicted in volcano plots in which the red lines show the thresholds that were used for significance and gene expression changes. Significantly regulated genes are highlighted in black. Genes significantly regulated in only one cell are highlighted in blue. ScRNA-seq analysis and data interpretation in collaboration with Sophie Tritschler from the Institute of Computational Biology, Helmholtz Zentrum München. Figures 7a-e with permission from Sachs et al. 2020a.

Pseudotemporal ordering of healthy and mSTZ-treated β-cells revealed transitions and gradual gene expression changes from mature to immature to mSTZ-derived β-cells (Figure 8a). Again, this suggested continuous conversions between β1-, β2-, and mSTZ β-cells rather than discrete β-cell phenotypes. Remaining mSTZ β-cells expressed low mRNA levels of β-cell maturity and functionality markers, e.g. *Ins1* and/or *Ins2*, *Ucn3* and *Slc2a2* (*Glut2*) (Figure 8a). Reduced protein expression of Ucn3 confirmed β-cell immaturity in mSTZ-diabetic mice (Figure 8c). β-cell identity TFs, such as *Nkx6.1*, *NeuroD1, Nkx2.2*, *Pdx1*, *Pax6*, *and Isl1* were

progressively downregulated from mature to diabetic β-cells (Figure 8a). Accordingly, downregulated genes in mSTZ β-cells were enriched in pathways associated with β-cell maturity and functionality (Figure 8b). Upregulated genes in remaining mSTZ β-cells are involved in ontologies related to endoplasmic reticulum (ER) stress and oxidative phosphorylation (Figure 8b).

In genetic mouse models, β-cell dedifferentiation was associated with an upregulation of TFs associated with pancreatic and endocrine progenitors (Rui et al., 2017; Talchai et al., 2012; Wang et al., 2014). Expression of *Sox9* and *Ngn3* (endocrine progenitor markers), or the pluripotency gene *Oct3/4* (*Pou5f1*) were unchanged in mSTZ-treated β-cells (Figure 8d). However, we found a gradually increased expression of the recently described β-cell dedifferentiation markers *Aldh1a3* and *Gastrin* (Cinti et al., 2016; Dahan et al., 2017; Kim-Muller et al., 2016) on the transcript and protein level (Figures 8a, e).

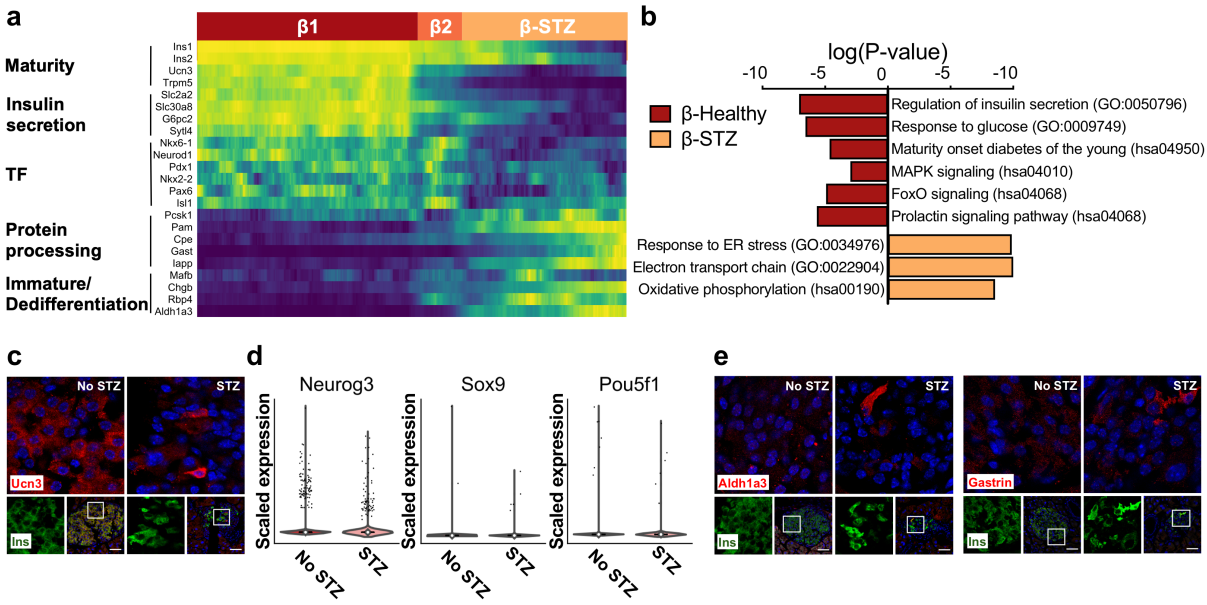

Figure 8: β-cell dedifferentiation on the single cell level.

(a) β-cell identity, maturation, and functionality genes along the inferred trajectory. As there were more healthy β-cells, β1-cells were downsampled (1500 cells). This enables a better visualization of gene expression changes. **(b)** Genes that were up- and downregulated in mSTZ β-cells compared to healthy β-cells were used for gene ontology and KEGG pathway enrichment analyses. The cutoff for regulated gene ontologies and KEGG pathways was log fold change>0.25 for upregulation and log fold change<-0.25 for downregulation. Selected ontologies and pathways are depicted. **(c)** Ucn3 immunohistochemistry at study end. **(d)** Expression of endocrine developmental genes in mSTZ-diabetic and healthy β-cells. **(e)** Aldh1a3 and Gastrin immunohistochemistry at study end. All scale bars, 50 µm. ScRNA-seq analysis and data interpretation in collaboration with Sophie Tritschler from the Institute of Computational Biology, Helmholtz Zentrum München. Figures 8a-e with permission from Sachs et al. 2020a.

In the absence of genetic lesions, our scRNA-seq analysis allowed the identification of genes that are usually not expressed or only subtly expressed in mature, functional murine β-cells, but are upregulated in remaining mSTZ β-cells (Figure 9a). Immunohistochemistry of e.g. Cck

and Slc5a10 confirmed increased protein expression in mSTZ-diabetic mice (Figure 9b). Some of the identified targets were also identified in pancreata and β-cells of human T1D and T2D (Camunas-Soler et al., 2019; Solimena et al., 2018) (Figures 9c, d). These results suggest that remaining β-cells of the mSTZ model are dedifferentiated after long-term hyperglycemia. This makes mSTZ a good diabetes model to study β-cell de- and redifferentiation in the absence of genetic lesions.

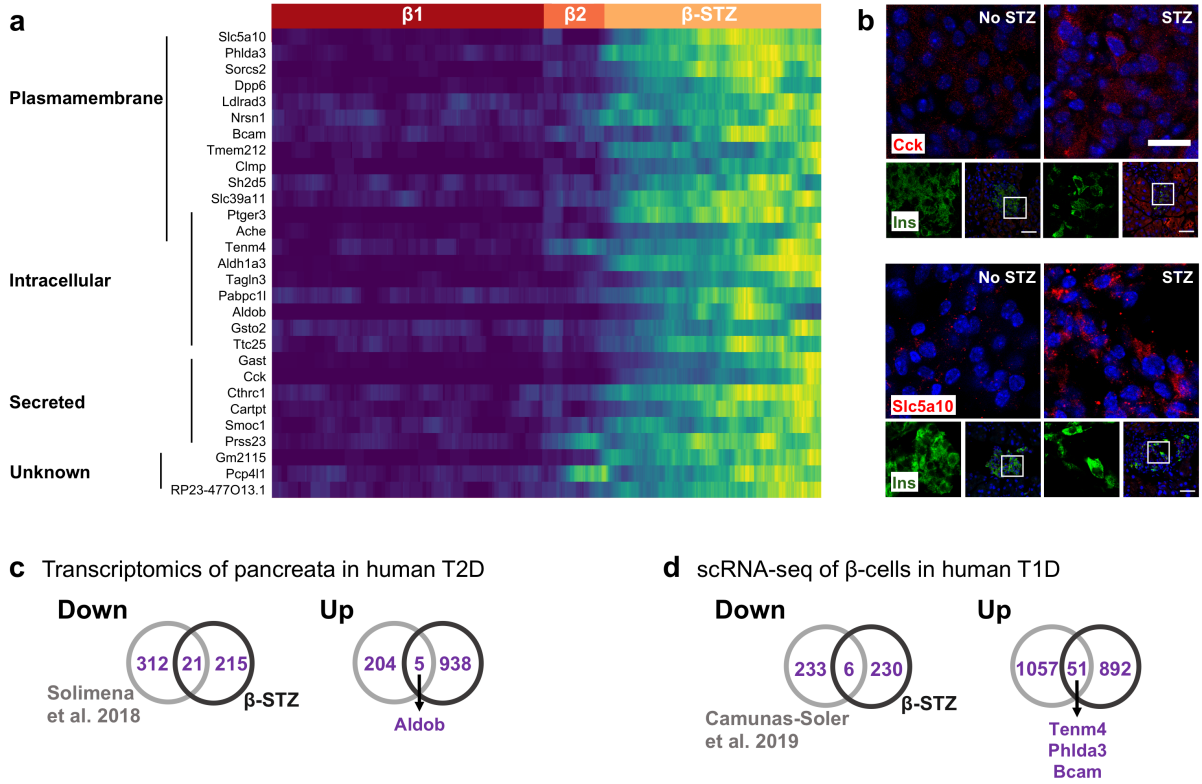

Figure 9: Potential markers of dedifferentiated β-cells.

(a) Gene expression along the trajectory from β1 to β-STZ of specifically increased genes in β-cells from mSTZ treated mice (expression in <5% of no STZ β-cells and >25% of mSTZ β-cells, 29 genes in total) with their cellular location. **(b)** Cck and Slc5a10 immunohistochemistry at study end. All scale bars, 50 µm. Dysregulated genes in mSTZ β-cells and **(c)** human T2D pancreata (RNA-seq) and **(d)** human T1D β-cells (scRNA-seq). Overlapping gene names to **(a)** are indicated. ScRNA-seq analysis and data interpretation in collaboration with Sophie Tritschler from the Institute of Computational Biology, Helmholtz Zentrum München. Figures 9a-d with permission from Sachs et al. 2020a.

4.1.2 β-cell regeneration in mSTZ-diabetic mice

β-cell dysfunction at treatment start

We used the mSTZ model to examine the effects of drug treatment to regenerate functional β-cells. Ten days after the last STZ injection, mSTZ-treated mice were hyperglycemic (Figure 10a) and showed a significant reduction in β-cell function (Figures 10b, c) along with a decrease in insulin area (Figure 10d). β-cell proliferation was unchanged in mSTZ-treated mice (Figure 10e), whereas we detected a significant increase in β-cell apoptosis (Figure 10f). mSTZ-treated mice exhibited severe impairment in islet integrity and composition with a

significant increase in non-β-cells (Figure 10g). Protein levels of β-cell maturation markers including Ucn3 (Figure 10h), Glut2 (Figure 10i), Nkx6.1 (Figure 10j), and the GLP-1R (Figure 10k) were reduced. This indicates loss of identity and function of remaining β-cells. Hence, compound treatment was initiated at this time point when mSTZ-treated mice were diabetic, but still contained a substantial proportion of insulin positive cells.

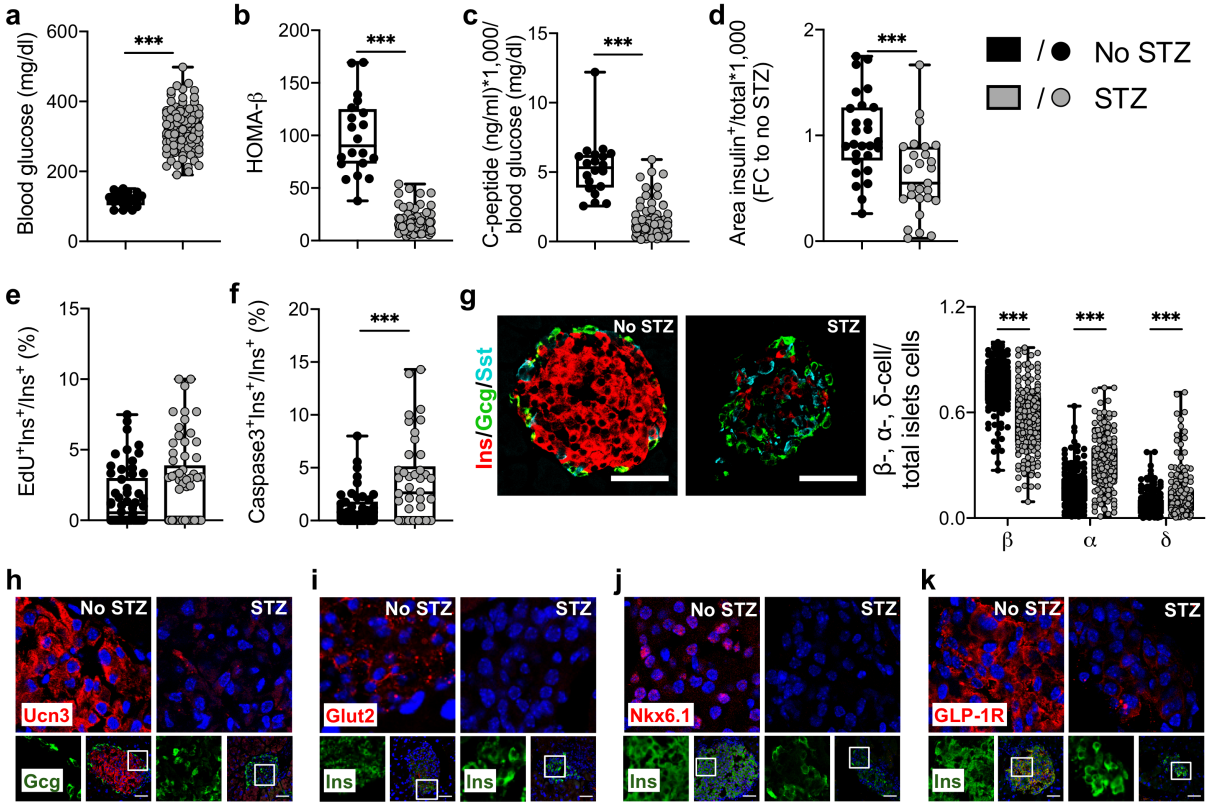

Figure 10: Remaining β-cells lose cell identity 10 days after last STZ injection.

(a) Fasting blood glucose (No STZ: n= 20, STZ: n=107; ***P<0.001, unpaired two-sided t-test), **(b)** the homeostatic model assessment of β-cell function (HOMA-β) (No STZ: n= 20, STZ: n=107; ***P<0.001, unpaired two-sided t-test), **(c)** the ratio of fasting C-peptide to fasting blood glucose (No STZ: n= 20, STZ: n=106; ***P<0.001, unpaired two-sided t-test), **(d)** the insulin positive area within pancreatic sections (No STZ: 27 sections of n=3 mice; STZ: 27, n=3; ***P<0.001, unpaired two-sided t- test), **(e)** the proliferation (No STZ: 58 islets of n=3 mice; STZ: 69, n=3; ***P<0.001, unpaired two-sided t-test t=1.707, df=125) and **(f)** apoptosis rate of β-cells (No STZ: 46 islets of n=3 mice; STZ: 42, n=3; ***P<0.001, unpaired two-sided t-test), **(g)** pancreatic islets histology (No STZ: 179 islets of n=3 mice, STZ: 182, n=3; ***P<0.001, unpaired two-sided t-test) as well as the expression of β-cell marker Ucn3 **(h),** Glut2 **(i)**, Nkx6.1 **(J)**, and GLP-1R **(K)** ten days after vehicle or mSTZ injections. Boxplots covering all data points are presented. All figures scale bar, 50 µm. Figures 10a-i with permission from Sachs et al. 2020a.

Insulin and GLP-1/estrogen regenerate functional β-cell mass in mSTZ-diabetic mice

After disease onset, mSTZ-diabetic mice were treated daily with subcutaneous injections for 100 days (Figure 11a). Vehicle treated mSTZ-diabetic mice remained hyperglycemic over the course of study (Figures 11b-e). We used a pegylated insulin analog (PEG-insulin, once daily) to correct the insulin deficiency in mSTZ-diabetic mice. Insulin treatment normalized blood

glucose (Figure 11b), progressively increased fasting C-peptide levels (Figure 11c), improved islet structure (Figure 11d), and increased the number of insulin positive cells within pancreatic sections (Figure 11e). Shortcomings like increased risk of hypoglycemia, unintended weight gain (especially in T2D), and the development or existence of insulin autoantibodies limit the broader use of insulin also as a preventive drug in human T1D and T2D. This underlines the need of novel pharmacological approaches to ameliorate hyperglycemia and improve β-cell function.

Due to insulinotropic and β-cell protective effects, GLP-1 and estrogen have been repeatedly implicated in the treatment of diabetes (Drucker, 2018; Tiano and Mauvais-Jarvis, 2012). In this study, neither estrogen nor GLP-1 treatment improved mSTZ-diabetes (Figures 11b-e). Treatment with a novel GLP-1/estrogen conjugate has shown synergistic metabolic effects through specific targeting and delivery of estrogen into GLP-1R positive cells (Finan et al., 2012). In line with these data, chronic GLP-1/estrogen conjugate treatment more efficiently reduced hyperglycemia (Figure 11b), increased fasting C-peptide levels (Figure 11c), and increased the number of insulin positive cells within pancreatic sections in mSTZ-diabetic mice (Figures 11d, e).

Moreover, we tested a triple pharmacological approach of insulin and GLP-1/estrogen co-treatment in order to enhance the efficacy of both compounds while reducing the insulin dose, which can theoretically reduce unintended weight gain and the risk of hypoglycemia. The co-therapy normalized glycemia (Figure 11b) and increased fasting C-peptide levels (Figure 11c) in mSTZ-diabetic mice. Although the co-injection of PEG-insulin and GLP-1/estrogen did not differentiate from their individual treatment arms regarding glycemic parameters (Figures 11b, c), we noticed an additional effect of the co-treatment in regard to insulin area, suggesting a superior effect of the co-treatment on β-cell mass regeneration compared to the insulin monotreatment (Figures 11d, e).

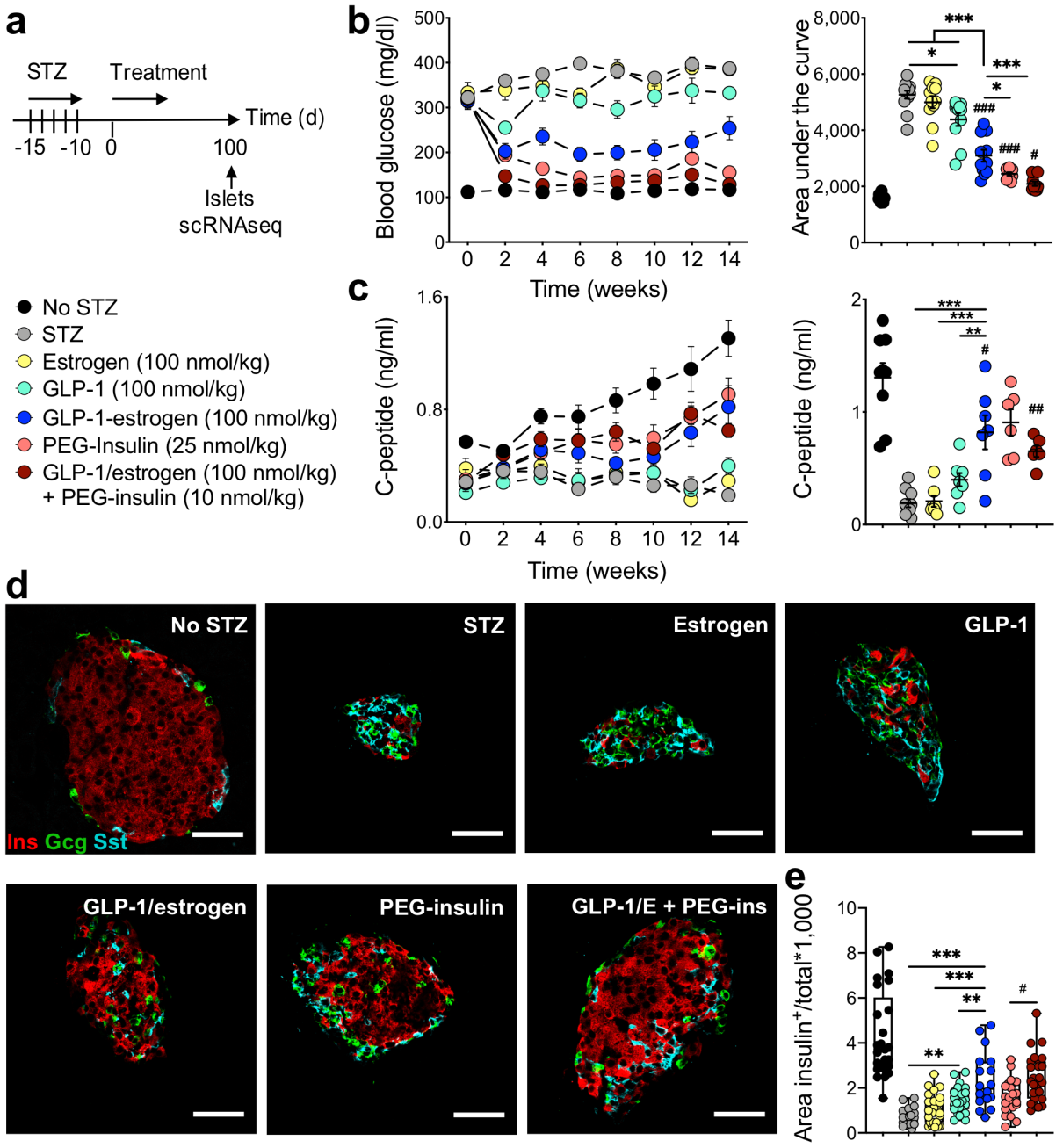

Figure 11: GLP-1/estrogen and PEG-insulin recover functional β-cells in mSTZ-diabetes.

(a) 8-week old C57Bl6/J mice were treated with daily subcutaneous injections of either vehicle (n=12, no STZ), vehicle (n=13, STZ), a GLP-1 analog (n=11), estrogen (n=11), the GLP-1/estrogen conjugate (n=11), PEG-insulin (n=9), or GLP-1/estrogen and PEG-insulin (n=10) ten days after the last STZ injection at the indicated doses for 100 days. Effects on fasting **(b)** blood glucose and **(c)** C-peptide levels of treated mice. Data are mean ± SEM. *P < 0.05, **P < 0.01, ***P < 0.001, among STZ, estrogen, GLP-1 and GLP-1/estrogen treated mice (one-way ANOVA with Tukey post-hoc test). *P < 0.05, **P < 0.01, ***P < 0.001 to compound injections; $^{\#}$P < 0.01, $^{\#\#\#}$P < 0.001 to no STZ mice, comparing no STZ, GLP-1/estrogen, PEG-insulin, and co-treated mice (one-way ANOVA and Tukey post-hoc). **(d)** Immunostaining for insulin, glucagon, and somatostatin of pancreatic sections shows effects on islet architecture after 100 days of treatment. **(e)** Quantitative comparison of total insulin area in pancreatic sections (No STZ; 25 sections of n=3 mice), vehicle (STZ; 21, n=3 mice), estrogen (27, n=3 mice), GLP-1 (26, n=3 mice), GLP-1/estrogen (18, n=2 mice), PEG-insulin (24, n=3 mice), or GLP-1/estrogen and PEG-insulin co-therapy (27, n=3 mice). **P < 0.01, ***P < 0.001, among STZ, estrogen, GLP-1 and

GLP-1/estrogen treated mice (one-way ANOVA with Tukey post-hoc test). #P < 0.05, among GLP-1/estrogen, PEG-insulin, and co-treated mice (one-way ANOVA with Tukey post-hoc). Figures 11a-e with permission from Sachs et al. 2020a.

In line with improved islet histology, GLP-1/estrogen, PEG-insulin, and GLP-1/estrogen and PEG-insulin co-therapy increased β-cell numbers concomitant with decreased numbers of α- and δ-cells per endocrine islet (Figure 12a). This was accompanied by recovery of a core-mantel pancreatic islet architecture characterized by an insulin-forming core surrounded by α- and δ-cells (Figures 11d, and 12b-e). Neither estrogen nor GLP-1 alone caused similar improvements (Figure 12).

a

Treatment	Islets (n)	Insulin cells/ total cells	Glucagon cells/ total cells	Somatostatin cells/ total cells	Cells/islet
No STZ	196	0.77 ± 0.01	0.19 ± 0.01	0.05 ± 0.00	288.71 ± 17.68
STZ	180	0.26 ± 0.02 *** &&& §§§	0.61 ± 0.02 *** &&& §§§	0.15 ± 0.01 *** &&&	118.57 ± 6.28 **
Estrogen	177	0.37 ± 0.02 ***	0.51 ± 0.02 ***	0.15 ± 0.02 *** §§§	114.15 ± 6.30 *** §
GLP-1	199	0.41 ± 0.01 ***	0.48 ± 0.01 ***	0.11 ± 0.01	141.42 ± 7.76
GLP-1/estrogen	175	0.52 ± 0.01 ###	0.39 ± 0.01 ###	0.09 ± 0.01	156.66 ± 8.85 $ ###
PEG-insulin	119	0.53 ± 0.01 ###	0.40 ± 0.01 ###	0.07 ± 0.01	152.31 ± 8.41 $ ###
GLP-1/estrogen + PEG-insulin	166	0.53 ± 0.01 ###	0.40 ± 0.01 ###	0.08 ± 0.01 #	204.63 ± 13.00 ###

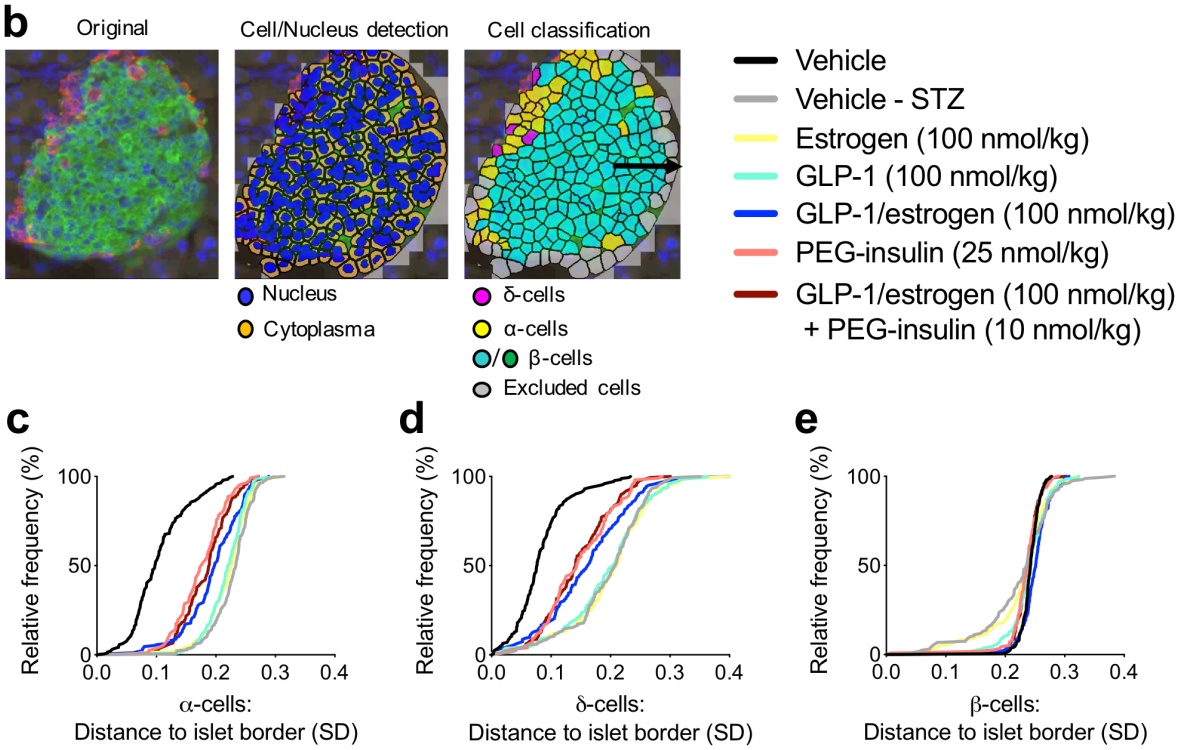

Figure 12: GLP-1/estrogen and PEG-insulin and recover islet structure.

(a) Cell composition of endocrine islets in the end of the study (No STZ: 196 islets of n=3 mice; STZ: 180, n=3; Estrogen: 177, n=3; GLP- 1: 199, n=3; GLP-1/estrogen: 175, n=2; PEG-insulin: 119, n=3; co-therapy: 166, n=3). Data are mean ± SEM. **P < 0.01 and ***P < 0.001 indicate significance to GLP-

1/estrogen treated mice. &&&P < 0.001 indicates significance to estrogen treated mice. §P < 0.05 and §§§P < 0.001 indicate significance to GLP-1 treated mice. $P < 0.05 indicates significance to GLP-1/estrogen plus PEG-insulin treatment. #P < 0.05 and ###P < 0.001 indicates significance to healthy controls (one-way ANOVA with Tukey post-hoc). **(b)** Scheme of automatic islet cell detection and classification. The black arrow indicates the measurement of the distance of each cell to its nearest border. We calculated the mean distance for each cell type and then took the standard deviation (SD) of each cell to estimate the cell distribution within an islet. Thereby, a low SD indicates a similar cell distribution within islets, whereas a high SD suggests a broader distribution of cells. Islets from vehicle (n = 3, no STZ), vehicle (n = 3, STZ), a GLP-1 analog (n = 3), estrogen (n = 3), the GLP- 1/estrogen conjugate (n = 3), PEG-insulin (n = 3), or the adjunctive therapy of GLP- 1/estrogen and PEG-insulin (n = 3) were analyzed. Effects of compound treatments on the relative cumulative frequency distribution of the SD of the distance of **(c)** α-, **(d)** δ-, and **(e)** β-cells within an islet to its nearest border. Figure 12a with permission from Sachs et al. 2020a.

Importantly, the additional effect of GLP-1/estrogen and PEG-insulin co-therapy to increase β-cell numbers compared to the insulin alone translated into superior glycemic control (Figure 13a) and increased pancreatic insulin content (Figure 13b), while limiting body weight gain (Figures 13c, d). Thus, we were able to reduce daily insulin requirements by 60% compared to the insulin monotreatment and still achieved superior therapeutic outcomes. Of note, GLP-1/estrogen treatment alone did not induce weight loss in our lean mice (Figures 13c, d), despite pronounced body weight lowering effects in DIO mice (Finan et al., 2012).

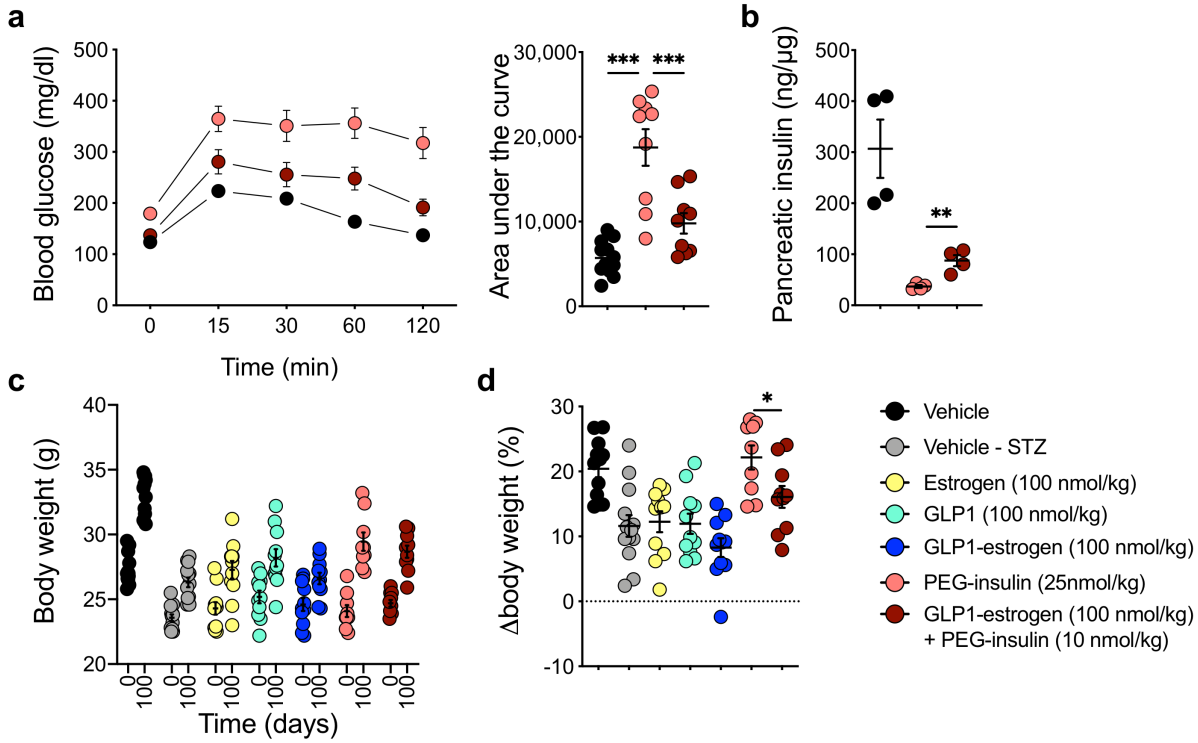

Figure 13: Superior effects of GLP-1/estrogen and PEG-insulin co-therapy in mSTZ mice.

(a) Glucose tolerance after a single intraperitoneal glucose injection (0.5g/kg) at week 12 (***P<0.001, one-way ANOVA with Tukey post-hoc) and **(b)** the insulin content of pancreas at study end (**P<0.01, unpaired two-sided t-test). **(c)** Body weight in the end of study and **(d)** body weight change (%) from

study start to study end (*P < 0.05, unpaired two-sided t-test). Data are mean ± SEM. Figures 13a-d with permission from Sachs et al. 2020a.

Sustained β-cell beneficial effects after treatment stop

To test whether treatment induced improvements on glucose and islet homeostasis were sustained, some GLP-1/estrogen treated mice were treated with GLP-1/estrogen for 12 weeks and then switched to two weeks of vehicle injections. Beneficial effects of GLP-1/estrogen treatment to reduce fasting glycemia (Figure 14a), enhance C-peptide levels (Figure 14b), and improve the β-cell maturation state (Figures 14c, d) were still evident after two weeks of vehicle injections.

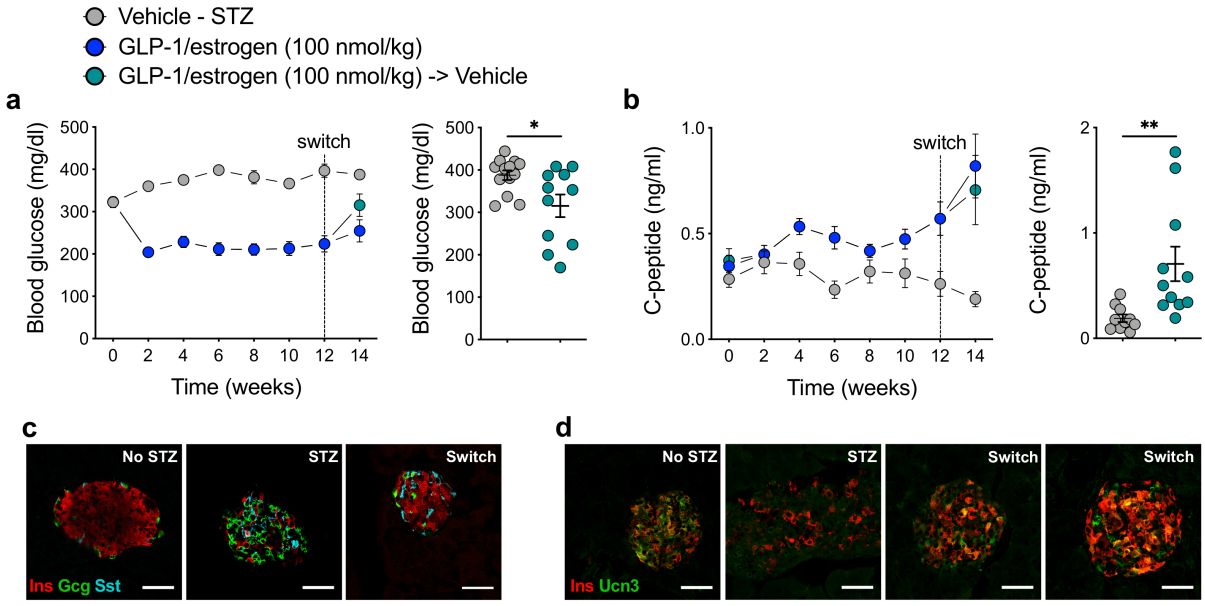

Figure 14: Sustained beneficial effects of GLP-1/estrogen in mSTZ mice.

Fasting **(a)** blood glucose (*P < 0.05, unpaired two-sided t-test) and **(b)** C-peptide levels at week 14 (*P < 0.05, unpaired two-sided t-test). **(c)** Immunohistochemistry of representative pancreatic islets. **(f)** Ucn3 immunohistochemistry at week 14. Figures 14a-d with permission from Sachs et al. 2020a.

4.1.3 GLP-1/estrogen improves human β-cell function

The human relevance of the findings was tested by treating human micro-islets with GLP-1/estrogen and the mono-agonists in the absence/presence of β-cell stressors (cytokine cocktail). After acute compound exposure and in absence of cytotoxic stress, GLP-1/estrogen more efficaciously increased GSIS from human micro-islets compared to either mono-agonists (Figure 15a). To test whether GLP-1/estrogen treatment protects against stress-induced impairment of GSIS, human micro-islets were exposed to a cytokine cocktail concurrent with compound exposure (Figure 15b). After seven days of treatment, GLP-1/estrogen enhanced GSIS, thereby exceeding effects of either mono-components (Figure 15b). Moreover, GLP-1/estrogen, but not the mono-treatments, increased total insulin content of cytokine exposed human micro-islets (Fig. 15c). Altogether, these results demonstrate that GLP-1/estrogen is

superior to both single agonists to improve β-cell function in homeostasis and upon diabetic stress in mouse and human.

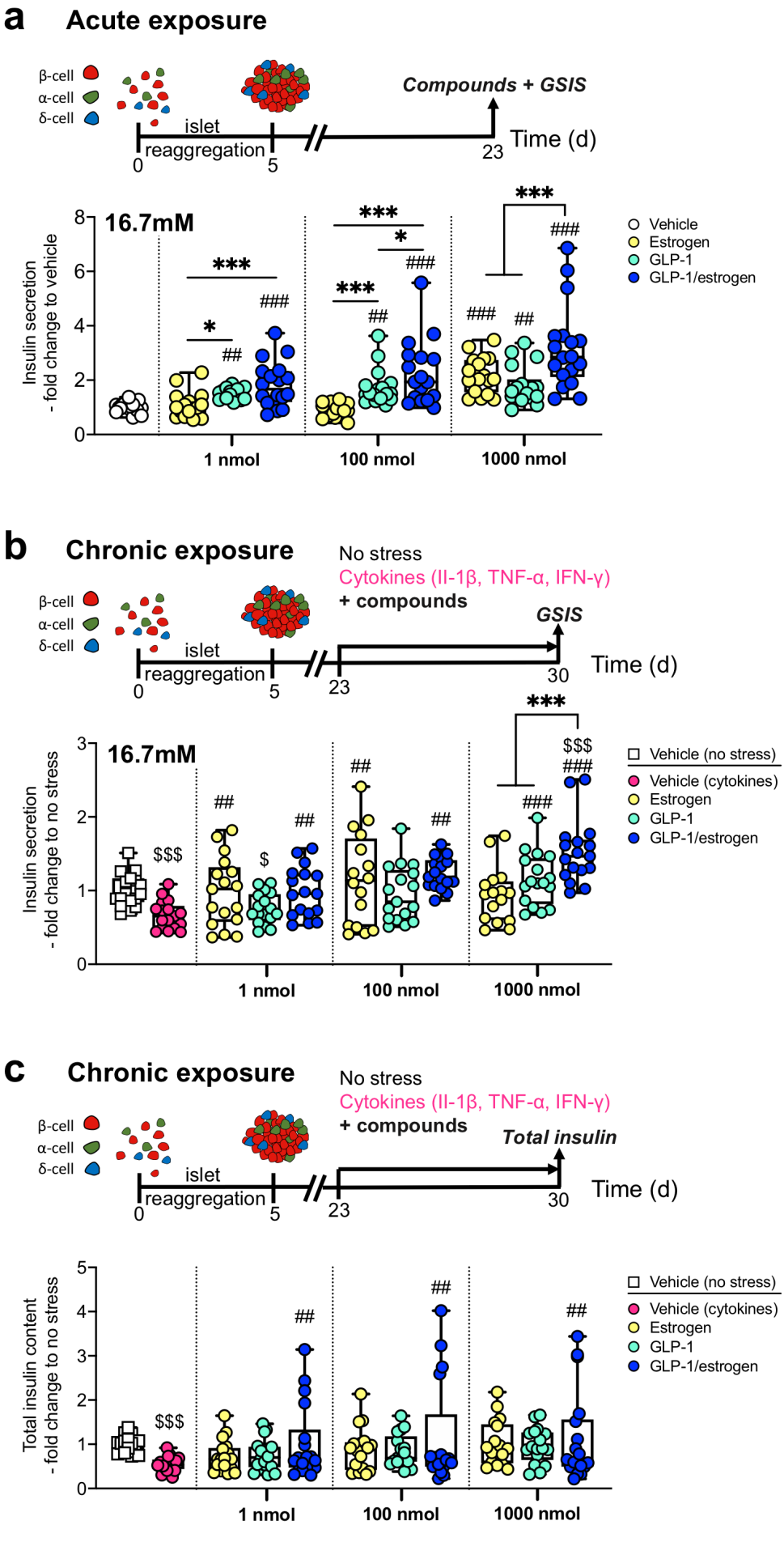
a
Acute exposure
β-cell
α-cell
δ-cell
islet
reaggregation
0
5
23
Compounds + GSIS
Time (d)
16.7mM
Insulin secretion
- fold change to vehicle
1 nmol
100 nmol
1000 nmol
Vehicle
Estrogen
GLP-1
GLP-1/estrogen
b
Chronic exposure
No stress
Cytokines (Il-1β, TNF-α, IFN-γ)
+ compounds
GSIS
30
16.7mM
Insulin secretion
- fold change to no stress
Vehicle (no stress)
Vehicle (cytokines)
c
Chronic exposure
Total insulin
Total insulin content
- fold change to no stress

Figure 15: GLP-1/estrogen improves function of human micro-islets.

(a) Human micro-islet insulin secretion after acute exposure to vehicle, estrogen, GLP-1, or GLP-1/estrogen at three escalating doses at a glucose concentration of 16.7mM. N= 5-6 micro-islets of n=3 human donors for each condition. Secretion (mean±SEM) after vehicle exposure of donor1 = 0.36±0.01 ng/ml, donor2 = 0.37±0.02 ng/ml, and donor3 = 0.29±0.03 ng/ml. $^{\#\#}$P<0.01, $^{\#\#\#}$P<0.001, to vehicle treatment. *P<0.05, **P<0.01, ***P<0.001, among compound treatments. Significance by one-way ANOVA with donor as random effect followed by Tukey post-hoc. Boxplot of all data points. **(b)** Human micro-islet insulin secretion after 7-day cytokine stress exposure and effects of vehicle, estrogen, GLP-1, and GLP-1/estrogen treatment. N= 5-6 micro-islets of n=3 human donors for each condition. Secretion (mean±SEM) of donor1 = 0.13±0.02 ng/ml, donor2 = 0.56±0.04 ng/ml, and donor3 = 0.51±0.06 ng/ml after chronic vehicle (no stress) exposure. $^{\$\$\$}$P<0.001, between healthy and cytokine exposed islets (unpaired two-sided t-test). $^{\#\#}$P<0.01, $^{\#\#\#}$P<0.001, to cytokine exposed islets. *P<0.05, ***P<0.001, among treatments. $^{\$}$P<0.05, $^{\$\$\$}$P<0.001, to healthy islets. Significance by one-way ANOVA with donor as random effect followed by Tukey post-hoc. Boxplot of all data points. **(c)** Human micro-islet total insulin content after 7-day cytokine stress exposure and effects of vehicle, estrogen, GLP-1, or GLP-1/estrogen. N= 5-6 micro-islets of n=3 human donors for each condition. Insulin content (mean±SEM) of donor1 = 41.11±3.73 ng/islet, donor2 = 30.86±3.36 ng/islet, and donor3 = 82.73±3.99 ng/islet after chronic vehicle (no stress) exposure. $^{\$\$\$}$P<0.001, between healthy and cytokine exposed islets (unpaired two-sided t-test). $^{\#\#}$P<0.01, to cytokine exposed islets. Significance by one-way ANOVA with donor as random effect followed by Tukey post-hoc. Boxplot of all data points. Compound studies on human micro-islets were performed in collaboration with Dr. Burcak Yesildag from InsPhero, Zürich. Figures 15a-c with permission from Sachs et al. 2020a.

4.1.4 Paths and mechanisms of β-cell regeneration on single cell level

In order to get insights into the paths and mechanisms underlying β-cell regeneration after compound treatment in mSTZ-diabetic mice, we performed scRNA-seq of isolated islets from treatment responding mice (Figure 16).

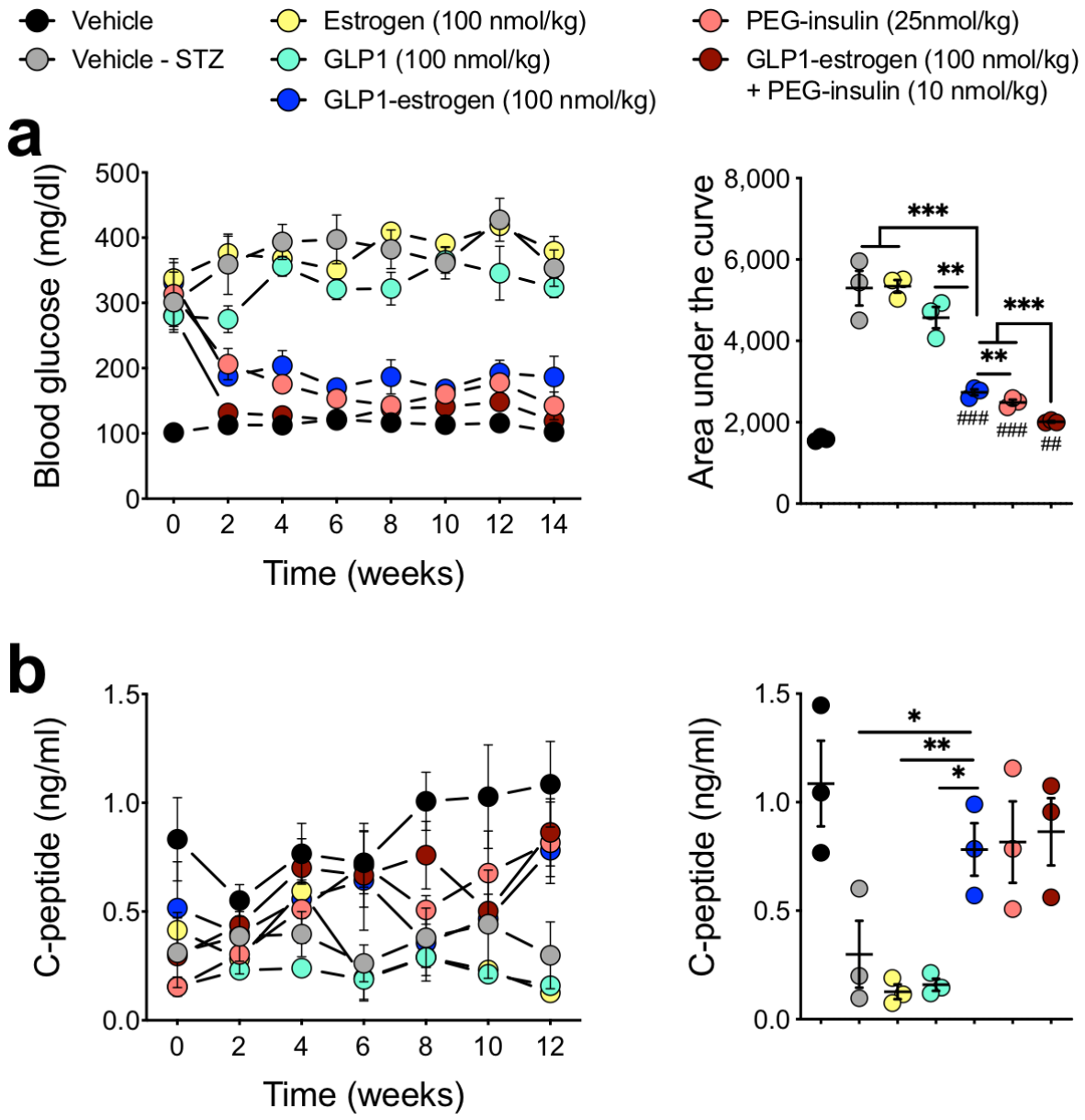

Figure 16: Physiological characteristics of mice used for scRNA-seq.

(a) Fasting blood glucose levels. **P < 0.01, ***P < 0.001, among STZ, estrogen, GLP-1 and GLP-1/estrogen treated mice (one-way ANOVA with Tukey post-hoc test). *P < 0.01, ***P < 0.001 to compound injections; ##P<0.01, ###P<0.001 to no STZ mice, comparing no STZ, GLP-1/estrogen, PEG-insulin, and co-treated mice (one-way ANOVA with Tukey post-hoc). **(b)** Fasting C-peptide levels. *P < 0.05, **P < 0.01, among STZ, estrogen, GLP-1, and GLP-1/estrogen treated mice (one-way ANOVA with Tukey post-hoc). Data are mean ± SEM. N=3 for all treatments. Representative mice that responded to treatment were used for scRNA-seq. Figures 16a-b with permission from Sachs et al. 2020a.

β-cell redifferentiation by GLP-1/estrogen, PEG-insulin, and the co-therapy

In line with the physiological data, single cell analysis revealed that β-cells of vehicle, estrogen, and GLP-1 treated mSTZ-diabetic mice were dedifferentiated, while increased fractions of GLP-1/estrogen treated β-cells clustered with immature β-cells (Figures 17a-d). Almost no

dedifferentiated β-cell remained after PEG-insulin and GLP-1/estrogen and PEG-insulin co-therapy and most cells clustered with immature β2-cells (Figures 17e, f).

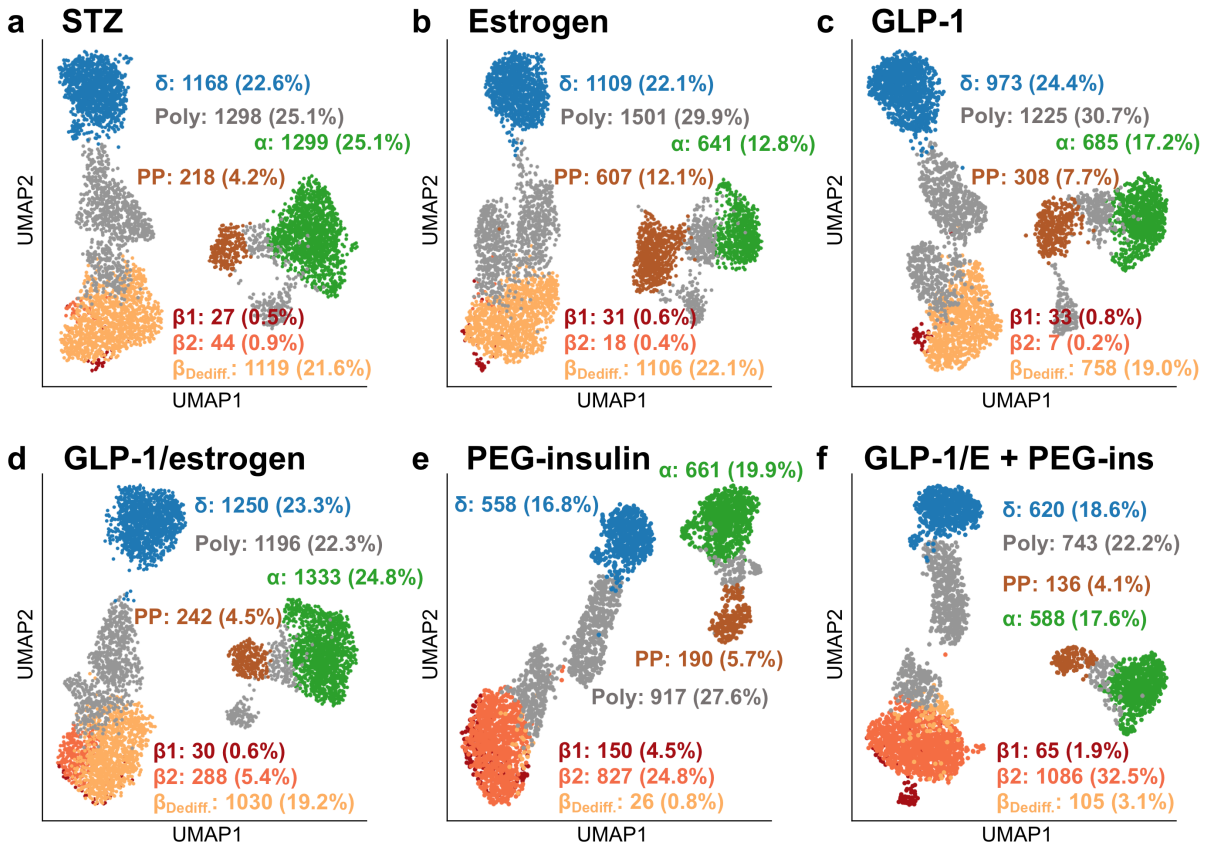

Figure 17: Effects of drug treatment on endocrine cells after 100 days of treatment.

UMAP and total cell number for **(a)** mSTZ-diabetic mice 5001, for **(b)** estrogen treated mice 4889, for **(c)** GLP-1 treated mice 3874, for **(d)** GLP-1/estrogen treated mice 5201, for **(e)** PEG-insulin treated mice 3217, and for **(f)** GLP-1/estrogen (GLP-1/E) and PEG-insulin (PEG-ins) co-treated mice 3276. Total cells and relative proportions of each cell cluster are indicated. ScRNA-seq analysis and data interpretation in collaboration with Sophie Tritschler from the Institute of Computational Biology, Helmholtz Zentrum München. Figures 17a-f with permission from Sachs et al. 2020a.

To assess the transcriptional state of β-cells after treatment, we calculated a cell-to-cell distance. This allows ordering of β-cells along a 1D-trajectory. The distance between two cells in this 1D-trajectory describes the similarity of their transcriptome. Thereby, diabetic β-cells from vehicle, estrogen, and GLP-1 treated mice had the biggest distance to healthy β-cells (Figures 18a, b). β-cells from GLP-1/estrogen treated mice moved on the 1D-trajectory more towards healthy β-cells and were distinct from β-cells from estrogen and GLP-1 mono-treated mice (Figures 18a, b). β-cells of PEG-insulin and the GLP-1/estrogen and PEG-insulin co-treatment were closest to healthy β-cells, but clustered in distinct β-cell subpopulations (Figures 18a, b).

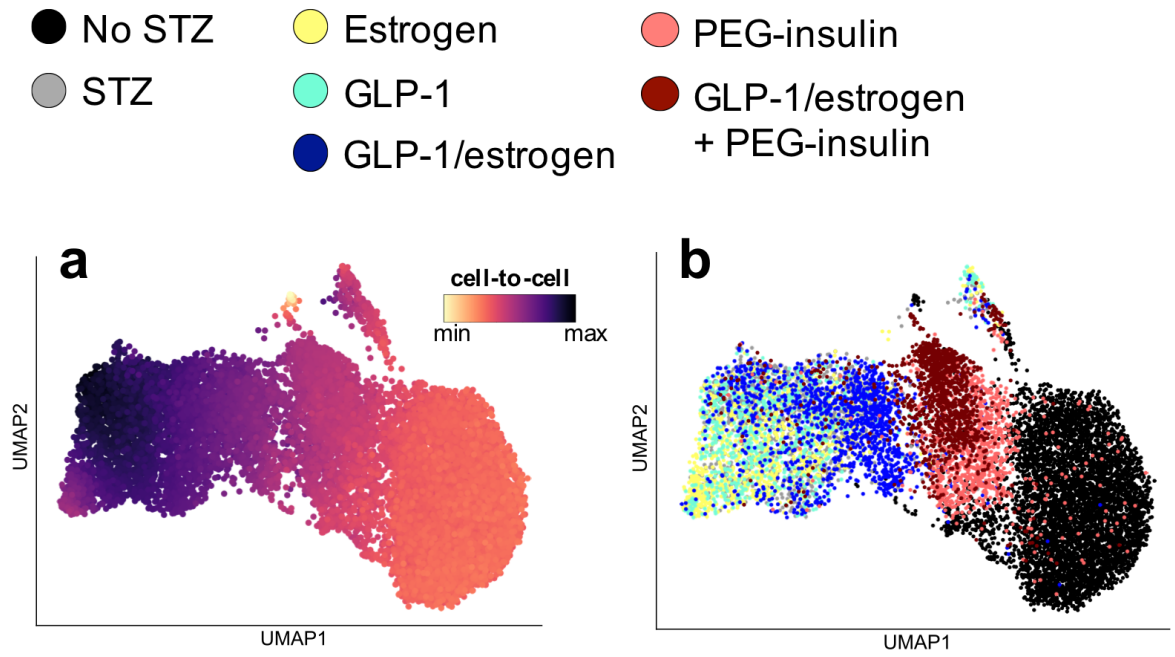

Figure 18: Transcriptional β-cell state after drug treatment in a UMAP.

Color indicates **(a)** random-walk-based cell-to-cell distance and **(b)** treatment groups. ScRNA-seq analysis and data interpretation in collaboration with Sophie Tritschler from the Institute of Computational Biology, Helmholtz Zentrum München. Figures 18a-b with permission from Sachs et al. 2020a.

Along the 1D-trajectory form diabetic to healthy β-cells, we found that β-cell dedifferentiation markers progressively decreased (e.g. *Aldh1a3*, *Gast*, *Cck*), while markers of β-cell maturity and function increased (e.g. *Ucn3*, *Slc2a2* (*Glut2)*, *Nkx6.1*) (Figures 19a, b). Thereby, we found a continuum transition from different β-cells of different treatment groups rather than discrete β-cell phenotypes, which indicates β-cell redifferentiation (Figures 19a, b). Exemplary immunostainings of Ucn3 and the Nkx6.1 TF confirmed reacquisition of β-cell function upon GLP-1/estrogen, PEG-insulin, and GLP-1/estrogen and PEG-insulin co-treatment (Figure 19c).

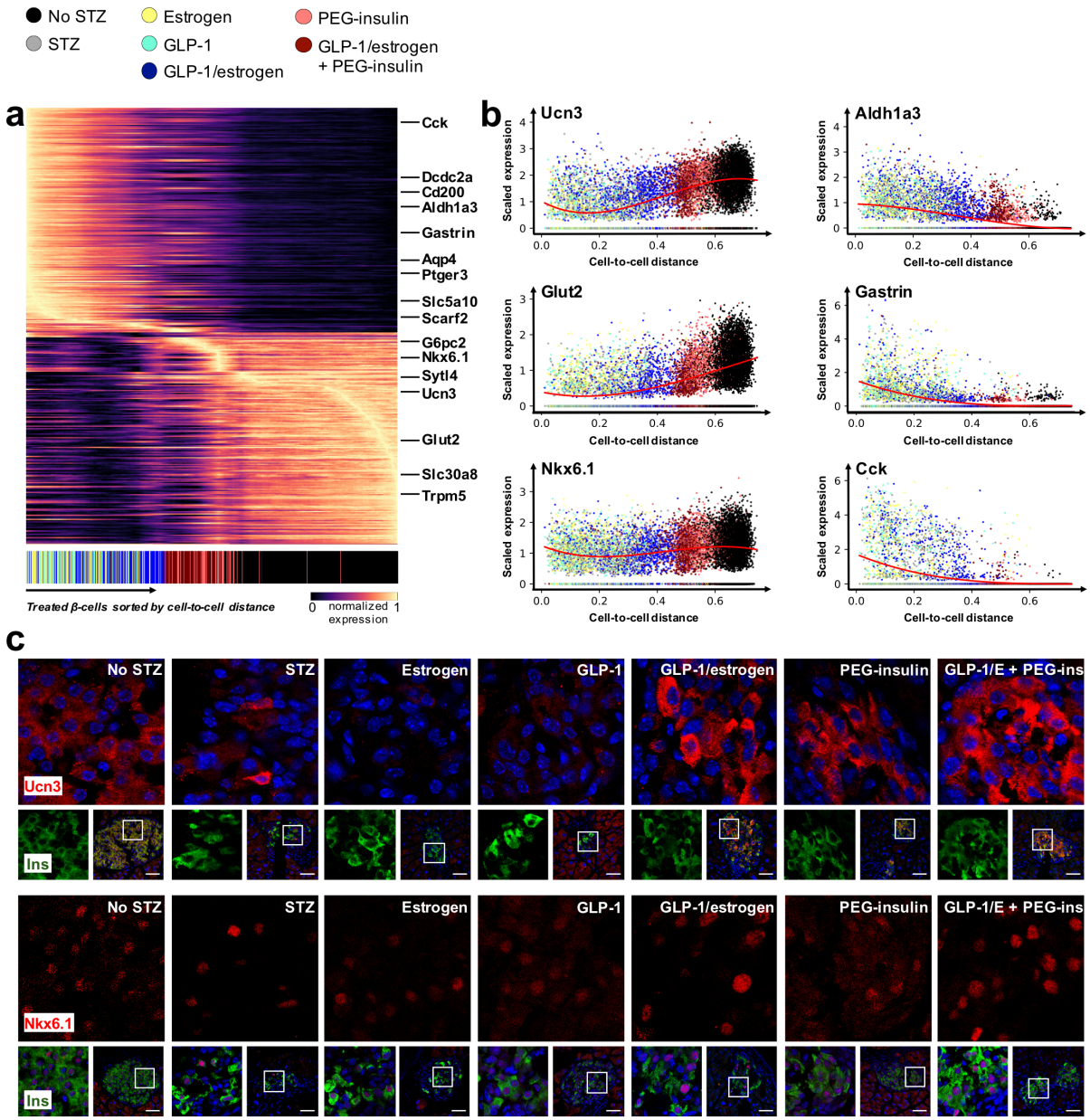

Figure 19: β-cell redifferentiation by GLP-1/estrogen, PEG-insulin, and the co-therapy.

(a) 200 up- and downregulated genes in mSTZ β-cells along the inferred trajectory. **(b)** Cells are ordered along the cell-to-cell distance and the gene expression of selected markers is depicted. Superimposed red lines are polynomial regression fits. **(c)** Ucn3 and Nkx6.1 immunohistochemistry revealed increased expression upon GLP-1/estrogen, PEG-insulin, and the co-therapy. All scale bars, 50 µm. ScRNA-seq analysis and data interpretation in collaboration with Sophie Tritschler from the Institute of Computational Biology, Helmholtz Zentrum München. Figures 19a-c with permission from Sachs et al. 2020a.

No on-going non-β to β-cell transdifferentiation

To explore whether other endocrine cells contributed to the increased functional β-cell mass after GLP-1/estrogen, PEG-insulin, and the co-treatment, we used PAGA and RNA velocity estimations (Figure 20). While PAGA measures the relative relatedness of single cell clusters (Wolf et al., 2019), RNA velocity tries to predict the future state of single cells by calculating a ratio of spliced and unspliced gene transcripts (La Manno et al., 2018). First, we used

endocrine cells from mSTZ-diabetic mice as starting point to investigate if cells move from that baseline towards endocrine cells from different treatment groups (Figure 20a). There was no direct connection from α-, δ-, or PP-cells towards regenerated β-cells (Figure 20a). Similarly, by including endocrine cells from healthy mice, we tried to predict the future state of cells from GLP-1/estrogen, PEG-insulin, and co-treated mice. This also suggested no direct movement from other (non-β) cell populations to regenerated immature β-cells (Figure 20b). Instead, some of the immature β-cells pointed to the more mature healthy β-cells (Figure 20b).

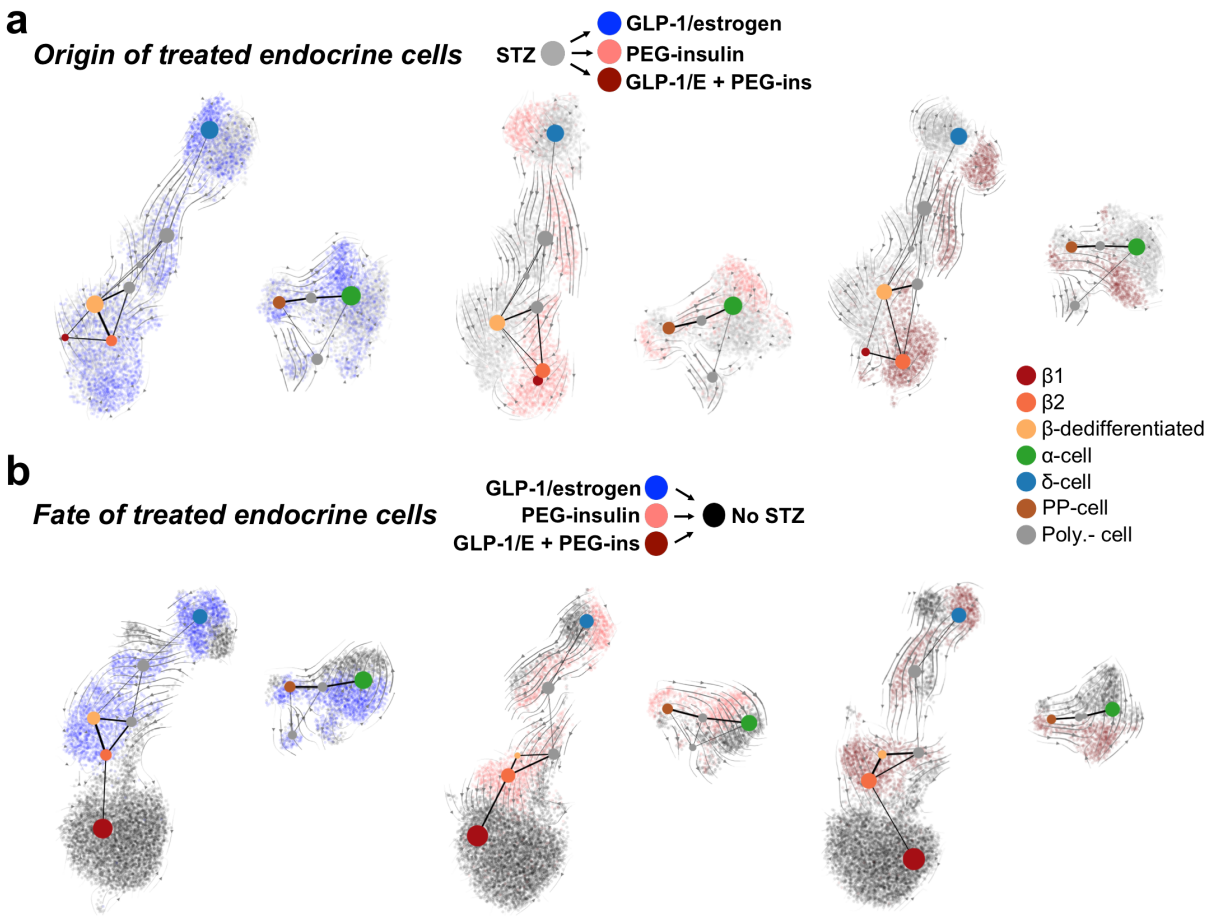

Figure 20: Origin and fate of endocrine cells after drug treatment.

(a) Endocrine cells from mSTZ and GLP-1/estrogen (left), PEG-insulin (middle) or GLP-1/estrogen plus PEG-insulin (right) treated mice. mSTZ were set as origin/starting point. Lines in PAGA and velocity suggest a movement towards treated cells. **(b)** Endocrine cells from healthy and GLP-1/estrogen (left), PEG-insulin (middle) or GLP-1/estrogen plus PEG-insulin (right) treated mice. Lines in PAGA and velocity suggest a movement towards healthy cells (fate). ScRNA-seq analysis and data interpretation in collaboration with Sophie Tritschler from the Institute of Computational Biology, Helmholtz Zentrum München. Figures 20a-b with permission from Sachs et al. 2020a.

No indication of β-cell neogenesis

Ngn3 is a regulator of embryonic endocrine cell development and thus a putative marker of endocrine cell neogenesis (Gradwohl et al., 2000). We found no induction of *Ngn3* expression in endocrine cells by scRNA-seq after 100 days of treatment (Figure 21a).

Immunohistochemistry confirmed the absence of Ngn3 positive endocrine progenitor cells in pancreatic islets of mSTZ-diabetic as well as GLP-1/estrogen, PEG-insulins, and GLP-1/estrogen and PEG-insulin co-treated mice during the course of the study (Figure 21b). Altogether these results suggest that functional β-cells in the mSTZ model after GLP-1/estrogen, PEG-insulin, and GLP-1/estrogen and PEG-insulin co-treatment are redifferentiated β-cells along the β-cell lineage trajectory.

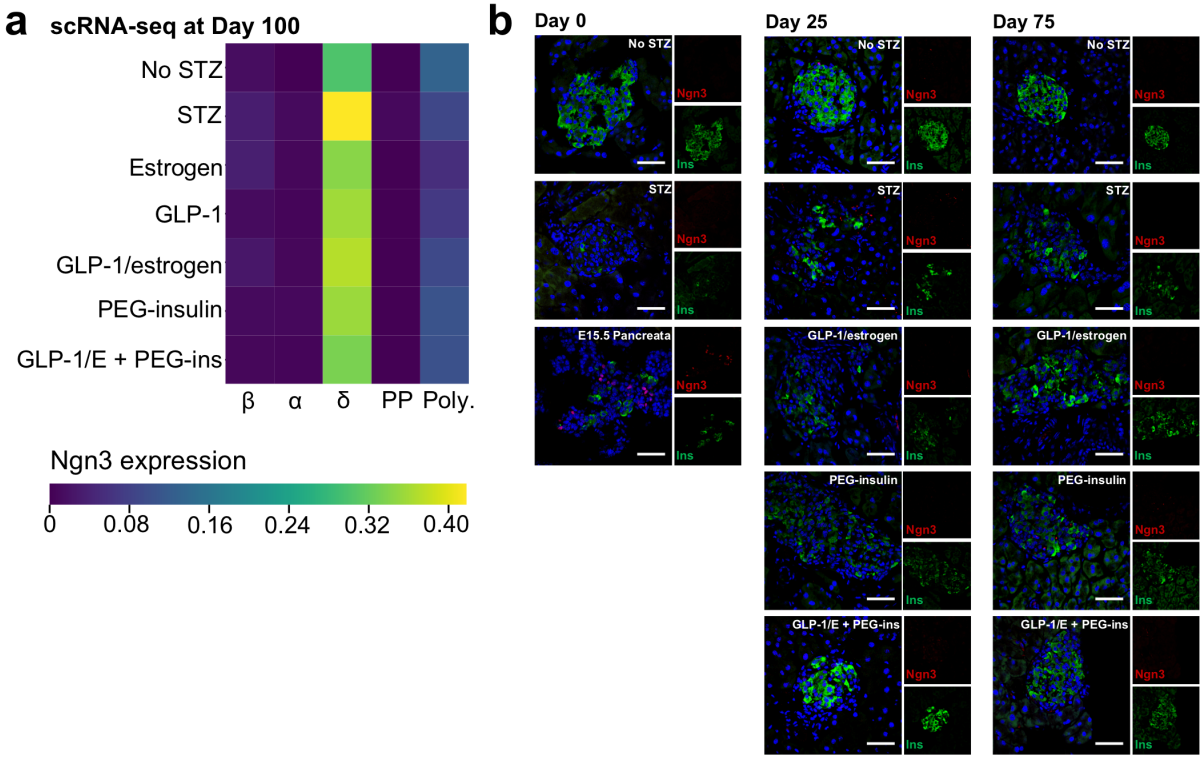

Figure 21: Absence of neogenesis in endocrine cells of treated mice as assessed by Ngn3 gene and protein expression.

(a) *Ngn3* expression in endocrine cells after 100 days of treatment. **(b)** Ngn3 immunohistochemistry during the study with mouse E15.5 pancreas as positive control. All scale bars, 50µm. ScRNA-seq analysis and data interpretation in collaboration with Sophie Tritschler from the Institute of Computational Biology, Helmholtz Zentrum München. Figures 21a-b with permission from Sachs et al. 2020a.

4.1.5 Estrogen and insulin signaling reactivate a molecular β-cell identity program

Redifferentiated β-cells of PEG-insulin and GLP-1/estrogen and PEG-insulin co-treated mice clustered in distinct β-cell subpopulations (Figure 18b). This indicates treatment specific mechanisms of actions (MOAs) for functional β-cell recovery. To obtain treatment-specific and glucose-dependent profiles after glycemia normalization, we compared β-cell-specific transcriptional signatures of PEG-insulin and co-treated mice to mSTZ-derived β-cells (Figure 22a). Both treatments stimulated the expression of β-cell markers and pathways indicative of improved β-cell function and are thus likely due to similar blood glucose corrections and/or the activation of similar or additive pathways in β-cells (Figure 22a). Of important note, genes specifically upregulated in β-cells after PEG-insulin treatment were enriched in pathways and

ontologies indicative of an increased insulin signaling cascade such as the recently described RNA polymerase II mediated pathway (Figure 22a) (Hancock et al., 2019).

Our goal was to use the GLP-1/estrogen conjugate to specifically deliver the steroid cargo into β-cells. We found an induction of the ER-associated degradation (ERAD) pathway and tRNA signaling specifically in β-cells of GLP-1/estrogen and PEG-insulin co-treated mice (Figure 22a). Unresolved ER stress contributes to functional β-cell mass loss in T1D and T2D (Fonseca et al., 2011). Estrogen mitigates β-cell ER stress of diabetic Akita mice by stabilizing ERAD, which depends on nuclear estrogen receptor alpha signaling, and leads to diabetes protection in this mouse model (Xu et al., 2018). tRNA signaling is a target of estrogen receptor activation and is associated with increased cell proliferation (Torrent et al., 2018; Zhu et al., 2018). Consequently, GLP-1/estrogen and PEG-insulin co-treatment stimulated β-cell proliferation (Figures 22b, c). Upon hyperglycemic stress, β-cells decrease GLP-1R expression (Fritsche et al., 2000; Xu et al., 2007). We hypothesized that the co-therapy more potently restored GLP-1R expression on β-cells compared to GLP-1/estrogen monotherapy, which allowed increased estrogen delivery. Indeed, GLP-1R expression increased with improved glucose levels (Figure 22d).

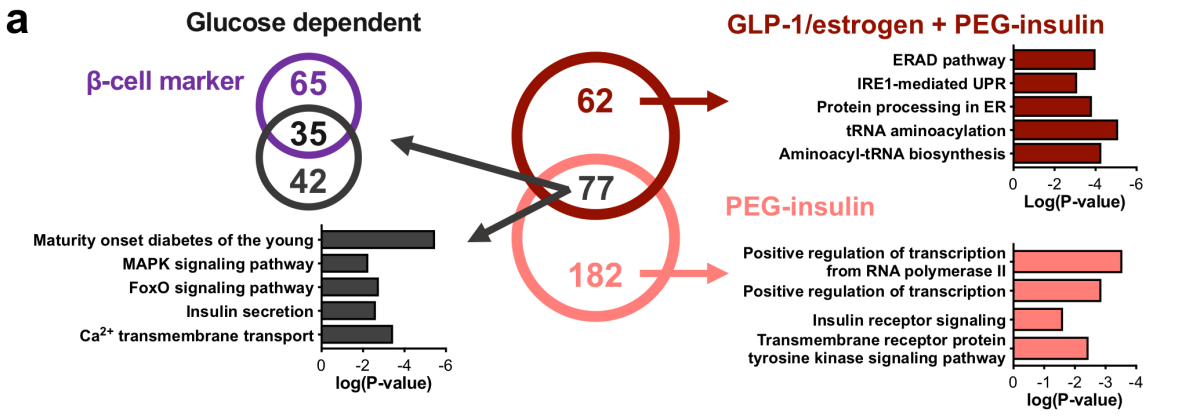

b

	β-cells	α-cells	δ-cells	PP-cells	Poly.-cells
No STZ	18/5643 (0.32 %)	0/781 (0 %)	0/493 (0 %)	0/70 (0 %)	2/436 (0.46 %)
STZ	4/1186 (0.34 %)	2/617 (0.32 %)	0/218 (0 %)	0/118 (0 %)	4/2870 (0.14 %)
Estrogen	8/1147 (0.7 %)	3/384 (0.78 %)	1/606 (0.17 %)	0/45 (0 %)	2/2459 (0.08 %)
GLP-1	3/795 (0.38 %)	2/683 (0.29 %)	1/972 (0.1 %)	0/308 (0 %)	11/1140 (0.96 %)
GLP-1/estrogen	3/1345 (0.22 %)	2/1328 (0.15 %)	0/1249 (0 %)	0/242 (0 %)	7/1061 (0.66 %)
PEG-insulin	3/998 (0.3 %)	0/660 (0 %)	0/558 (0 %)	0/190 (0 %)	2/852 (0.23 %)
GLP-1/E + PEG-ins	14/1239 (1.13 %)	0/588 (0 %)	3/616 (0.49 %)	0/136 (0 %)	7/696 (1.01 %)

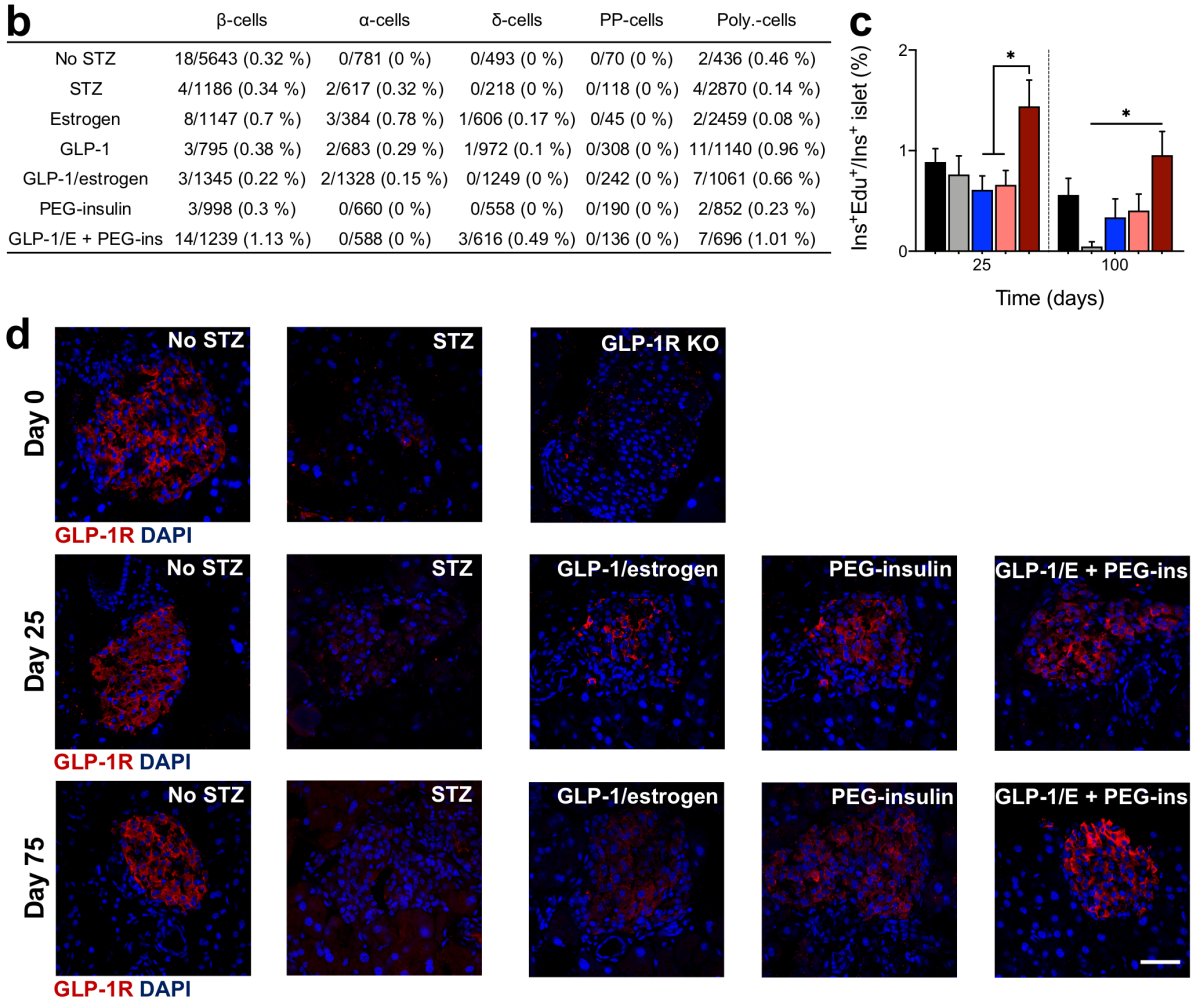

Figure 22: β-cell specific insulin and estrogen targeting.

(a) Venn diagram of β-cell specific upregulated genes (log fold change > 0.25, FDR < 0.01) of PEG-insulin and GLP-1/estrogen plus PEG-insulin co-treated mice compared to mSTZ treated mice (left) (selected GO terms/KEGG pathways). **(b-c)** β-cell proliferation after drug treatment in mSTZ mice. **(b)** β-cell proliferation assessed by scRNA-seq at study end. **(c)** β-cell proliferation assessed by EdU staining during the study. Day 25: No STZ, 73 islets of n=3 mice; STZ, 36 islets, n=3; GLP-1/estrogen, 37 islets, n=3; PEG-insulin, 61 islets, n=3; GLP-1/estrogen and PEG-insulin, 50 islets, n=3. Day 100: No STZ, 47 islets of n=3 mice; STZ, 47 islets, n=3; GLP-1/estrogen, 36 islets, n=2; PEG-insulin, 43 islets, n=3; GLP-1/estrogen and PEG-insulin, 47 islets, n=3. Data are mean ± SEM. *P<0.05, comparing indicated treatments at either day 25 or day 100 by one-way ANOVA followed by Tukey post-hoc

comparison. **(d)** GLP-1R immunohistochemistry. GLP-1R knock-out (GLP-1R KO) mouse shows GLP-1R antibody specificity. Scale bar, 50 µm. Figures 22a-d with permission from Sachs et al. 2020a.

Part II

4.2 Shared benefits of GLP-1/GIP dual-agonism in mice and bariatric surgery in humans

There is an urgent need of new treatments options that safely mimic the multi-target beneficial effects of bariatric surgery to correct obesity. This can not only lead to T2D prevention but also reversal of β-cell dysfunction. In this thesis we compared the plasma proteome of GLP-1/GIP co-agonist treated male and female DIO mice to that of humans who underwent RYGB to better understand whether this polypharmacological approach could better mimic the benefits of bariatric surgery compared to a GLP-1 and GIP mono-treatment.

4.2.1 GLP-1/GIP decreases adiposity with equal efficacy in both sexes

Female C57Bl6/J mice gain weight slower that male counterparts (Yang et al., 2014). In order to obtain body weight and age-matched obese male and female mice we delayed the onset of HFD-feeding in male mice. After four and 29 weeks on HFD respectively, age-matched male and female mice were body weight matched (Figure 23a). Due to inherent sex differences, male DIO mice had less fat (Figure 23b) and more lean mass (Figure 23c) compared to female DIO mice.

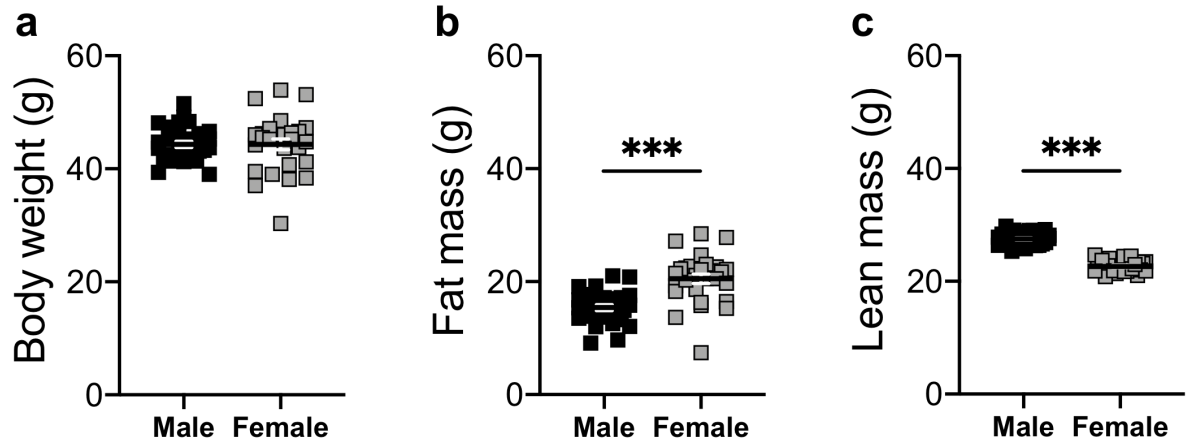

Figure 23: Body composition of male and female DIO mice at treatment initiation.

Male (n = 30) and female (n = 28) mice after HFD feeding for four and 29 weeks, respectively. Panels show (a) body weight, (b) fat mass and (c) lean mass at treatment start. Data represent means ± SEM. ***P < 0.001, unpaired two-sided t-test. Figures 23a-c with permission from Sachs et al. 2020b.

In male DIO mice, GLP-1/GIP treatment decreased body weight to a greater extent than activity matched GLP-1 and GIP mono-agonists (Figure 24a). Body weight loss was mainly driven by a loss of fat and not lean mass (Figure 24b). Food intake reduction was similar between GLP-1 and GLP-1/GIP treated mice, indicating food intake-independent mechanisms of GLP-1/GIP to reduce body weight of male DIO mice (Figure 24c). Also for female DIO mice, GLP-1/GIP treatment reduced body weight more potently by stimulating fat but not lean mass

loss compared to either mono-treatment (Figures 24d, e). The superior weight loss induced by GLP-1/GIP over GLP-1 therapy emerged earlier in female than male DIO mice (day 15 vs. 19) (Figures 24a, d). In contrast to males, GLP-1/GIP treated females consumed less food than those treated with GLP-1 (Figures 24c, f). In both sexes, GIP treatment has no effect on body weight or food intake (Figure 24).

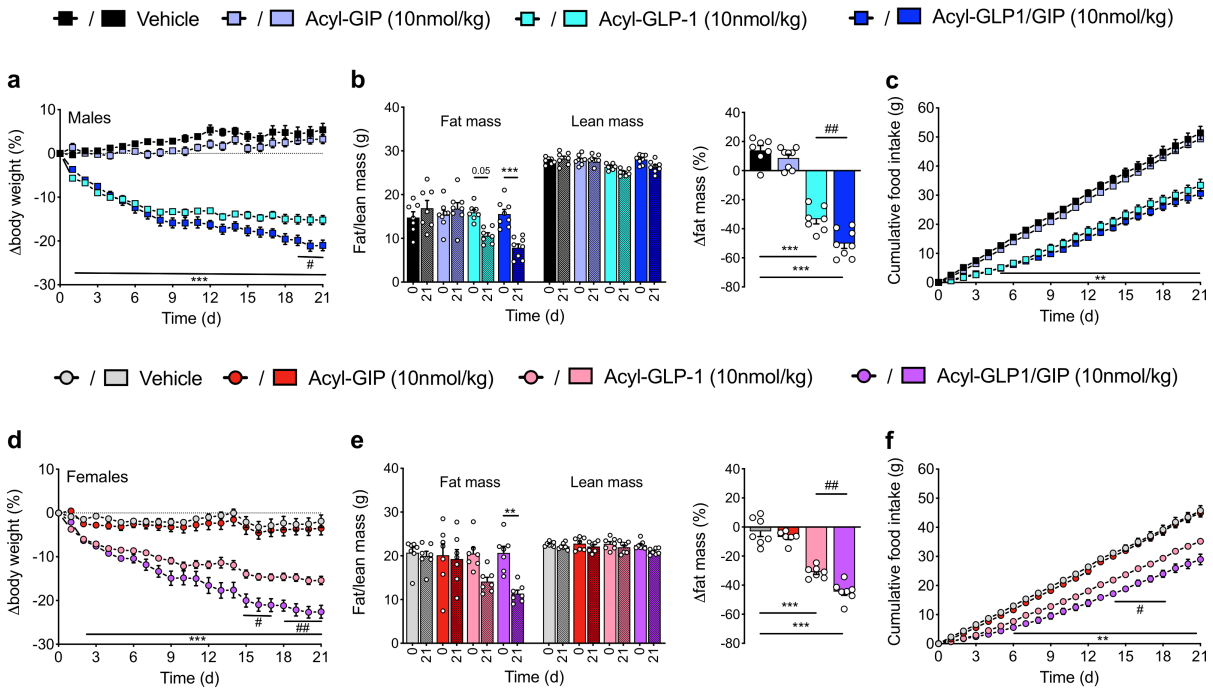

Figure 24: Superior effect of GLP-1/GIP to reduce body weight in both sexes.

(a and d) Body weight loss in percentage, **(b and e)** total fat and lean mass and change of fat mass to study start as well as **(c and f)** cumulative food intake of male (a-c) and female (d-f) mice during the study: vehicle (n (female) = 7, n (male) = 7), acyl-GIP (10nmol/kg; n (female) = 7, n (male) = 8), acyl-GLP-1 (10nmol/kg; n (female) = 7), n (male) = 7), acyl-GLP1/GIP (10nmol/kg; n (female) = 7, n (male) = 8). Data represent means ± SEM. **P < 0.01, ***P < 0.001, determined by two-way ANOVA comparing vehicle with the acyl-GLP1/GIP co-agonist. $^{\#}$P < 0.05, $^{\#\#}$P < 0.01 determined by two-way ANOVA comparing acyl-GLP-1 with the acyl-GLP1/GIP co-agonist. ANOVA was followed by Tukey post hoc multiple comparison analysis to determine statistical significance. Figures 24a-f with permission from Sachs et al. 2020b.

Vehicle treated male mice gained weight during the study as they had not yet reached their body weight plateau (Figures 25a, b). Female mice had been on HFD for 29 weeks prior study start and already reached their maximal body weight (Figures 25a, b). Body weight loss of GLP-1 and GLP-1/GIP treated males and females was similar compared to their initial body weight (Figure 25). As vehicle treated males gained weight during the study, the relative difference to GLP-1 and GLP-1/GIP treated mice was bigger in the end of the study compared to that of treated females (Figure 25).

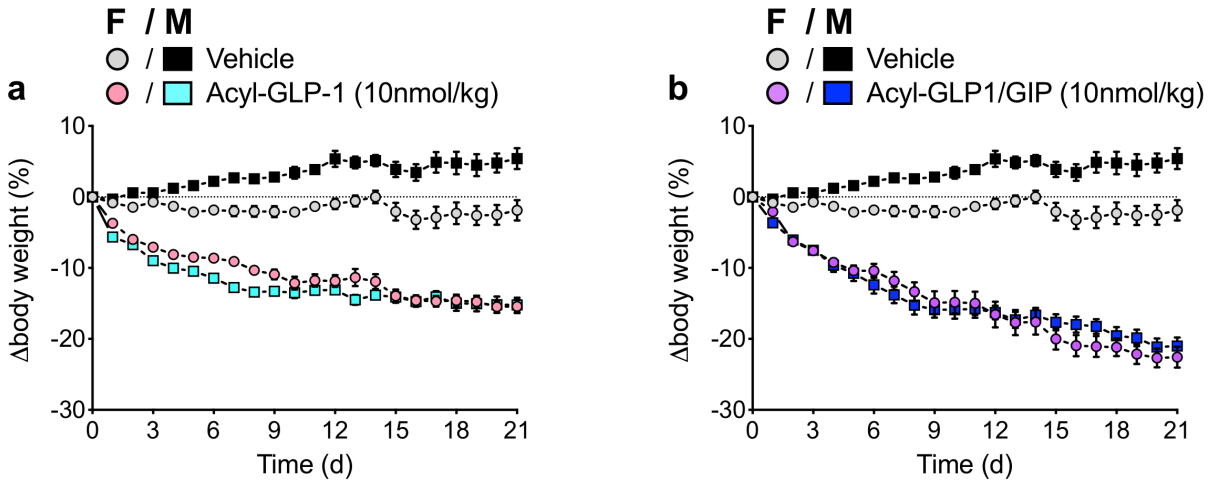

Figure 25: Body weight lowering of GLP-1 and GLP1/GIP treated male and female DIO mice.

(a) Percentage of body weight loss by GLP-1 (10nmol/kg; n (female) = 7, n (male) = 7) compared to vehicle treatment in male and female DIO mice (n (female) = 7, n (male) = 7). GLP-1-induced body weight loss to treatment start was similar in both sexes. Vehicle treated males gained weight during the study. This caused a relative bigger weight loss of vehicle to GLP-1 treated males in the end of the study compared to vehicle and GLP-1 treated females (males: 20.39 ± 1.28% vs. females: 13.76 ± 3.21% comparing the body weight of vehicle and GLP-1 treated mice at study day 21). **(b)** Percentage of body weight loss by GLP-1/GIP (10nmol/kg; n (female) = 7, n (male) = 8) compared to vehicle treatment of male and female DIO mice (n (female) = 7, n (male) = 7). Vehicle treated males gained weight during the study. This caused a relative bigger weight loss of vehicle to GLP-1/GIP treated males in the end of the study compared to vehicle and GLP-1/GIP treated females (males: 23.45 ± 1.76% vs. females: 22.22 ± 2.07% comparing the body weight of vehicle and GLP-1 treated mice at study day 21). Data represent means ± SEM. Figures 25a-b with permission from Sachs et al. 2020b.

4.2.2 GLP-1/GIP improves glucose metabolism in both sexes

Fasting blood glucose and glucose tolerance was significantly improved by GLP-1/GIP treatment in male and female DIO mice (Figures 26a, b, e, f). In male mice, GLP-1 and GLP-1/GIP treatment reduced fasting insulin (Figure 26c) and fasting HOMA-IR (Figure 26d), implying enhanced insulin sensitivity. Fasting insulin levels were low in female DIO mice and were not further reduced by either mono- or dual-agonist treatment (Figure 26g). Still, GLP-1/GIP treatment improved HOMA-IR in female DIO mice (Figure 26f). Treatment with GIP improved glucose tolerance in both sexes (Figures 26a, b, e, f) without reducing fasting insulin (Figures 26c, g) or reducing HOMA-IR (Figures 26d, h). This might suggest direct effects of GIP treatment on pancreatic β-cells to increase GSIS (incretin effect).

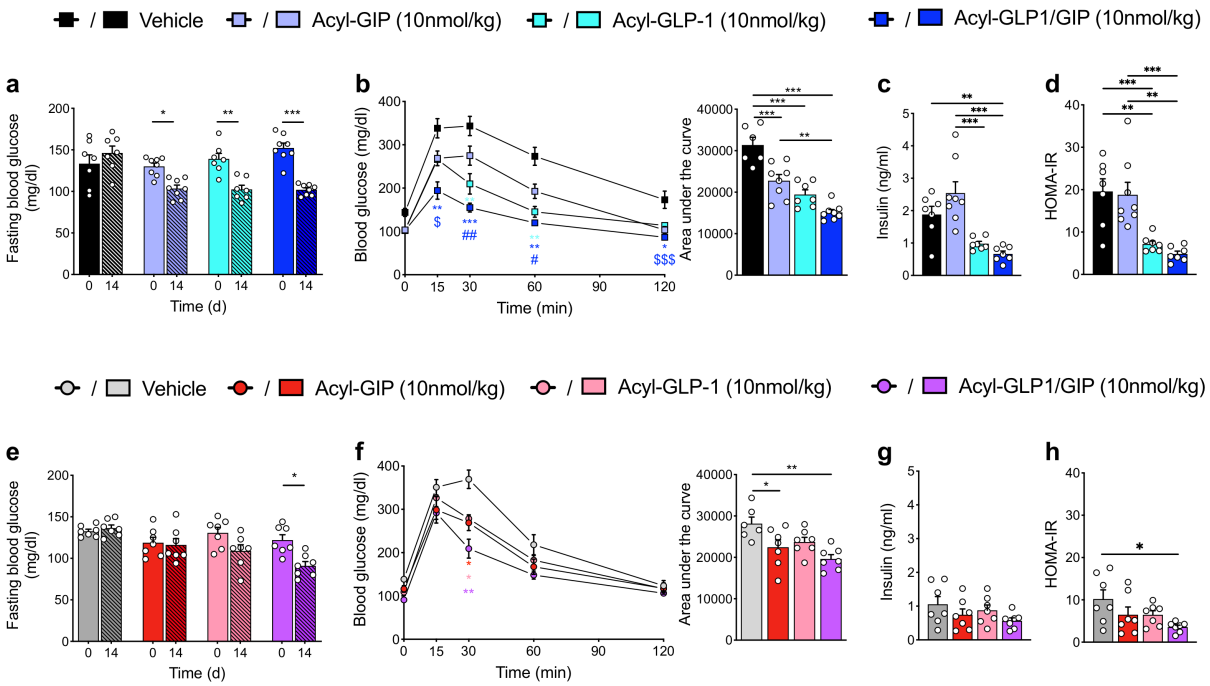

Figure 26: GLP-1/GIP improves glucose metabolism in male and female DIO mice.

(a and e) Fasting blood glucose at study day 0 and 14, **(b and f)** glucose excursions during an intraperitoneal glucose tolerance test (ipGTT) (2g glucose/kg body weight) at study day 14, **(c and g)** fasting plasma insulin levels, and the calculated insulin sensitivity as HOMA-IR value **(d and h)** of male (a-d) and female (e-h) mice: vehicle (n (female) = 7, n (male) = 7), acyl-GIP (10nmol/kg; n (female) = 7, n (male) = 8), acyl-GLP-1 (10nmol/kg; n (female) = 7, n (male) = 7), acyl-GLP1/GIP (10nmol/kg; n (female) = 7, n (male) = 8). Data represent means ± SEM. ipGTT in **(b)** and **(f)**: *P < 0.05, **P < 0.01, *** P < 0.001, determined by two-way ANOVA comparing vehicle with compound treatments; $^{\#}$P < 0.05, $^{\#\#}$P < 0.01, determined by two-way ANOVA comparing acyl-GLP-1/GIP with the acyl-GIP mono-agonist; $^{\$}$P < 0.05, $^{\$\$\$}$P < 0.001, determined by two-way ANOVA comparing acyl-GLP-1/GIP with the acyl-GLP-1 mono-agonist. Otherwise, *P < 0.05, **P < 0.01, *** P < 0.0001, determined by one-way ANOVA. ANOVA was followed by Tukey post hoc multiple comparison analysis to determine statistical significance. Figures 26a-h with permission from Sachs et al. 2020b.

4.2.3 GLP-1/GIP synergistically improves lipid metabolism

GLP-1/GIP treatment synergistically reduced total plasma cholesterol levels in both sexes (Figures 27a, c). In males, GLP-1/GIP-mediated reduction of plasma cholesterol was predominately attributable to a reduction in LDL cholesterol, with only subtle changes of HDL cholesterol (Figure 27b). Similarly, GLP-1 treatment reduced LDL levels, but to a lesser extent compared to the co-agonist (Figure 27b). In females, only GLP-1/GIP treatment reduced plasma LDL, whereas both GLP-1 and GLP-1/GIP similarly increased HDL levels (Figure 27d). GIP had no effect on plasma cholesterol in body weight-matched male and female DIO mice (Figure 27). In both sexes, GLP-1 and GLP-1/GIP significantly reduced the lipid positive area in hepatic tissue sections (Figure 28).

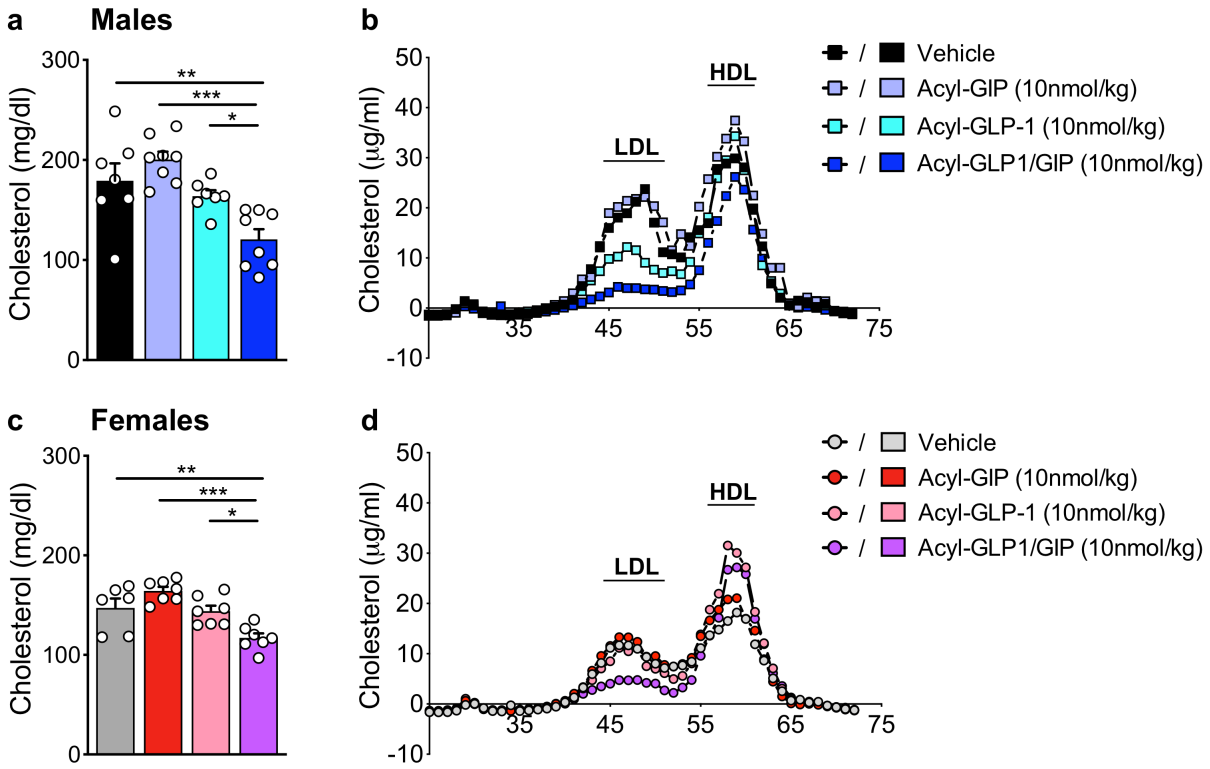

Figure 27: GLP-1/GIP synergistically improves lipid metabolism in male and female DIO mice.

(a) Plasma cholesterol and **(b)** plasma lipoprotein fractions of male mice and **(c)** plasma cholesterol and **(d)** plasma lipoprotein fractions of female mice treated daily with either vehicle (n (female) = 7, n (male) = 7), acyl-GIP (10nmol/kg; n (female) = 7, n (male) = 8), acyl-GLP-1 (10nmol/kg; n (female) = 7, n (male) = 7), or acyl-GLP1/GIP (10nmol/kg; n (female) = 7, n (male) = 8). Data represent means ± SEM and are derived from blood at study end. *P < 0.05, **P < 0.01, *** P < 0.001, determined by one-way ANOVA followed by Tukey post hoc multiple comparison analysis to determine statistical significance. Figures 27a-d with permission from Sachs et al. 2020b.

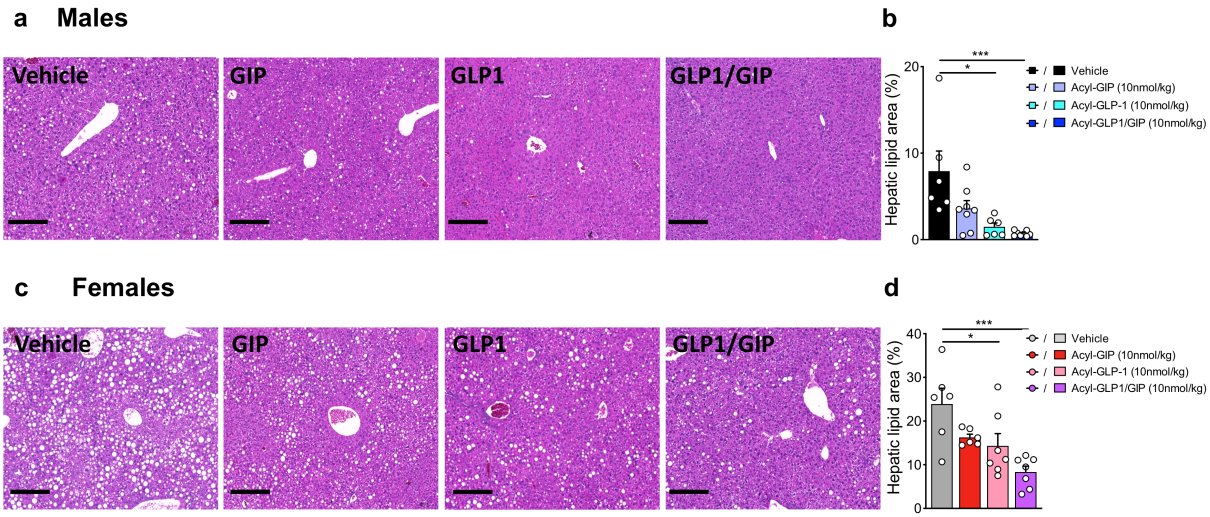

Figure 28: GLP-1/GIP reduces hepatic steatosis in male and female DIO mice.

(a and c) Histology of the liver and **(b and d)** the lipid area of hepatic sections of male (a-b) and female (c-d) female mice: vehicle (n (female) = 7, n (male) = 7), acyl-GIP (10nmol/kg; n (female) = 7, n (male) = 8), acyl-GLP-1 (10nmol/kg; n (female) = 7, n (male) = 7), acyl-GLP1/GIP (10nmol/kg; n (female) = 7,

n (male) = 8). Data represent means ± SEM. b: *P < 0.05, *** P < 0.001, determined by Kruskal-Wallis test followed by Dunn's multiple comparison test to determine statistical significance. d: *P < 0.05, *** P < 0.001, determined by one-way ANOVA followed by Tukey post hoc multiple comparison analysis to determine statistical significance. Figures 28a-d with permission from Sachs et al. 2020b.

4.2.4 Plasma proteome profiling reveals sex-specific differences

We used plasma from untreated obese mice to examine sex-specific differences of the plasma proteome. Remarkably, the plasma proteome separated male and female mice by one-dimensional principal-component analysis (PCA) (Figure 29a). This indicated strong sex-specific differences in the plasma proteome. Of the 563 identified plasma proteins, 75 proteins were differentially regulated between male and female DIO mice (P<0.01; Figure 29b).

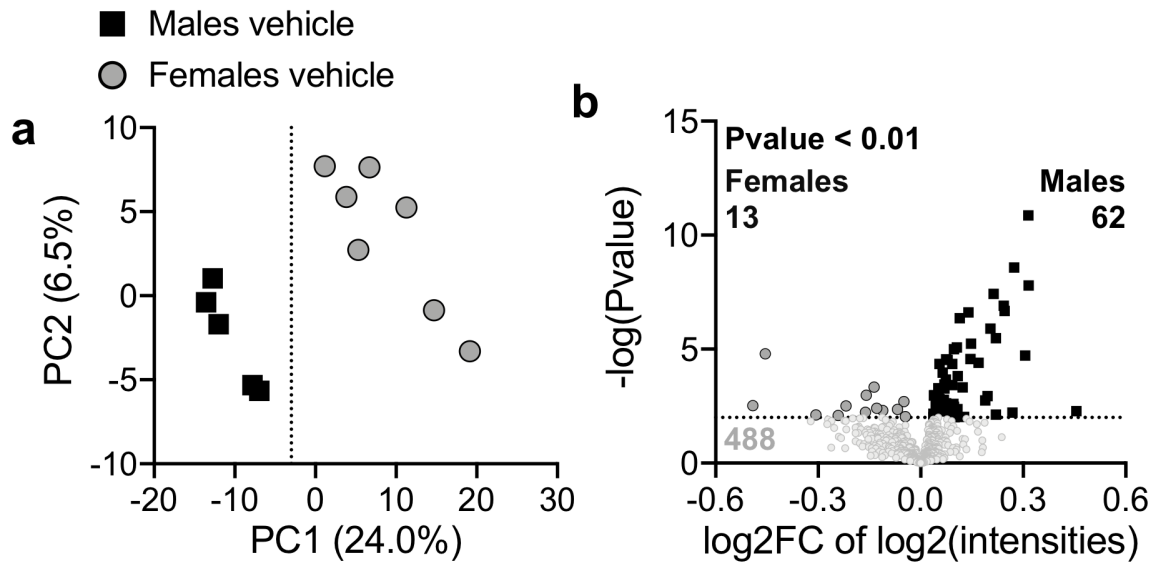

Figure 29: Distinct plasma proteome of body weight matched male and female DIO mice.

(a) The first two components of a principle component analysis (PCA) of vehicle treated male and female DIO mice. All proteins were used for PCA calculation. **(b)** Volcano plot comparing male and female plasma proteins. Differentially regulated proteins (p < 0.01) are marked. 62 proteins were high in male DIO plasma, while 13 proteins were increased in female DIO mice. Dashed line indicates P<0.01. Figures 29a-b with permission from Sachs et al. 2020b.

Previously it has been shown that women and female mice have lower levels and activity of plasma complement components compared to their male counterparts (Gaya da Costa et al., 2018; Kotimaa et al., 2016). Similarly, 31 of the 62 proteins with increased abundancy in DIO males relative to DIO females were associated with the complement system and inflammation (Figure 30a). Consistent with increased total plasma cholesterol, LDL, and HDL in males relative to female DIO mice, constituents of the HDL (e.g. Apod and Apoa1) and LDL particle (e.g. Apoc1, Apoc3, and Apoc4; all P<0.05) were higher in males (Figure 30a). In addition, male DIO mice had high protein abundancies of major urinary proteins (Mup2, Mup3, Mup17) (Figure 30a), which are male pheromone carrier proteins (Stopková et al., 2007) indicating that

sex inherent differences were captured by PPP. Among proteins of increased abundancies in female compared to male DIO mice, we found Aldolase B (Aldob), Sorbitol dehydrogenase (Sord), Aspartate aminotransferase (or Glutamic-oxaloacetic transaminase (Got1)), Serum amyloid P-component (Apcs), Dipeptidyl peptidase-4 (Dpp4), Leucine aminopeptidase 3 (Lap3), NADP-dependent malic enzyme (Me1), and Glutamyl aminopeptidase (Enpep) (Figure 30b). While Got1 is already used as biomarker for liver diseases in the clinic (Kotronen et al., 2009), increased protein levels of Aldob, Sord, Apcs, Dpp4, Lap3, Me1, and Enpep were recently found in humans with NAFLD and heavily obese male mice and are thus novel potential biomarkers of liver disease (Niu et al., 2019). This difference is reflected by a higher percentage of hepatic fat in female DIO mice compared to body weight matched male DIO mice (Figures 28b, d). Importantly, few regulated proteins also belonged to one of the three main contamination panels (erythrocyte, platelet, coagulation), suggesting that identified proteins could be derived from a true biological effect (Figure 30c).

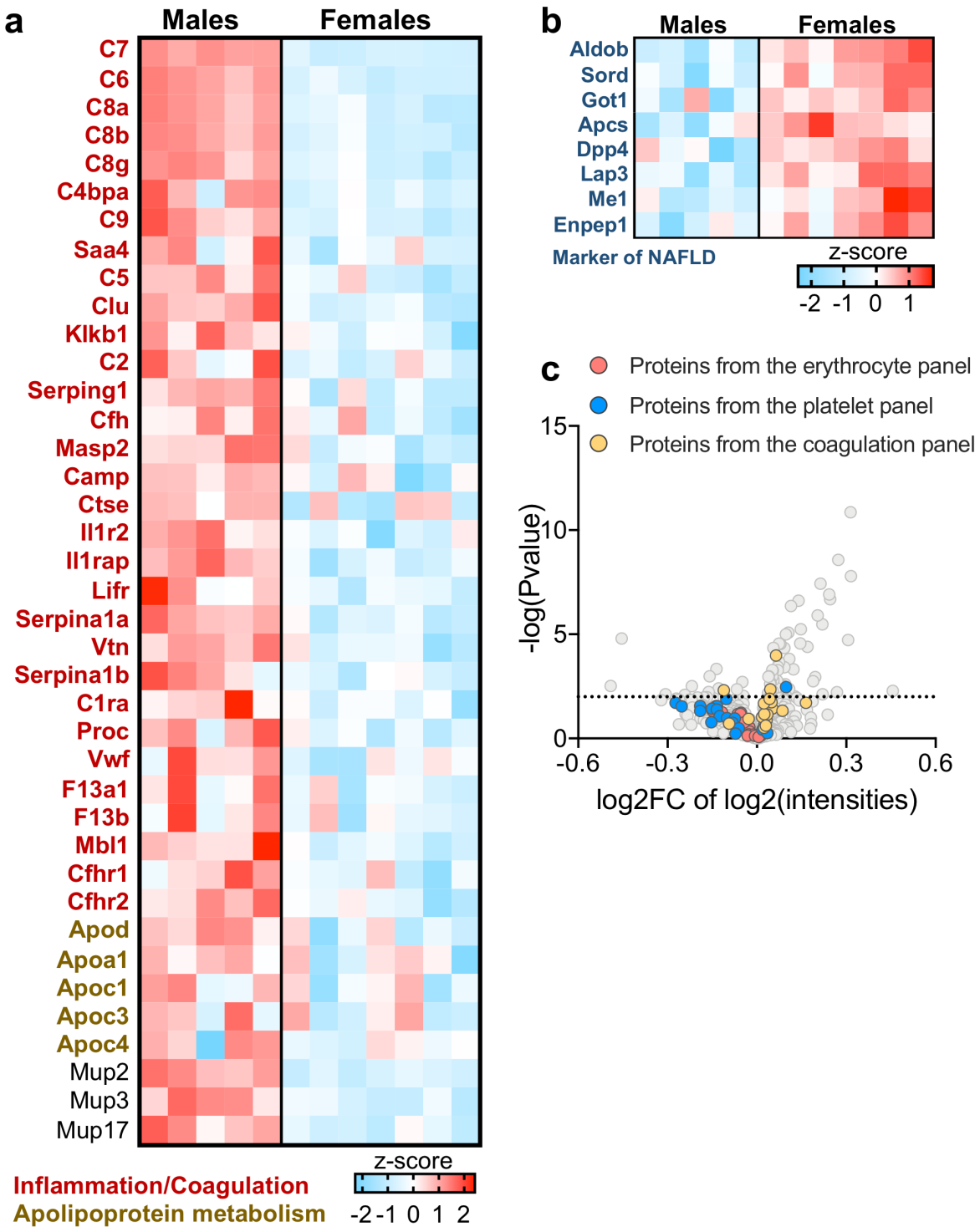

Figure 30: Sex specific proteins of body weight matched male and female DIO mice.

(a) Upregulated proteins in male compared to female DIO mice ($P < 0.01$; selected proteins are depicted). **(b)** Upregulated in DIO female compared to DIO male mice ($P < 0.05$; selected proteins are depicted). Protein intensities were log2-transformed. The Z-score normalized protein levels across samples. **(c)** The volcano plot shows the comparison between male and female vehicle treated DIO mice. The red, blue, and yellow color marks proteins from the erythrocyte, platelet, and coagulation contamination panel (Geyer et al., 2019). The dashed line indicates significance (p-value < 0.01). Figures 30a-c with permission from Sachs et al. 2020b.

4.2.5 Plasma proteome profile shows translational properties from mice to humans

MS-based PPP allows comparisons across species as it does not rely on specific protein epitopes (Geyer et al., 2017; Niu et al., 2019). In humans, RYGB most significantly altered proteins attributed to systemic inflammation and lipid metabolism, which were grouped into two panels consisting of 49 and 24 unique proteins, respectively (Wewer Albrechtsen et al., 2018). We detected 37 of the 49 inflammation markers and 20 of the 24 lipid transport associated proteins also in our plasma proteome analysis of treated male and female mice (Figure 31). Hence, the overall high degree of overlap allows direct comparisons of these panels between compound treated mice and RYGB in humans.

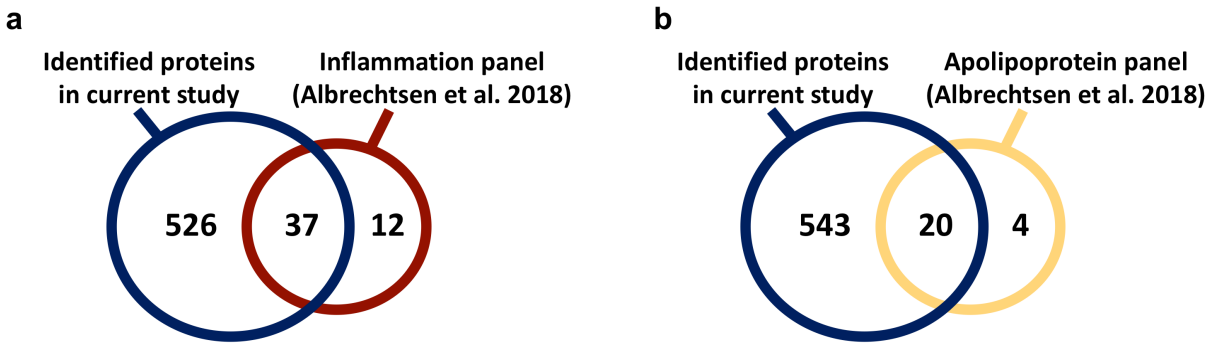

Figure 31: Plasma proteome profile shows translational properties from mice to humans.

Venn diagrams showing the overlap of proteins that were detected in our study with the inflammation **(a)** and lipid transport **(b)** panel defined by Wewer Albrechtsen et al., 2018.

4.2.6 Plasma proteome profile after GLP-1/GIP treatment mimics proteomic changes after RYGB

Due to the marked sex-differences, we first analyzed treatment responses in male and female mice separately, before we interpreted individual plasma proteins that were modulated in both sexes. We compared the plasma proteome of vehicle treated mice to that of either GIP, GLP-1, or GLP-1/GIP treated mice to obtain treatment-specific plasma proteome changes. Importantly, only very few differentially regulated proteins cluster in one of the contamination panels defined by Geyer et al. 2019 (Geyer et al., 2019), which indicates that most highlighted proteins are likely a true treatment effect (Figure 32).

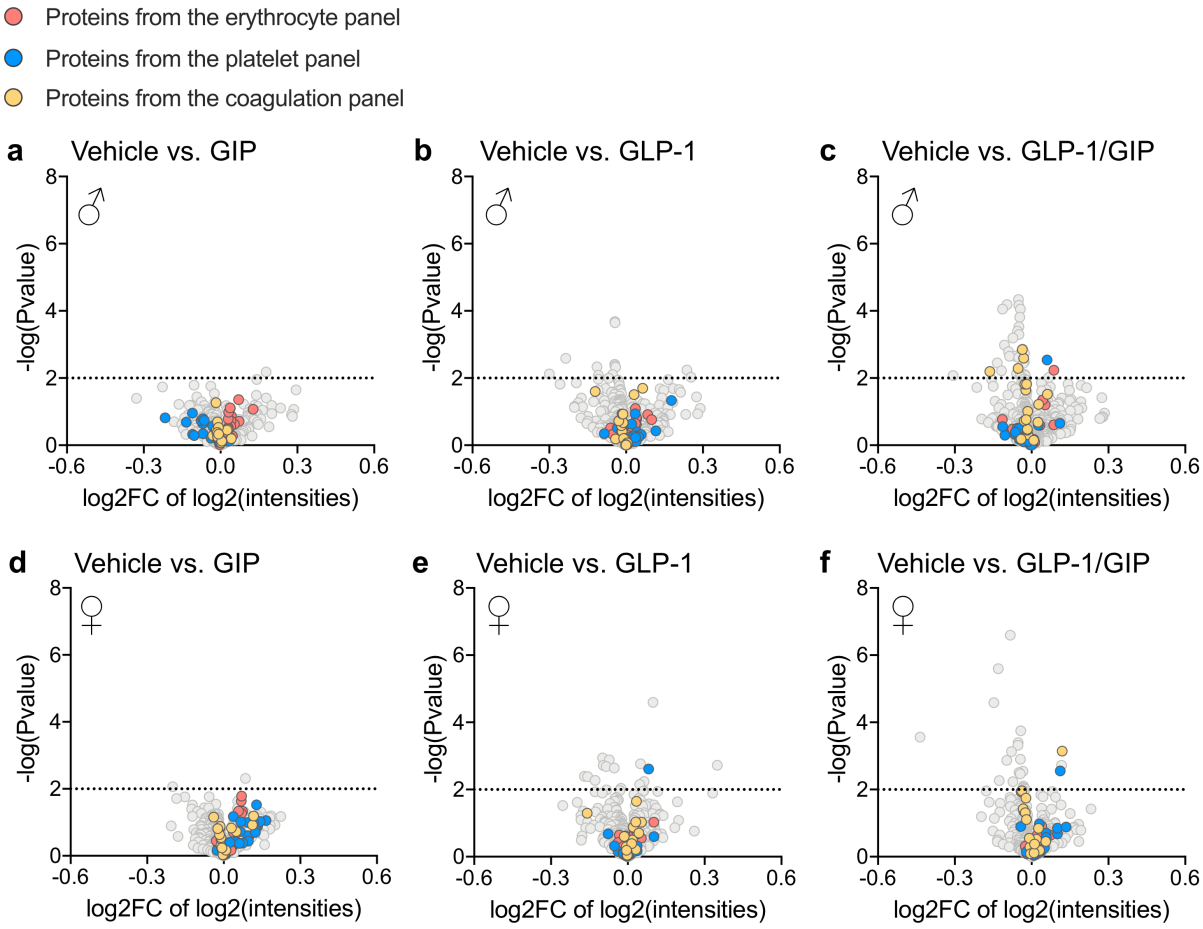

Figure 32: Volcano plots assessing quality bias in two-group comparisons of treated mice.

Proteins indicating potential contamination defined by Geyer at al. derived from erythrocyte, platelet, and coagulation proteins are highlighted in red, blue, and yellow (Geyer et al., 2019). The dashed line indicates significance (p-value < 0.01). Comparison of male vehicle vs. male GIP **(a)**, GLP-1 **(b)**, and GLP-1/GIP **(c)** treated mice. In (c) significantly regulated proteins: Pkm (platelet panel); F11, Apoc3, Gpld1, and F2 (coagulation panel); Aldoa (erythrocyte panel). **(d)** Comparison of female vehicle vs. female GIP **(d)**, GLP-1 **(e)**, and **(f)** GLP-1/GIP treated mice. In **(e)** significantly regulated proteins: F13a1 (platelet panel). In **(f)** significantly regulated proteins: Thbs1 (platelet panel); Pf4 (coagulation panel). Figures 32a-f with permission from Sachs et al. 2020b.

4.2.7 GLP-1/GIP treatment resolves systemic inflammation in male mice

In male DIO mice, compound treatment induced a stronger down- than upregulation of plasma proteins (Figure 33a). There was no overlap of upregulated proteins between different treatments (Figure 33a). Among GLP-1/GIP upregulated proteins, we found Complement C1q C Chain (C1qc) and Pyruvate kinase (Pkm) (Figure 33b). Pkm belongs to the platelet contamination panel, but the increase in all GLP-1/GIP treated mice suggest a treatment specific effect rather than a contamination of specific samples (Figure 33b). Both, C1qc and Pkm are associated with the polarization of anti-inflammatory macrophages (Palsson-McDermott et al., 2015; Spivia et al., 2014). GLP-1/GIP treatment decreased 33 proteins in contrast to GLP-1 that only reduced ten proteins and GIP had no effect (Figure 33a). We found an overlap of six proteins between GLP-1 and GLP-1/GIP downregulated proteins (Figures

33a, c). These results indicated that co-agonist treatment induced broader changes of the plasma proteome than mono-agonist treatment, underscoring the additional effect of GLP-1/GIP to reduce body weight and improve glucose and lipid metabolism in male DIO mice.

RYGB-induced body weight loss in humans has been shown to chronically reduce systemic inflammation (Wewer Albrechtsen et al., 2018). Hence, we were interested in the anti-inflammatory effect of GLP-1 and GLP-1/GIP treatment in obese male mice. Among the GLP-1/GIP downregulated proteins, eight proteins overlapped with the 37 proteins of the inflammation panel defined by Wewer Albrechtsen et al. (Figure 33a) (Wewer Albrechtsen et al., 2018). Only three of them (Serum amyloid A1 (Saa1), Alpha-1-acid glycoprotein 1 (Orm1), and Peptidoglycan recognition protein 2 (Pglyrp2)) were also downregulated by GLP-1 (Figures 33a, c). GLP-1/GIP additionally reduced plasma proteins levels of Alpha-1-acid glycoprotein 2 (Orm2), Serum amyloid A4 (Saa4), Mannan-binding lectin-associated serine proteases (Masp2), Plasma blood coagulation factor II (F2), and Plasma protease C1 inhibitor (Serping1) (Figure 33c). We calculated the systemic inflammation status of mice by taking the median expression of these eight proteins. Thereby, we found that only GLP-1/GIP treatment synergistically improved the inflammation status of male DIO mice (Figure 27d). Additionally, GLP-1/GIP treatment more potently reduced plasma protein abundancies of Serpin family A member 10 (Serpina10), Carboxypeptidase B2 (Cpb2), and Plasma blood coagulation factor XI (F11) (Figure 33d), which are involved in inflammatory processes or the complement system but were not affected by RYGB in humans (Wewer Albrechtsen et al., 2018). Leucine-rich alpha-2-glycoprotein (Lrg1), Hemoglobin subunit beta-1 (Hbb1), Melanoma cell adhesion molecule (Mcam), Cell growth regulator with EF hand domain protein 1 (Cgref1), and Phosphatidylinositol-glycan-specific phospholipase D (Gpld1) are recently suggested biomarkers for cardiovascular disease (Luo et al., 2017; O'Brien et al., 1996; Pek et al., 2018; Puig et al., 2011; Watanabe et al., 2007). Both, GLP-1 and GLP-1/GIP treatment reduced plasma Lrg1 levels (Figure 33c). In contrast, the co-agonist more potently reduced Hbb1, Mcam, Cgref1, and Gpld1 compared to both single agonists (Figure 33c). Together with reduced levels of the apolipoproteins Apoc2, Apoc3, and Apoc4 (Figure 33c), additional changes in the plasma proteome highlight the additional, potentially beneficial effects of GLP-1/GIP in treating cardio-metabolic disease.

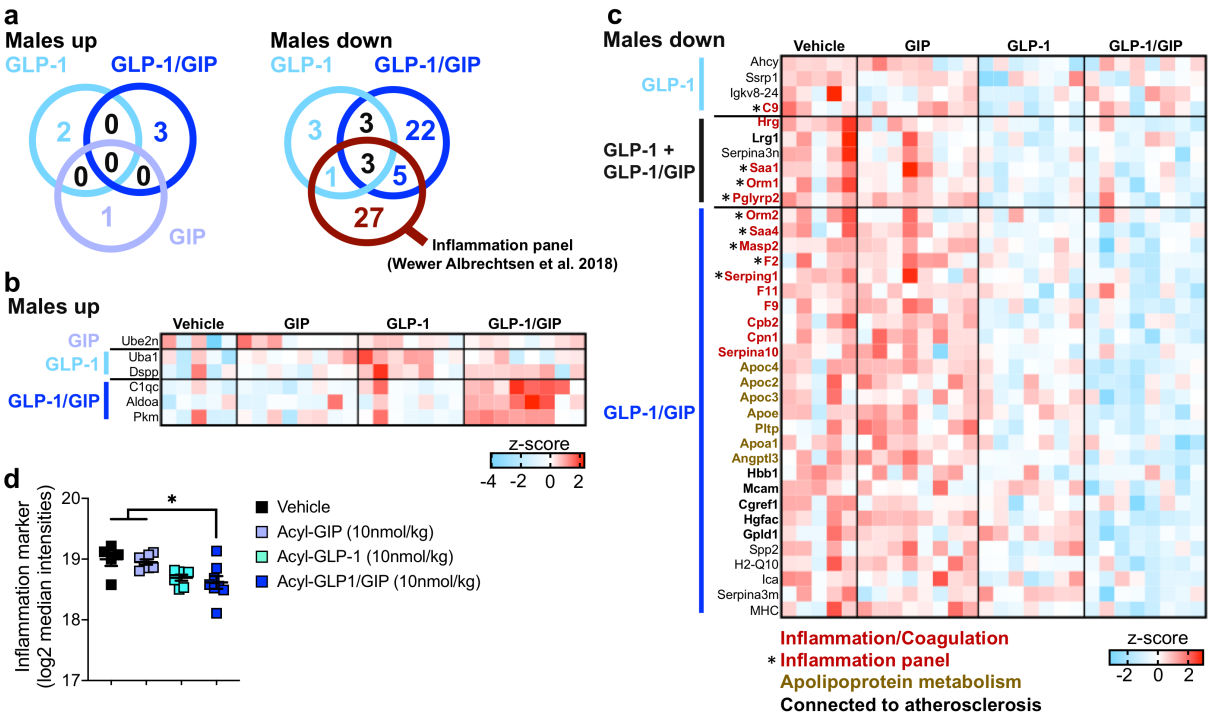

Figure 33: GLP1/GIP resolves systemic inflammation in male DIO mice.

(a) Overlap of up- and downregulated proteins by the specific treatment compared to vehicle treatment depicted in a Venn diagram ($p < 0.01$). **(b)** Upregulated proteins depicted in a heat map. **(c)** Downregulated proteins depicted in a heat map. Protein intensities were log2-transformed. The Z-score normalized protein levels across samples. **(d)** Systemic inflammation (proteins marked with asterisk in (c) – proteins regulated by bariatric surgery in humans and GLP-1/GIP treatment in mice) after compound treatment. Vehicle: n = 5; GIP: n = 8; GLP-1: n = 7: GLP-1/GIP: n = 8. Figures 33a-d with permission from Sachs et al. 2020b.

4.2.8 Broader plasma protein changes by GLP-1/GIP in female DIO mice

Similarly to males, also in female DIO mice, there was a stronger down- than upregulation of plasma proteins (Figure 34a). There was no overlap among the one, six, and three upregulated proteins by GIP, GLP-1, and GLP-1/GIP treatment (Figure 34a). GIP increased protein levels of Lactate dehydrogenase A (Ldha), which is a monomeric subunit of lactate hydrogenase, the rate-limiting enzyme in anaerobic glycolysis (Figure 34b). GLP-1 treatment was associated with increased levels of Coagulation factor XIII B chain (F13b), Coagulation factor XIII A chain (F13a1), and Protein Hc (Hc, also known as α1-microglobulin) (Figure 34b). F13b and F13a1 are components of the plasma factor XIII tetramer, which catalyzes the last step of blood coagulation. F13a1 belongs to the fibrinogenic contamination panel (Figure 32e), but similar to F13b, its plasma levels are specifically increased after GLP-1 treatment (Figure 34b). We found increased levels of Platelet factor 4 (Pf4, also known as C-X-C motif chemokine 4, Cxcl4) and Thrombospondin 1 (Thbs1) in plasma of female DIO mice after GLP-1/GIP treatment (Figure 34b). Cxcl4 and Thbs1 belong to the platelet and/or coagulation contamination panel (Figure 32f), but were specifically increased by co-agonist treatment (Figure 34b). Hence, due

to the specific increase of F13a1 (GLP-1) as well as of Cxcl4 and Thbs1 (GLP-1/GIP), we cannot exclude a true treatment specific effect on these plasma proteins.

Among the downregulated proteins, we found that GIP reduced circulating levels of Collagen type XVIII alpha 1 chain (Col18a1), a suggested biomarker for cardiovascular disease (Yin et al., 2014) (Figure 34c). We found five overlapping proteins between the nine GLP-1 and 19 GLP-1/GIP downregulated proteins in female mice (Figures 34a, c). GLP-1 more potently reduced plasma levels of inflammation-associated Dipeptidase 2 (Dpep2) and Proteoglycan 4 (Prg4) (Figure 34c). Interestingly, GLP-1 and GLP-1/GIP therapy reduced NAFLD markers Aldob, Lap3, and Me1, with an additional effect of GLP-1/GIP to reduce Enpep, another recently identified NAFLD marker (Figure 34c) (Niu et al., 2019). Moreover, GLP-1/GIP treatment reduced proteins associated with inflammation (Serine palmitoyltransferase, long chain base subunit 2 (Sptlc2), Cd5 Molecule Like (Cd5l), Carboxypeptidase B2 (Cpb2), Carboxypeptidase N (Cpn1)), lipid transport (Apoc4, Angiopoietin-related protein 3 (Angptl3), Phospholipid transfer protein (Pltp)), as well as a novel CVD biomarker (Hepatocyte growth factor activator (Hgfac)) (Figure 34c). Out of the RYGB-associated inflammatory panel solely Pglyrp2 was reduced after GLP-1 and GLP-1/GIP treatment in female DIO mice (Figure 34c). This is in stark contrast to reduction of the inflammation panel by GLP-1/GIP in male DIO mice and underlines the aforementioned DIO-associated sex-specific differences.

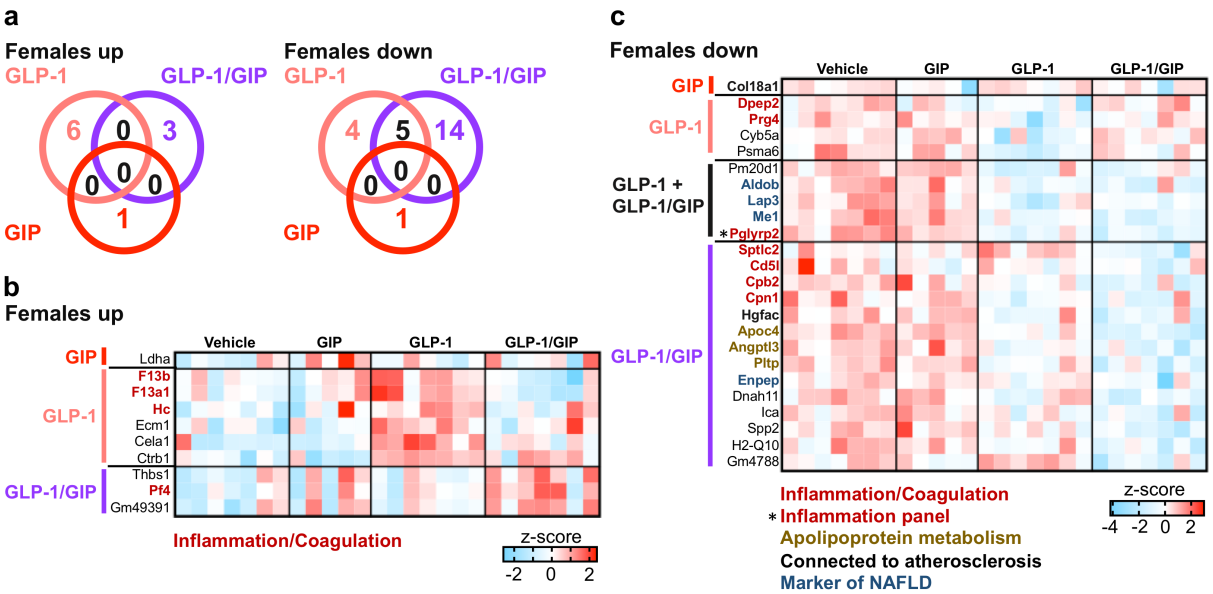

Figure 34: GLP1/GIP induced broader changes in the plasma proteome of female mice.

(a) Overlap of up- and downregulated proteins by the specific treatment compared to vehicle treatment depicted in a Venn diagram ($p < 0.01$). **(b)** Upregulated proteins depicted in a heat map. **(c)** Downregulated proteins depicted in a heat map. Protein intensities were log2-transformed. The Z-score normalized protein levels across samples. Vehicle: n = 7; GIP: n = 5 GIP; GLP-1: n = 7; GLP-1/GIP: n = 7 GLP-1/GIP. Figures 34a-c with permission from Sachs et al. 2020b.

4.2.9 Comparison of regulated proteins between male and female mice after treatment

Overall, we found little overlap between differentially regulated proteins after GIP, GLP-1, and GLP-1/GIP treatment in male and female DIO mice (Figure 35). Still, we identified ten proteins that were downregulated by GLP-1/GIP treatment compared to vehicle treatment in males and females (Figure 35c). Among the commonly decreased proteins we found Pltp and Angptl3, which are both involved in lipid metabolism and high plasma levels are associated with obesity, T2D, and cardiovascular disease in humans (Jiang, 2018; Tikka and Jauhiainen, 2016). Reduction of plasma Apoc4 levels in both sexes are in accordance with decreased LDL levels after GLP-1/GIP treatment in male and female DIO mice (Figures 21b, d). We also found lower levels of Hgfac in both sexes. Hgfac converts hepatocyte growth factor (Hgf) to its active form and increased levels of Hgf have been associated with a more severe progression of atherosclerosis in humans (Bell et al., 2018).

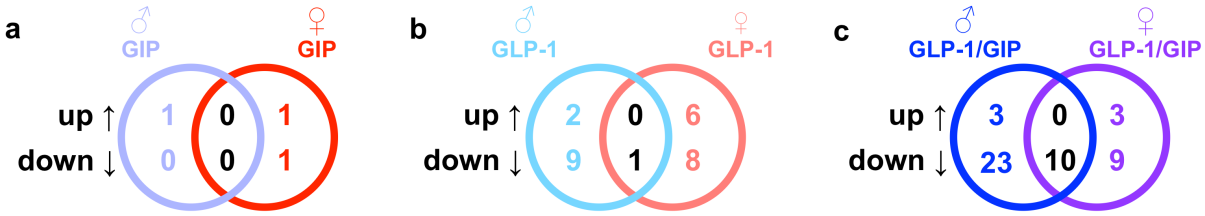

Figure 35: Common and differentially regulated plasma proteins after mono-agonist and co-agonist treatment in male and female DIO mice.

Differentially and common up- and downregulated plasma proteins of DIO male and female mice after GIP **(a)**, GLP-1 **(b)**, and GLP-1/GIP **(c)** treatment depicted in Venn diagrams. Figures 35a-c with permission from Sachs et al. 2020b.

5. Discussion

5.1 Targeted pharmacological therapy restores β-cell function for diabetes remission

This study describes the fate of islet endocrine cells using massive parallel scRNA-seq of more than 36.000 islet cells in health state as well as in mSTZ-diabetes and after compound treatment to dissect paths and mechanisms of β-cell failure and regeneration. In healthy mice, mature (β1) and immature and/or proliferative β-cells (β2) co-exist in pancreatic islets (Bader et al., 2016). After mSTZ-induced β-cell ablation, changes in islet niche and 100 days of long-term hyperglycemia, remaining β-cells dedifferentiate to a dysfunctional state. Intensive insulin therapy not only relieves β-cells from systemic hyperglycemia, but also activates insulin signaling directly in β-cells for mSTZ-diabetes remission. Combining insulin with GLP-1/estrogen therapy reduced insulin requirements by 60% and elicits an estrogen transcriptional response specifically in β-cells, which was accompanied by increased β-cell number and improved β-cell function compared to either monotherapy. Thereby, blood glucose normalization restored β-cell GLP-1R expression that potentially facilitated the enhanced delivery, uptake and action of estrogen and might also increase GLP-1 signaling in β-cells. Hence, targeted delivery of estrogen via GLP-1 and intensive insulin therapy leads to β-cell redifferentiation by distinct mechanisms of action. These results demonstrate that the mSTZ model is valuable to study islet cell regeneration after severe islet damage and demonstrate that combinatorial therapy has the potential to regenerate β-cells.

5.1.1 The mSTZ model reveals important markers and paths of β-cell failure and dedifferentiation

Since its first description in 1963, the streptozotocin-induced mouse diabetes model has been studied for more than 50 years (Rakieten et al., 1963). As for every preclinical model, the transferable value of the mSTZ model for human diabetes is questionable. This study showed that mSTZ leads to massive β-cell death, hyperglycemia, islet distortion, relative increase of α- and δ-cells, and surprisingly, also to substantial β-cell dedifferentiation. Dedifferentiated β-cells have been observed in multiple mouse models of hyperglycemia and human T1D and T2D, suggesting a conserved mechanism of β-cell failure (Brereton et al., 2014; Cinti et al., 2016; Jonas et al., 1999; Lam et al., 2018; Laybutt et al., 2002; Md Moin et al., 2016; Rui et al., 2017; Seiron et al., 2019; Talchai et al., 2012; Wang et al., 2014). However, most findings from dedifferentiated β-cells result from genetic mouse models of diabetes. There is a debate to weather β-cell dedifferentiation resembles a reversal to a pluripotent (Oct3/4, Nanog, Sox2) or endocrine progenitor state (Ngn3), or reflects normal β-cell heterogeneity, or is a glucotoxic-induced reversible state (Weir and Bonner-Weir, 2013). Thereby, it is important to understand if β-cells are degranulated, dedifferentiated, (partially) transdifferentiated, dysfunctional or lost, to find paths for regenerative therapy. Using scRNA-seq in healthy and mSTZ-diabetic mice, some of the questions were resolved.

The scRNA-seq profile of healthy mature and immature β-cells clearly aligned along a 1D trajectory close to dedifferentiated β-cells from mSTZ-diabetic mice. Calculating a cell-to-cell distance according to transcriptional nearest neighbors, clearly separates other non-β-cells from insulin positive cells. This was further substantiated by no on-going transition from α-, δ-, or PP-cells to dedifferentiated β-cells using velocity predictions. Although, we cannot completely exclude that dedifferentiated β-cells are partially formed by neogenesis as potential sources like acinar or duct cells were not sufficiently captured by our islet isolation method, we found no Ngn3 induction in islets of mSTZ-diabetic and compound treated mice. Together with recent lineage tracing experiments (Brereton et al., 2014; Wang et al., 2014), this strongly suggests that remaining β-cells of the mSTZ model are dedifferentiated β-cells. Thereby, upregulation of the endocrine master regulator *Ngn3* might depend on hyperglycemia severity: high glucose levels (> 33 mM) were shown to induce *Ngn3* expression (Talchai et al., 2012; Wang et al., 2014), whereas lower levels (< 25mM) were not (this study; Brereton et al., 2014; Jonas et al., 1999; Laybutt et al., 2002). Interestingly, mSTZ-diabetic β-cells increased Gastrin and Cck expression, which are also transiently expressed during pancreatic development (Brand et al., 1984; Liu, 2001; Suissa et al., 2013). Recently, Dahan et al. reported a *Ngn3* independent ectopic Gastrin expression in β-cells of diabetic rodents and T2D humans (Dahan et al., 2017). Together, these results indicate that β-cells of mSTZ-diabetic mice dedifferentiate to an earlier embryonic endocrine state after Ngn3 induction.

Remaining β-cells of mSTZ-treated mice acquire the expression of the only currently known β-cell dedifferentiation markers Aldh1a3 and Gastrin (Cinti et al., 2016; Dahan et al., 2017) as well as a panel of so far undescribed dedifferentiation markers (e.g. *Aqp4*, *Scarf2*, *Ptger3, Slc5a10, Aldob*). Careful systems biology and transcriptomic studies of hundreds of organ donors from individuals with T2D (Solimena et al., 2018) has identified many dysregulated genes, which we also find in this study, such as e.g. *CD44*, *G6PC2*, *PPP1R1A*, *SLC2A2*, *CD200*, *IAPP*, *RBP4*, *SLC30A8*, *SYT13*, and *ALDOB*. Similarly, as for the mSTZ β-cells, genes like e.g. *Aldh1a3*, *Cd200*, *Chgb*, *Gpx3*, *Slc2a2*, *Ppp1r1a*, *Trpm5*, and *Cox6a2* were dysregulated in sorted β-cells of DIO mice (Dusaulcy et al., 2019).

β-cells that do not contain any secretory granules are found in rodent and human diabetes (Brereton et al., 2014; Cinti et al., 2016; Marselli et al., 2014). It is not clear whether these degranulated β-cells are in fact “empty” cells without any insulin or insulin expression is just not detected by standard immunohistochemistry due to very low insulin levels in these cells. Recently, Lam et al. found substantial numbers of insulin positive cells by improving the staining protocol in recent onset and long-term T1D (Lam et al., 2018). Both, degranulated and dedifferentiated β-cells are characterized by decreased insulin expression accompanied by β-cell dysfunction to secrete insulin. Some degranulated or “empty” β-cells of human T2D expressed the β-cell dedifferentiation marker ALDH1A3 (Cinti et al., 2016). Glycemia normalization reversed β-cell degranulation and/or dedifferentiation in genetic mouse models of diabetes (Brereton et al., 2014). Hence, degranulated and dedifferentiated β-cells potentially refers to the same dysfunctional β-cell state. In the future, it will be especially interesting and

important to validate the large list of upregulated β-dedifferentiation markers in human studies and tissue collections. This will identify potential entry sites to target dedifferentiated β-cells in diabetes and further resolve the semantic debate on β-cell degranulation and dedifferentiation.

5.1.2 Regeneration of β-cells by GLP-1/estrogen and/or insulin treatment

mSTZ-treated mice remained diabetic with no increase of functional β-cell mass over the course of the study (> 100 days). Importantly, these results suggest that β-cells remain dedifferentiated upon sustained hyperglycemia and cannot be regenerated from endogenous cell sources to improve the disease state. Glycemia normalization by intensive insulin therapy has been shown to transiently reverse β-cell dysfunction in T1D and T2D (Harrison et al., 2012; Kramer et al., 2013, 1998). Two recent genetic lineage tracing studies have indicated that upon blood glucose normalization dedifferentiated β-cells were redifferentiated by insulin or anti-diabetic drug treatment (Brereton et al., 2014; Wang et al., 2014). It remains uncertain if these redifferentiated β-cells reacquire functionality due to the genetic burden of the used mouse models. ScRNA-seq allowed the dissection of endocrine subtype-specific transcriptional responses after chronic compound treatment. Thereby, the insulin monotreatment triggered a transcriptional response specific for β-cells, which is connected to insulin and/or IRS signaling. This supports the idea that besides relieving β-cells from glucotoxic stress, direct insulin/IGF signaling improves β-cell health and can regenerate functional β-cells in diabetes (Ueki et al., 2006). Importantly, insulin treatment redifferentiated functional β-cells in the mSTZ model, which responded to physiological stimuli as indicated by increased plasma C-peptide levels. These results show functional β-cell recovery upon glycemia normalization and extents findings from insulin treatment in genetically modified mouse models (Brereton et al., 2014; Wang et al., 2014).

GLP-1 analogs and estrogen mimetics prevent the onset of STZ-induced diabetes (Le May et al., 2006; Li et al., 2003; Puah and Bailey, 1985). Here, we started the compound treatment after mSTZ-induced hyperglycemia and β-cell dysfunction manifested. In this restorative therapeutic setting, neither estrogen nor GLP-1 monotherapy reduced glucose levels or improved β-cell function at the doses tested herein. GLP-1R expression is reduced in rodent models of hyperglycemia (Xu et al., 2007; mSTZ in this thesis). In glucose intolerant and T2D humans, the GLP-1 responsiveness is partially maintained, but the GLP-1 induced insulin secretion is ameliorated (Fritsche et al., 2000). Hence, inadequate β-cell GLP-1R expression might contribute to the lack of efficacy of GLP-1 analogs to improve or prevent the progressive loss of β-cell function in human T1D and T2D as well as mSTZ-diabetic mice (Chon and Gautier, 2016; Drucker et al., 2017). Strikingly, the GLP-1/estrogen conjugate synergistically improved mSTZ-diabetes. With prolonged treatment duration, reduced glucose levels likely increased β-cell GLP-1R expression accompanied by improved β-cell function, as indicated by increased fasting C-peptide levels and partial re-expression of β-cell maturation markers. GLP-1/estrogen and insulin co-therapy enhanced GLP-1R expression on dedifferentiated β-cells, which further increased the susceptibility of targeted estrogen delivery. Accordingly, the

combo-treatment triggered the ERAD pathway and tRNA signaling specifically in β-cells, which are both described targets of estrogen receptor activation (Torrent et al., 2018; Xu et al., 2018; Zhu et al., 2018). Altogether, these results demonstrate that the GLP-1 peptide can be used to specifically shuttle estrogen into GLP-1R expressing β-cells for β-cell redifferentiation and diabetes remission in mSTZ mice.

Moreover, this thesis shows that the induction of redifferentiation from dedifferentiated β-cells could be a new therapeutic approach for the treatment of diabetes, which does not involve the creation of new cells *per se*. Analyzing the fate of endocrine cells after 100 days of drug treatment implied neither a transition from α-, nor δ- , or PP-cells towards insulin positive β-cells. These results suggest that dedifferentiated β-cell are redifferentiated along the β-cell lineage with no major contribution of other endocrine cells to increase the functional β-cell mass after GLP-1/estrogen, PEG-insulin, and co-treated mice.

5.2 Shared benefits of GLP-1/GIP dual-agonism in mice and bariatric surgery in humans

RYGB is still the most effective intervention for morbidly obese patients to reduce body weight and improve disease related co-morbidities. Its underlining mechanisms are still poorly understood. Due to technological improvements in analyzing the plasma proteome, Wewer Albrechtsen recently showed that RYGB-induced body weight loss in humans is accompanied by a reduction of systemic inflammation and improvements in lipid homeostasis potentially contributing to the overall improved disease state after RYGB (Wewer Albrechtsen et al., 2018). Clinically advancing monomeric peptide co-agonists with balanced activity for the GLP-1R and GIPR are currently the most effective treatment option to reduce body weight and improve glucose homeostasis in obese type 2 diabetic subjects and outperform best in class GLP-1R mono-agonists (Frias et al., 2018). The underlining mechanisms of superior efficacy of GLP-1R and GIPR co-agonism over mono-agonism are still unclear. Therefore, we applied PPP to examine whether chronic GLP-1/GIP treatment of male and female DIO mice more closely mimics metabolic benefits of RYGB compared to the individual components. Similarly to RYGB in humans, GLP1-GIP co-agonism reduced protein markers of systemic inflammation and lipid metabolism, thereby being more effective than treatment with either mono-agonist. In both sexes, the GLP-1/GIP co-agonist decreased plasma LDL cholesterol levels and improves NAFLD to a larger extent than mono-agonist treatment. Especially in male DIO mice, PPP revealed that treatment with the co-agonist more efficiently reduced proteins indicative of systemic inflammation.

5.2.1 GLP-1/GIP corrects obesity in male and female DIO mice

GLP-1/GIP treatment reduced body weight with comparable efficacy in both sexes. In female mice, the additional weight loss of the GLP-1/GIP co-agonist compared to the GLP-1 mono-agonist was accompanied by an increased anorectic effect of the co-agonism. Contrary, the additional weight loss of GLP-1/GIP treatment could not be explained by an additional anorectic effect compared to the GLP-1 treatment in male DIO mice. Finan et al. recently showed that GLP-1/GIP treatment of heavily obese male mice did not increase energy expenditure, but induced a greater weight loss compared to pair-fed animals (Finan et al., 2013). Together, these results indicate that other mechanisms such as malabsorption or decreased feeding efficiency might contribute to the GLP-1/GIP-induced body weight loss in male DIO mice, and interestingly, this might be differentially regulated in female DIO mice.

5.2.2 PPP revealed resolution of systemic inflammation by GLP-1/GIP in male DIO mice

The plasma proteome substantially differed between age- and body weight-matched male and female obese mice. It has been shown that men and male mice have increased plasma abundancies and activity of complement proteins compared to female counterparts (Gaya da Costa et al., 2018; Kotimaa et al., 2016). Unbiased and undirected PPP revealed increased protein levels of markers for systemic inflammation and the complement and coagulation

cascade in male compared to female DIO mice. Obesity has been associated with increased circulating components of the fibrinolytic and haemostatic system, which might partially explain the bigger cardiovascular risk in these individuals (Kaye et al., 2012; Mertens and Van Gaal, 2002). Whether the protection of female C57Bl6/J mice against DIO-complications results from such alterations in the plasma complement and coagulation pathways remains uncertain. Still, due to the described sex-specific differences, the effect of GLP-1/GIP to reduce plasma proteins involved in inflammatory and immunological processes was much more pronounced in male than in female DIO mice. Thereby, co-agonist treatment of male DIO mice more closely mimicked the resolution of systemic inflammation as observed after RYGB in humans compared to either mono-agonist (Wewer Albrechtsen et al., 2018). However, the additional anti-inflammatory phenotype after GLP-1/GIP treatment might have resulted from the superior weight loss (Geyer et al., 2016b; Wewer Albrechtsen et al., 2018), although direct immunoregulatory mechanisms of GLP-1 and/or GIP are also conceivable (Fishman et al., 2019).

5.2.3 GLP-1/GIP reduced the cardiovascular risk profile in both sexes

After 12-weeks of treatment, a fatty-acylated GLP-1/GIP co-agonist with balanced activity at each receptor (GLP-1R EC_{50} = 5pM ; GIPR EC_{50} = 3pM; 1.8mg/day) reduced body weight and improved glucose metabolism compared with placebo in T2D patients (Frias et al., 2017). More clinical studies like a dose-finding trail including a refined escalation schedule and, importantly, a trial with longer treatment duration is needed to completely assess the metabolic efficacy of this co-agonist in humans (NNC0090-2746 (Frias et al., 2017)). However, in the 12-week study, NNC0090-2746 was able to reduce plasma cholesterol compared to the placebo control group (Frias et al., 2017). As the GLP-1 control group had no effect, these results suggest a body weight-independent additional effect of the GLP-1R/GIPR co-agonist (Frias et al., 2017). Intrudingly, chronic GLP-1/GIP treatment synergistically reduced fasting plasma cholesterol levels in male and female DIO mice, which was predominantly attributable to a decrease in LDL lipid fractions and was superior to effects by GIP or GLP-1 mono-treatment. PPP further revealed a more efficient reduction of apolipoproteins pertinent to LDL particles by GLP-1R/GIPR co-agonism in both sexes. In addition, plasma protein markers of CVD risk in male (e.g. Hbb1, Mcam, Cgref1, Hgfac, Gpld1, Pltp, Angptl3) and female (e.g. Hgfac, Pltp, Angptl3) DIO mice were potently reduced by GLP-1/GIP treatment. These results underline the power of PPP. This unbiased approach not only measures multiple lipid particles in more detail and depth but also detects other metabolic risk factors simultaneously. Thereby, PPP requires much less blood/plasma volume, which usually limits such biomarker discovery and validation in preclinical pharmacological studies. Altogether, treatment with the GLP-1/GIP co-agonist more potently improved the cardiovascular risk profile of male and female DIO mice compared to treatment with each mono-agonist.

5.2.4 GLP-1/GIP as potential treatment for NAFLD

NAFLD is the hepatic manifestation of the metabolic syndrome and shares almost identical risk factors (Tilg et al., 2017). NAFLD describes a range of liver diseases from nonalcoholic fatty liver (NAFL) without inflammation to nonalcoholic steatohepatitis (NASH) that can ultimately lead to liver cirrhosis and cancer (Friedman et al., 2018). There is no approved drug to treat the disease that complements the recommended, but often not effective lifestyle change. Clinical trials investigating GLP-1R agonists for the treatment of NAFLD are currently conducted and have already shown promising results to reduce hepatic fat content and inflammation that may go beyond reducing body weight *per se* (Armstrong et al., 2016; Seghieri et al., 2018). As both, NAFL and NASH are reversible conditions, it is of importance to prevent further progression of disease. Therefore, plasma biomarkers that predict the disease risk and can indicate the therapy response are needed (Friedman et al., 2018). Niu et al. recently applied PPP to male mice and humans to identify novel biomarkers of liver disease, which potentially distinguish reversible NAFLD from irreversible liver cirrhosis (Niu et al., 2019). Plasma levels of proteins that belong to this biomarker panel of NAFLD including Aldob, Sord, Apcs, Dpp4, Lap3, Me1, and Enpep were higher in female compared to male DIO mice, which was in line with the increased hepatic lipid content of females and probably due to the different duration of HFD exposure (32 weeks in female vs. 7 weeks in male vehicle treated mice). In female DIO mice, GLP-1 and GLP-1/GIP treatment reduced plasma levels of Aldob, Lap3, and Me1 with an additional effect of the co-agonist to reduce plasma levels of Enpep. Altogether, these results not only suggest that the recently identified NAFLD biomarkers translate to both sexes, but also respond to compound treatment. In addition, GLP-1/GIP treatment decreased plasma Cd5l in female DIO mice. Increased plasma levels of Cd5l are found in women compared to men and pathological increased levels of Cd5l were found in patients with liver cirrhosis and thus suggestive as a biomarker for liver fibrosis (Sanjurjo et al., 2015). These results demonstrate the power of PPP to simultaneously detect multiple plasma markers of disease state and highlight the potential use of a GLP-1/GIP co-agonist to treat NAFLD in both sexes.

The results of this study indicate that GLP-1R/GIPR co-agonism more closely mimics the metabolic improvements of RYGB than GLP-1R or GIPR mono-agonism. This supports the rationale for integrating multiple hormones in a single entity to close the gap to metabolic benefits usually achieved only by bariatric surgery. Treatment with a GLP-1/GIP co-agonist is more effective than treatment with either mono-agonist to reduce body weight, to improve glucose tolerance, to ameliorate systemic inflammation, to improve dyslipidemia, to reduce cardiovascular risk, and to reduce the hepatic lipid content of male and female DIO mice. Altogether, the anti-obesity effects of GLP-1/GIP treatment can potentially prevent the progressive decline of functional β-cell mass in T2D.

6. Outlook and Perspectives

A major achievement of this thesis was to establish the mSTZ model of diabetes as preferable model to study β-cell dysfunction and dedifferentiation in the absence of genetic lesions. This allowed the discovery of many novel markers of β-cell dedifferentiation. Many of them code for surface molecules and receptors that might allow the detection, isolation, and characterization of dedifferentiated β-cells in order to reveal pathophysiological mechanisms of human T1D and T2D. Moreover, some of these markers might by unique therapeutic targets for β-cell redifferentiation.

GLP-1/estrogen, PEG-insulin, and GLP-1/estrogen plus PEG-insulin co-therapy regenerated functional β-cells in the mSTZ-diabetes model by distinct MOA's. Insulin treatment is being used for more than a century to substitute for inadequate endogenous insulin production and secretion in diabetes. The results of this thesis provide evidence that insulin treatment, beside reducing β-cell glucotoxicity, directly acts on β-cells to induce β-cell redifferentiation and reinstall β-cell identity and function. Direct metabolic actions of insulin on β-cells have been suggested before, but have never been formally proven on the single cell level. These results further support future clinical trials with intensive insulin treatment to disrupt the decline of functional β-cell mass in T1D and T2D. However, newly generated functional β-cells need to be protected against auto-immune killing to translate to T1D therapy. Recently, anti-CD3 immunotherapy halted progression of T1D for two years by preventing the auto-immune destruction of β-cells (Herold et al., 2002, 2013, 2019). Hence, insulin and anti-CD3 co-treatment might further delay the progression to T1D, by a combination of immune-protection, glucose lowering, and direct effects of insulin on β-cell regeneration. Based on the results presented herein of GLP-1/estrogen and GLP-1/estrogen and insulin co-therapy to regenerate functional β-cells in mSTZ-diabetic mice, even a quadruple pharmacological approach of anti-CD3, insulin, and GLP-1/estrogen combinatorial therapy might further prolong or even prevent T1D onset. Thereby, GLP-1 peptide targeting can be used to increase β-cell mass. ScRNA-seq revealed an induction of ER stress in dedifferentiated β-cells of mSTZ-diabetic mice. Recent evidence suggests ER stress as a major mechanism of functional β-cell mass loss in T1D and T2D (Back and Kaufman, 2012; Fonseca et al., 2011). Alleviating ER stress by new pharmacological means may thus afford future opportunities for disease modification in patients suffering from diabetes (Ghosh et al., 2019). Results of this thesis show that targeted delivery of estrogen via GLP-1 activates the ERAD pathway specifically in β-cells, which is a known mechanism to mitigate ER stress (Engin et al., 2013; Qi et al., 2017; Xu et al., 2018). There is now an increasing interest in the design and optimization of novel molecules to target ER stress in various diseases including β-cell loss in diabetes (Hetz et al., 2019). In the future, the GLP-1 peptide could be used to deliver such novel and more specific ER stress relievers into β-cells. As these small molecules are regarded as safe (Hetz et al., 2019), the fear of unintended plasma cleavage from the carrier peptide would be relatively little compared to the

GLP-1/estrogen conjugate. Still, the anti-obesity effects of GLP-1/estrogen (Finan et al., 2012) together with β-cell protection (Schwenk et al., 2015) and β-cell regeneration (this thesis), make GLP-1/estrogen a strong translational candidate for obesity treatment as well as T2D prevention/treatment.

GLP-1/GIP co-agonists are currently the best pharmacological approach to manage body weight and glucose metabolism in preclinical models and human T2D (Finan et al., 2013; Frias et al., 2018). While the strong anti-obesity effect potentially prevents the development of T2D, it is not clear yet whether these agonists also directly improve β-cell health or even regenerate declining β-cell mass. Interestingly, GIPR activation on β-cells triggers distinct beneficial pathways that preserve function and survival of diabetic β-cells and could thus complement β-cell GLP-1R stimulation (Campbell et al., 2016). In this context, a triple pharmacological approach of a covalently linkage of the GLP-1/GIP peptide to estrogen or other small molecules might further enhance the metabolic benefits compared to each individual treatment. The benefit of such a polypharmacological approach could be to reduce dosage while simultaneously synergize metabolic benefits and reduce the risk of side effects.

References

Ackermann, A.M., Moss, N.G., and Kaestner, K.H. (2018). GABA and Artesunate Do Not Induce Pancreatic α-to-β Cell Transdifferentiation In Vivo. Cell Metabolism *28*, 787-792.e3.

Ackermann Misfeldt, A., Costa, R.H., and Gannon, M. (2008). -Cell Proliferation, but Not Neogenesis, Following 60% Partial Pancreatectomy Is Impaired in the Absence of FoxM1. Diabetes *57*, 3069–3077.

Agersø, H., Jensen, L.B., Elbrønd, B., Rolan, P., and Zdravkovic, M. (2002). The pharmacokinetics, pharmacodynamics, safety and tolerability of NN2211, a new long-acting GLP-1 derivative, in healthy men. Diabetologia *45*, 195–202.

Aguilar-Olivos, N.E., Almeda-Valdes, P., Aguilar-Salinas, C.A., Uribe, M., and Méndez-Sánchez, N. (2016). The role of bariatric surgery in the management of nonalcoholic fatty liver disease and metabolic syndrome. Metabolism *65*, 1196–1207.

Ahrén, B. (2005). Type 2 diabetes, insulin secretion and beta-cell mass. Curr. Mol. Med. *5*, 275–286.

Al-Hasani, K., Pfeifer, A., Courtney, M., Ben-Othman, N., Gjernes, E., Vieira, A., Druelle, N., Avolio, F., Ravassard, P., Leuckx, G., et al. (2013). Adult Duct-Lining Cells Can Reprogram into β-like Cells Able to Counter Repeated Cycles of Toxin-Induced Diabetes. Developmental Cell *26*, 86–100.

Alonso-Magdalena, P., Ropero, A.B., Carrera, M.P., Cederroth, C.R., Baquié, M., Gauthier, B.R., Nef, S., Stefani, E., and Nadal, A. (2008). Pancreatic Insulin Content Regulation by the Estrogen Receptor ERα. PLoS ONE *3*, e2069.

Alpert, S., Hanahan, D., and Teitelman, G. (1988). Hybrid insulin genes reveal a developmental lineage for pancreatic endocrine cells and imply a relationship with neurons. Cell *53*, 295–308.

Alvarsson, M., Sundkvist, G., Lager, I., Henricsson, M., Berntorp, K., Fernqvist-Forbes, E., Steen, L., Westermark, G., Westermark, P., Orn, T., et al. (2003). Beneficial Effects of Insulin Versus Sulphonylurea on Insulin Secretion and Metabolic Control in Recently Diagnosed Type 2 Diabetic Patients. Diabetes Care *26*, 2231–2237.

Anderson, S.L., and Trujillo, J.M. (2016). Basal Insulin Use With GLP-1 Receptor Agonists. Diabetes Spectrum *29*, 152–160.

Angrisani, L., Santonicola, A., Iovino, P., Formisano, G., Buchwald, H., and Scopinaro, N. (2015). Bariatric Surgery Worldwide 2013. Obesity Surgery *25*, 1822–1832.

Ariyachet, C., Tovaglieri, A., Xiang, G., Lu, J., Shah, M.S., Richmond, C.A., Verbeke, C., Melton, D.A., Stanger, B.Z., Mooney, D., et al. (2016). Reprogrammed Stomach Tissue as a Renewable Source of Functional β Cells for Blood Glucose Regulation. Cell Stem Cell *18*, 410–421.

Armstrong, M.J., Gaunt, P., Aithal, G.P., Barton, D., Hull, D., Parker, R., Hazlehurst, J.M., Guo, K., Abouda, G., Aldersley, M.A., et al. (2016). Liraglutide safety and efficacy in patients with non-alcoholic steatohepatitis (LEAN): a multicentre, double-blind, randomised, placebo-controlled phase 2 study. The Lancet *387*, 679–690.

Aroda, V.R., Bain, S.C., Cariou, B., Piletič, M., Rose, L., Axelsen, M., Rowe, E., and DeVries, J.H. (2017). Efficacy and safety of once-weekly semaglutide versus once-daily insulin glargine as add-on to metformin (with or without sulfonylureas) in insulin-naive patients with type 2 diabetes (SUSTAIN 4): a randomised, open-label, parallel-group, multicentre, multinational, phase 3a trial. The Lancet Diabetes & Endocrinology *5*, 355–366.

Ashcroft, F.M., Harrison, D.E., and Ashcroft, S.J.H. (1984). Glucose induces closure of single potassium channels in isolated rat pancreatic β-cells. Nature *312*, 446–448.

Back, S.H., and Kaufman, R.J. (2012). Endoplasmic Reticulum Stress and Type 2 Diabetes. Annual Review of Biochemistry *81*, 767–793.

Bader, E., Migliorini, A., Gegg, M., Moruzzi, N., Gerdes, J., Roscioni, S.S., Bakhti, M., Brandl, E., Irmler, M., Beckers, J., et al. (2016). Identification of proliferative and mature β-cells in the islets of Langerhans. Nature *535*, 430–434.

Bastidas-Ponce, A., Scheibner, K., Lickert, H., and Bakhti, M. (2017). Cellular and molecular mechanisms coordinating pancreas development. Development *144*, 2873–2888.

Beamish, A.J., Olbers, T., Kelly, A.S., and Inge, T.H. (2016). Cardiovascular effects of bariatric surgery. Nature Reviews Cardiology *13*, 730–743.

Becht, E., McInnes, L., Healy, J., Dutertre, C.-A., Kwok, I.W.H., Ng, L.G., Ginhoux, F., and Newell, E.W. (2018). Dimensionality reduction for visualizing single-cell data using UMAP. Nature Biotechnology *37*, 38–44.

Bell, E.J., Decker, P.A., Tsai, M.Y., Pankow, J.S., Hanson, N.Q., Wassel, C.L., Larson, N.B., Cohoon, K.P., Budoff, M.J., Polak, J.F., et al. (2018). Hepatocyte growth factor is associated with progression of atherosclerosis: The Multi-Ethnic Study of Atherosclerosis (MESA). Atherosclerosis *272*, 162–167.

Ben-Othman, N., Vieira, A., Courtney, M., Record, F., Gjernes, E., Avolio, F., Hadzic, B., Druelle, N., Napolitano, T., Navarro-Sanz, S., et al. (2017). Long-Term GABA Administration Induces Alpha Cell-Mediated Beta-like Cell Neogenesis. Cell *168*, 73-85.e11.

Blondel, V.D., Guillaume, J.-L., Lambiotte, R., and Lefebvre, E. (2008). Fast unfolding of communities in large networks. Journal of Statistical Mechanics: Theory and Experiment *2008*, P10008.

Bluestone, J.A., Herold, K., and Eisenbarth, G. (2010). Genetics, pathogenesis and clinical interventions in type 1 diabetes. Nature *464*, 1293–1300.

Blum, B., Hrvatin, S., Schuetz, C., Bonal, C., Rezania, A., and Melton, D.A. (2012). Functional beta-cell maturation is marked by an increased glucose threshold and by expression of urocortin 3. Nature Biotechnology *30*, 261–264.

Bonner-Weir, S., Baxter, L.A., Schuppin, G.T., and Smith, F.E. (1993). A Second Pathway for Regeneration of Adult Exocrine and Endocrine Pancreas: A Possible Recapitulation of Embryonic Development. Diabetes *42*, 1715–1720.

Bonner-Weir, S., Toschi, E., Inada, A., Reitz, P., Fonseca, S.Y., Aye, T., and Sharma, A. (2004). The pancreatic ductal epithelium serves as a potential pool of progenitor cells. Pediatric Diabetes *5*, 16–22.

Bonner-Weir, S., Inada, A., Yatoh, S., Li, W.-C., Aye, T., Toschi, E., and Sharma, A. (2008). Transdifferentiation of pancreatic ductal cells to endocrine β-cells. Biochemical Society Transactions *36*, 353–356.

Bouwens, L., and Pipeleers, D.G. (1998). Extra-insular beta cells associated with ductules are frequent in adult human pancreas. Diabetologia *41*, 629–633.

Brand, S.J., Andersen, B.N., and Rehfeld, J.F. (1984). Complete tyrosine-O-sulphation of gastrin in neonatal rat pancreas. Nature *309*, 456–458.

Brereton, M.F., Iberl, M., Shimomura, K., Zhang, Q., Adriaenssens, A.E., Proks, P., Spiliotis, I.I., Dace, W., Mattis, K.K., Ramracheya, R., et al. (2014). Reversible changes in pancreatic islet structure and function produced by elevated blood glucose. Nature Communications *5*, 4639.

Brestoff, J.R., and Artis, D. (2015). Immune Regulation of Metabolic Homeostasis in Health and Disease. Cell *161*, 146–160.

Brown, J.B., Nichols, G.A., and Perry, A. (2004). The burden of treatment failure in type 2 diabetes. Diabetes Care *27*, 1535–1540.

Brown, J.B., Conner, C., and Nichols, G.A. (2010). Secondary Failure of Metformin Monotherapy in Clinical Practice. Diabetes Care *33*, 501–506.

Buchwald, H., and Buchwald, J.N. (2019). Metabolic (Bariatric and Nonbariatric) Surgery for Type 2 Diabetes: A Personal Perspective Review. Diabetes Care *42*, 331–340.

Buchwald, H., Avidor, Y., Braunwald, E., Jensen, M.D., Pories, W., Fahrbach, K., and Schoelles, K. (2004). Bariatric Surgery: A Systematic Review and Meta-analysis. JAMA *292*, 1724.

Buchwald, H., Estok, R., Fahrbach, K., Banel, D., Jensen, M.D., Pories, W.J., Bantle, J.P., and Sledge, I. (2009). Weight and Type 2 Diabetes after Bariatric Surgery: Systematic Review and Meta-analysis. The American Journal of Medicine *122*, 248-256.e5.

Butler, A.E., Janson, J., Bonner-Weir, S., Ritzel, R., Rizza, R.A., and Butler, P.C. (2003). Beta-cell deficit and increased beta-cell apoptosis in humans with type 2 diabetes. Diabetes *52*, 102–110.

Butler, A.E., Cao-Minh, L., Galasso, R., Rizza, R.A., Corradin, A., Cobelli, C., and Butler, P.C. (2010). Adaptive changes in pancreatic beta cell fractional area and beta cell turnover in human pregnancy. Diabetologia *53*, 2167–2176.

Büttner, M., Miao, Z., Wolf, F.A., Teichmann, S.A., and Theis, F.J. (2019). A test metric for assessing single-cell RNA-seq batch correction. Nature Methods *16*, 43–49.

Camastra, S., Manco, M., Mari, A., Greco, A.V., Frascerra, S., Mingrone, G., and Ferrannini, E. (2007). -Cell Function in Severely Obese Type 2 Diabetic Patients: Long-term effects of bariatric surgery. Diabetes Care *30*, 1002–1004.

Campbell, J.E., and Drucker, D.J. (2015). Islet α cells and glucagon--critical regulators of energy homeostasis. Nat Rev Endocrinol *11*, 329–338.

Campbell, J.E., Ussher, J.R., Mulvihill, E.E., Kolic, J., Baggio, L.L., Cao, X., Liu, Y., Lamont, B.J., Morii, T., Streutker, C.J., et al. (2016). TCF1 links GIPR signaling to the control of beta cell function and survival. Nature Medicine *22*, 84–90.

Camunas-Soler, J., Dai, X., Hang, Y., Bautista, A., Lyon, J., Suzuki, K., Kim, S.K., Quake, S.R., and MacDonald, P.E. (2019). Pancreas patch-seq links physiologic dysfunction in diabetes to single-cell transcriptomic phenotypes. BioRxiv 555110.

Carlsson, L.M.S., Peltonen, M., Ahlin, S., Anveden, Å., Bouchard, C., Carlsson, B., Jacobson, P., Lönroth, H., Maglio, C., Näslund, I., et al. (2012). Bariatric Surgery and Prevention of Type 2 Diabetes in Swedish Obese Subjects. New England Journal of Medicine *367*, 695–704.

Chen, E.Y., Tan, C.M., Kou, Y., Duan, Q., Wang, Z., Meirelles, G., Clark, N.R., and Ma'ayan, A. (2013). Enrichr: interactive and collaborative HTML5 gene list enrichment analysis tool. BMC Bioinformatics *14*, 128.

Chen, Y.-J., Finkbeiner, S.R., Weinblatt, D., Emmett, M.J., Tameire, F., Yousefi, M., Yang, C., Maehr, R., Zhou, Q., Shemer, R., et al. (2014). De Novo Formation of Insulin-Producing "Neo-β Cell Islets" from Intestinal Crypts. Cell Reports *6*, 1046–1058.

Chera, S., Baronnier, D., Ghila, L., Cigliola, V., Jensen, J.N., Gu, G., Furuyama, K., Thorel, F., Gribble, F.M., Reimann, F., et al. (2014). Diabetes recovery by age-dependent conversion of pancreatic δ-cells into insulin producers. Nature *514*, 503–507.

Chiang, M.-K., and Melton, D.A. (2003). Single-Cell Transcript Analysis of Pancreas Development. Developmental Cell *4*, 383–393.

Chon, S., and Gautier, J.-F. (2016). An Update on the Effect of Incretin-Based Therapies on β-Cell Function and Mass. Diabetes & Metabolism Journal *40*, 99.

Cinti, F., Bouchi, R., Kim-Muller, J.Y., Ohmura, Y., Sandoval, P.R., Masini, M., Marselli, L., Suleiman, M., Ratner, L.E., Marchetti, P., et al. (2016). Evidence of β-Cell Dedifferentiation in Human Type 2 Diabetes. The Journal of Clinical Endocrinology & Metabolism *101*, 1044–1054.

Clemmensen, C., Finan, B., Müller, T.D., DiMarchi, R.D., Tschöp, M.H., and Hofmann, S.M. (2019). Emerging hormonal-based combination pharmacotherapies for the treatment of metabolic diseases. Nature Reviews Endocrinology *15*, 90–104.

Collombat, P., Xu, X., Ravassard, P., Sosa-Pineda, B., Dussaud, S., Billestrup, N., Madsen, O.D., Serup, P., Heimberg, H., and Mansouri, A. (2009). The Ectopic Expression of Pax4 in the Mouse Pancreas Converts Progenitor Cells into α and Subsequently β Cells. Cell *138*, 449–462.

Coskun, T., Sloop, K.W., Loghin, C., Alsina-Fernandez, J., Urva, S., Bokvist, K.B., Cui, X., Briere, D.A., Cabrera, O., Roell, W.C., et al. (2018). LY3298176, a novel dual GIP and GLP-1 receptor agonist for the treatment of type 2 diabetes mellitus: From discovery to clinical proof of concept. Molecular Metabolism *18*, 3–14.

Dahan, T., Ziv, O., Horwitz, E., Zemmour, H., Lavi, J., Swisa, A., Leibowitz, G., Ashcroft, F.M., In't Veld, P., Glaser, B., et al. (2017). Pancreatic β-Cells Express the Fetal Islet Hormone Gastrin in Rodent and Human Diabetes. Diabetes *66*, 426–436.

Dai, C., Hang, Y., Shostak, A., Poffenberger, G., Hart, N., Prasad, N., Phillips, N., Levy, S.E., Greiner, D.L., Shultz, L.D., et al. (2017). Age-dependent human β cell proliferation induced by glucagon-like peptide 1 and calcineurin signaling. Journal of Clinical Investigation *127*, 3835–3844.

Damond, N., Engler, S., Zanotelli, V.R.T., Schapiro, D., Wasserfall, C.H., Kusmartseva, I., Nick, H.S., Thorel, F., Herrera, P.L., Atkinson, M.A., et al. (2019). A Map of Human Type 1 Diabetes Progression by Imaging Mass Cytometry. Cell Metabolism *29*, 755-768.e5.

D'Amour, K.A., Bang, A.G., Eliazer, S., Kelly, O.G., Agulnick, A.D., Smart, N.G., Moorman, M.A., Kroon, E., Carpenter, M.K., and Baetge, E.E. (2006). Production of pancreatic hormone–expressing endocrine cells from human embryonic stem cells. Nature Biotechnology *24*, 1392–1401.

Davies, M. (2004). The reality of glycaemic control in insulin treated diabetes: defining the clinical challenges. International Journal of Obesity *28*, S14–S22.

Davies, M., Pieber, T.R., Hartoft-Nielsen, M.-L., Hansen, O.K.H., Jabbour, S., and Rosenstock, J. (2017). Effect of Oral Semaglutide Compared With Placebo and Subcutaneous Semaglutide on Glycemic Control in Patients With Type 2 Diabetes: A Randomized Clinical Trial. JAMA *318*, 1460.

Day, J.W., Ottaway, N., Patterson, J.T., Gelfanov, V., Smiley, D., Gidda, J., Findeisen, H., Bruemmer, D., Drucker, D.J., Chaudhary, N., et al. (2009). A new glucagon and GLP-1 co-agonist eliminates obesity in rodents. Nature Chemical Biology *5*, 749–757.

Dirice, E., Walpita, D., Vetere, A., Meier, B.C., Kahraman, S., Hu, J., Dančík, V., Burns, S.M., Gilbert, T.J., Olson, D.E., et al. (2016). Inhibition of DYRK1A Stimulates Human β-Cell Proliferation. Diabetes *65*, 1660–1671.

Domínguez-Bendala, J., Qadir, M.M.F., and Pastori, R.L. (2019). Pancreatic Progenitors: There and Back Again. Trends in Endocrinology & Metabolism *30*, 4–11.

Dor, Y., Brown, J., Martinez, O.I., and Melton, D.A. (2004). Adult pancreatic beta-cells are formed by self-duplication rather than stem-cell differentiation. Nature *429*, 41–46.

Drucker, D.J. (2018). Mechanisms of Action and Therapeutic Application of Glucagon-like Peptide-1. Cell Metabolism *27*, 740–756.

Drucker, D.J., Habener, J.F., and Holst, J.J. (2017). Discovery, characterization, and clinical development of the glucagon-like peptides. Journal of Clinical Investigation *127*, 4217–4227.

Dubuc, P.U. (1985). Effects of Estrogen on Food Intake, Body Weight, and Temperature of Male and Female Obese Mice. Experimental Biology and Medicine *180*, 468–473.

Dugger, S.A., Platt, A., and Goldstein, D.B. (2018). Drug development in the era of precision medicine. Nature Reviews Drug Discovery *17*, 183–196.

Dusaulcy, R., Handgraaf, S., Visentin, F., Howald, C., Dermitzakis, E.T., Philippe, J., and Gosmain, Y. (2019). High-fat diet impacts more changes in beta-cell compared to alpha-cell transcriptome. PLOS ONE *14*, e0213299.

Ediger, B.N., Du, A., Liu, J., Hunter, C.S., Walp, E.R., Schug, J., Kaestner, K.H., Stein, R., Stoffers, D.A., and May, C.L. (2014). Islet-1 Is Essential for Pancreatic -Cell Function. Diabetes *63*, 4206–4217.

El Ouaamari, A., Dirice, E., Gedeon, N., Hu, J., Zhou, J.-Y., Shirakawa, J., Hou, L., Goodman, J., Karampelias, C., Qiang, G., et al. (2016). SerpinB1 Promotes Pancreatic β Cell Proliferation. Cell Metabolism *23*, 194–205.

Elrick, H., Stimmler, L., Hlad, C.J., and Arai, Y. (1964). Plasma Insulin Response to Oral and Intravenous Glucose Administration1. The Journal of Clinical Endocrinology & Metabolism *24*, 1076–1082.

Eng, J. (1992). Exendin peptides. Mt. Sinai J. Med. *59*, 147–149.

Engin, F., Yermalovich, A., Nguyen, T., Hummasti, S., Fu, W., Eizirik, D.L., Mathis, D., and Hotamisligil, G.S. (2013). Restoration of the Unfolded Protein Response in Pancreatic Cells Protects Mice Against Type 1 Diabetes. Science Translational Medicine *5*, 211ra156-211ra156.

Faria, S.L., Faria, O.P., Cardeal, M. de A., Ito, M.K., and Buffington, C. (2014). Diet-induced thermogenesis and respiratory quotient after Roux-en-Y gastric bypass surgery: A prospective study. Surgery for Obesity and Related Diseases *10*, 138–143.

Farilla, L., Hui, H., Bertolotto, C., Kang, E., Bulotta, A., Di Mario, U., and Perfetti, R. (2002). Glucagon-Like Peptide-1 Promotes Islet Cell Growth and Inhibits Apoptosis in Zucker Diabetic Rats. Endocrinology *143*, 4397–4408.

Ferber, S., Halkin, A., Cohen, H., Ber, I., Einav, Y., Goldberg, I., Barshack, I., Seijffers, R., Kopolovic, J., Kaiser, N., et al. (2000). Pancreatic and duodenal homeobox gene 1 induces expression of insulin genes in liver and ameliorates streptozotocin-induced hyperglycemia. Nature Medicine *6*, 568–572.

Feuchtinger, A., Stiehler, T., Jütting, U., Marjanovic, G., Luber, B., Langer, R., and Walch, A. (2015). Image analysis of immunohistochemistry is superior to visual scoring as shown for patient outcome of esophageal adenocarcinoma. Histochemistry and Cell Biology *143*, 1–9.

Fiaschi-Taesch, N.M., Kleinberger, J.W., Salim, F.G., Troxell, R., Wills, R., Tanwir, M., Casinelli, G., Cox, A.E., Takane, K.K., Srinivas, H., et al. (2013a). Cytoplasmic-Nuclear Trafficking of G1/S Cell Cycle Molecules and Adult Human -Cell Replication: A Revised Model of Human -Cell G1/S Control. Diabetes *62*, 2460–2470.

Fiaschi-Taesch, N.M., Kleinberger, J.W., Salim, F.G., Troxell, R., Wills, R., Tanwir, M., Casinelli, G., Cox, A.E., Takane, K.K., Scott, D.K., et al. (2013b). Human Pancreatic -Cell G1/S Molecule Cell Cycle Atlas. Diabetes *62*, 2450–2459.

Finan, B., Yang, B., Ottaway, N., Stemmer, K., Müller, T.D., Yi, C.-X., Habegger, K., Schriever, S.C., García-Cáceres, C., Kabra, D.G., et al. (2012). Targeted estrogen delivery reverses the metabolic syndrome. Nature Medicine *18*, 1847–1856.

Finan, B., Ma, T., Ottaway, N., Muller, T.D., Habegger, K.M., Heppner, K.M., Kirchner, H., Holland, J., Hembree, J., Raver, C., et al. (2013). Unimolecular Dual Incretins Maximize Metabolic Benefits in Rodents, Monkeys, and Humans. Science Translational Medicine *5*, 209ra151-209ra151.

Finan, B., Yang, B., Ottaway, N., Smiley, D.L., Ma, T., Clemmensen, C., Chabenne, J., Zhang, L., Habegger, K.M., Fischer, K., et al. (2015). A rationally designed monomeric peptide triagonist corrects obesity and diabetes in rodents. Nature Medicine *21*, 27–36.

Finan, B., Clemmensen, C., Zhu, Z., Stemmer, K., Gauthier, K., Müller, L., De Angelis, M., Moreth, K., Neff, F., Perez-Tilve, D., et al. (2016). Chemical Hybridization of Glucagon and Thyroid Hormone Optimizes Therapeutic Impact for Metabolic Disease. Cell *167*, 843-857.e14.

Fishman, S., Zvibel, I., and Varol, C. (2019). Incretin Hormones in the Control of Immunometabolism. IJ

1, e190004.

Fonseca, S.G., Gromada, J., and Urano, F. (2011). Endoplasmic reticulum stress and pancreatic β-cell death. Trends in Endocrinology & Metabolism.

Frias, J.P., Bastyr, E.J., Vignati, L., Tschöp, M.H., Schmitt, C., Owen, K., Christensen, R.H., and DiMarchi, R.D. (2017). The Sustained Effects of a Dual GIP/GLP-1 Receptor Agonist, NNC0090-2746, in Patients with Type 2 Diabetes. Cell Metabolism *26*, 343-352.e2.

Frias, J.P., Nauck, M.A., Van, J., Kutner, M.E., Cui, X., Benson, C., Urva, S., Gimeno, R.E., Milicevic, Z., Robins, D., et al. (2018). Efficacy and safety of LY3298176, a novel dual GIP and GLP-1 receptor agonist, in patients with type 2 diabetes: a randomised, placebo-controlled and active comparator-controlled phase 2 trial. The Lancet *392*, 2180–2193.

Friedman, S.L., Neuschwander-Tetri, B.A., Rinella, M., and Sanyal, A.J. (2018). Mechanisms of NAFLD development and therapeutic strategies. Nature Medicine *24*, 908–922.

Fritsche, A., Stefan, N., Hardt, E., Häring, H., and Stumvoll, M. (2000). Characterisation of beta-cell dysfunction of impaired glucose tolerance: Evidence for impairment of incretin-induced insulin secretion. Diabetologia *43*, 852–858.

Furuyama, K., Chera, S., van Gurp, L., Oropeza, D., Ghila, L., Damond, N., Vethe, H., Paulo, J.A., Joosten, A.M., Berney, T., et al. (2019). Diabetes relief in mice by glucose-sensing insulin-secreting human α-cells. Nature *567*, 43-48.

Gao, Q., Mezei, G., Nie, Y., Rao, Y., Choi, C.S., Bechmann, I., Leranth, C., Toran-Allerand, D., Priest, C.A., Roberts, J.L., et al. (2007). Anorectic estrogen mimics leptin's effect on the rewiring of melanocortin cells and Stat3 signaling in obese animals. Nature Medicine *13*, 89–94.

Gao, T., McKenna, B., Li, C., Reichert, M., Nguyen, J., Singh, T., Yang, C., Pannikar, A., Doliba, N., Zhang, T., et al. (2014). Pdx1 Maintains β Cell Identity and Function by Repressing an α Cell Program. Cell Metabolism *19*, 259–271.

Gaya da Costa, M., Poppelaars, F., van Kooten, C., Mollnes, T.E., Tedesco, F., Würzner, R., Trouw, L.A., Truedsson, L., Daha, M.R., Roos, A., et al. (2018). Age and Sex-Associated Changes of Complement Activity and Complement Levels in a Healthy Caucasian Population. Frontiers in Immunology *9*.

Geyer, P.E., Kulak, N.A., Pichler, G., Holdt, L.M., Teupser, D., and Mann, M. (2016a). Plasma Proteome Profiling to Assess Human Health and Disease. Cell Systems *2*, 185–195.

Geyer, P.E., Wewer Albrechtsen, N.J., Tyanova, S., Grassl, N., Iepsen, E.W., Lundgren, J., Madsbad, S., Holst, J.J., Torekov, S.S., and Mann, M. (2016b). Proteomics reveals the effects of sustained weight loss on the human plasma proteome. Molecular Systems Biology *12*, 901.

Geyer, P.E., Holdt, L.M., Teupser, D., and Mann, M. (2017). Revisiting biomarker discovery by plasma proteomics. Molecular Systems Biology *13*, 942.

Geyer, P.E., Voytik, E., Treit, P.V., Doll, S., Kleinhempel, A., Niu, L., Müller, J.B., Buchholtz, M., Bader, J.M., Teupser, D., et al. (2019). Plasma Proteome Profiling to detect and avoid sample-related biases in biomarker studies. EMBO Molecular Medicine *11*.

Ghosh, R., Colon-Negron, K., and Papa, F.R. (2019). Endoplasmic reticulum stress, degeneration of pancreatic islet β-cells, and therapeutic modulation of the unfolded protein response in diabetes. Molecular Metabolism *27*, S60–S68.

Gloyn, A.L., Pearson, E.R., Antcliff, J.F., Proks, P., Bruining, G.J., Slingerland, A.S., Howard, N., Srinivasan, S., Silva, J.M.C.L., Molnes, J., et al. (2004). Activating Mutations in the Gene Encoding the ATP-Sensitive Potassium-Channel Subunit Kir6.2 and Permanent Neonatal Diabetes. New England Journal of Medicine *350*, 1838–1849.

Godsland, I.F. (2005). Oestrogens and insulin secretion. Diabetologia *48*, 2213–2220.

Göke, R., Larsen, P.J., Mikkelsen, J.D., and Sheikh, S.P. (1995). Distribution of GLP-1 Binding Sites in the Rat Brain: Evidence that Exendin-4 is a Ligand of Brain GLP-1 Binding Sites. European Journal of Neuroscience *7*, 2294–2300.

Gotfredsen, C.F., Molck, A.-M., Thorup, I., Nyborg, N.C.B., Salanti, Z., Knudsen, L.B., and Larsen, M.O. (2014). The Human GLP-1 Analogs Liraglutide and Semaglutide: Absence of Histopathological Effects on the Pancreas in Nonhuman Primates. Diabetes *63*, 2486–2497.

Gradwohl, G., Dierich, A., LeMeur, M., and Guillemot, F. (2000). neurogenin3 is required for the development of the four endocrine cell lineages of the pancreas. Proceedings of the National Academy of Sciences *97*, 1607–1611.

Granhall, C., Donsmark, M., Blicher, T.M., Golor, G., Søndergaard, F.L., Thomsen, M., and Bækdal, T.A. (2019). Safety and Pharmacokinetics of Single and Multiple Ascending Doses of the Novel Oral Human GLP-1 Analogue, Oral Semaglutide, in Healthy Subjects and Subjects with Type 2 Diabetes. Clinical Pharmacokinetics *58*, 781–791.

Gregg, B.E., Moore, P.C., Demozay, D., Hall, B.A., Li, M., Husain, A., Wright, A.J., Atkinson, M.A., and Rhodes, C.J. (2012). Formation of a Human β-Cell Population within Pancreatic Islets Is Set Early in Life. The Journal of Clinical Endocrinology & Metabolism *97*, 3197–3206.

Gu, C., Stein, G.H., Pan, N., Goebbels, S., Hörnberg, H., Nave, K.-A., Herrera, P., White, P., Kaestner, K.H., Sussel, L., et al. (2010). Pancreatic β Cells Require NeuroD to Achieve and Maintain Functional Maturity. Cell Metabolism *11*, 298–310.

Guo, S., Dai, C., Guo, M., Taylor, B., Harmon, J.S., Sander, M., Robertson, R.P., Powers, A.C., and Stein, R. (2013). Inactivation of specific β cell transcription factors in type 2 diabetes. Journal of Clinical Investigation *123*, 3305–3316.

Gutiérrez, G.D., Bender, A.S., Cirulli, V., Mastracci, T.L., Kelly, S.M., Tsirigos, A., Kaestner, K.H., and Sussel, L. (2016). Pancreatic β cell identity requires continual repression of non–β cell programs. Journal of Clinical Investigation *127*, 244–259.

Haghverdi, L., Büttner, M., Wolf, F.A., Buettner, F., and Theis, F.J. (2016). Diffusion pseudotime robustly reconstructs lineage branching. Nature Methods *13*, 845–848.

Hancock, M.L., Meyer, R.C., Mistry, M., Khetani, R.S., Wagschal, A., Shin, T., Ho Sui, S.J., Näär, A.M., and Flanagan, J.G. (2019). Insulin Receptor Associates with Promoters Genome-wide and Regulates Gene Expression. Cell *177*, 722-736.e22.

Hanley, S.C., Austin, E., Assouline-Thomas, B., Kapeluto, J., Blaichman, J., Moosavi, M., Petropavlovskaia, M., and Rosenberg, L. (2010). β-Cell Mass Dynamics and Islet Cell Plasticity in Human Type 2 Diabetes. Endocrinology *151*, 1462–1472.

Harrison, L.B., Adams-Huet, B., Raskin, P., and Lingvay, I. (2012). -Cell Function Preservation After 3.5 Years of Intensive Diabetes Therapy. Diabetes Care *35*, 1406–1412.

Hering, B.J., Clarke, W.R., Bridges, N.D., Eggerman, T.L., Alejandro, R., Bellin, M.D., Chaloner, K., Czarniecki, C.W., Goldstein, J.S., Hunsicker, L.G., et al. (2016). Phase 3 Trial of Transplantation of Human Islets in Type 1 Diabetes Complicated by Severe Hypoglycemia. Diabetes Care *39*, 1230–1240.

Herold, K.C., Hagopian, W., Auger, J.A., Poumian-Ruiz, E., Taylor, L., Donaldson, D., Gitelman, S.E., Harlan, D.M., Xu, D., Zivin, R.A., et al. (2002). Anti-CD3 Monoclonal Antibody in New-Onset Type 1 Diabetes Mellitus. New England Journal of Medicine *346*, 1692–1698.

Herold, K.C., Gitelman, S.E., Ehlers, M.R., Gottlieb, P.A., Greenbaum, C.J., Hagopian, W., Boyle, K.D., Keyes-Elstein, L., Aggarwal, S., Phippard, D., et al. (2013). Teplizumab (Anti-CD3 mAb) Treatment

Preserves C-Peptide Responses in Patients With New-Onset Type 1 Diabetes in a Randomized Controlled Trial: Metabolic and Immunologic Features at Baseline Identify a Subgroup of Responders. Diabetes *62*, 3766–3774.

Herold, K.C., Bundy, B.N., Long, S.A., Bluestone, J.A., DiMeglio, L.A., Dufort, M.J., Gitelman, S.E., Gottlieb, P.A., Krischer, J.P., Linsley, P.S., et al. (2019). An Anti-CD3 Antibody, Teplizumab, in Relatives at Risk for Type 1 Diabetes. New England Journal of Medicine *381*, 603-613.

Hetz, C., Axten, J.M., and Patterson, J.B. (2019). Pharmacological targeting of the unfolded protein response for disease intervention. Nature Chemical Biology *15*, 764–775.

Hofmann, S.M., Perez-Tilve, D., Greer, T.M., Coburn, B.A., Grant, E., Basford, J.E., Tschop, M.H., and Hui, D.Y. (2008). Defective Lipid Delivery Modulates Glucose Tolerance and Metabolic Response to Diet in Apolipoprotein E Deficient Mice. Diabetes *57*, 5–12.

Holst, J.J. (2007). The Physiology of Glucagon-like Peptide 1. Physiological Reviews *87*, 1409–1439.

Holst, J.J., Orskov, C., Nielsen, O.V., and Schwartz, T.W. (1987). Truncated glucagon-like peptide I, an insulin-releasing hormone from the distal gut. FEBS Lett. *211*, 169–174.

Husain, M., Birkenfeld, A.L., Donsmark, M., Dungan, K., Eliaschewitz, F.G., Franco, D.R., Jeppesen, O.K., Lingvay, I., Mosenzon, O., Pedersen, S.D., et al. (2019). Oral Semaglutide and Cardiovascular Outcomes in Patients with Type 2 Diabetes. New England Journal of Medicine *381*, 841–851.

Inagaki, N., Seino, Y., Takeda, J., Yano, H., Yamada, Y., Bell, G.I., Eddy, R.L., Fukushima, Y., Byers, M.G., Shows, T.B., et al. (1989). Gastric Inhibitory Polypeptide: Structure and Chromosomal Localization of the Human Gene. Molecular Endocrinology *3*, 1014–1021.

Jall, S., Sachs, S., Clemmensen, C., Finan, B., Neff, F., DiMarchi, R.D., Tschöp, M.H., Müller, T.D., and Hofmann, S.M. (2017). Monomeric GLP-1/GIP/glucagon triagonism corrects obesity, hepatosteatosis, and dyslipidemia in female mice. Molecular Metabolism *6*, 440–446.

Jiang, X.-C. (2018). Phospholipid transfer protein: its impact on lipoprotein homeostasis and atherosclerosis. Journal of Lipid Research *59*, 764–771.

Jo, J., Kilimnik, G., Kim, A., Guo, C., Periwal, V., and Hara, M. (2011). Formation of Pancreatic Islets Involves Coordinated Expansion of Small Islets and Fission of Large Interconnected Islet-like Structures. Biophysical Journal *101*, 565–574.

Jonas, J.C., Sharma, A., Hasenkamp, W., Ilkova, H., Patanè, G., Laybutt, R., Bonner-Weir, S., and Weir, G.C. (1999). Chronic hyperglycemia triggers loss of pancreatic beta cell differentiation in an animal model of diabetes. J. Biol. Chem. *274*, 14112–14121.

Jørgensen, M.C., Ahnfelt-Rønne, J., Hald, J., Madsen, O.D., Serup, P., and Hecksher-Sørensen, J. (2007). An Illustrated Review of Early Pancreas Development in the Mouse. Endocrine Reviews *28*, 685–705.

Jørgensen, N.B., Jacobsen, S.H., Dirksen, C., Bojsen-Møller, K.N., Naver, L., Hvolris, L., Clausen, T.R., Wulff, B.S., Worm, D., Lindqvist Hansen, D., et al. (2012). Acute and long-term effects of Roux-en-Y gastric bypass on glucose metabolism in subjects with Type 2 diabetes and normal glucose tolerance. American Journal of Physiology-Endocrinology and Metabolism *303*, E122–E131.

Kaneto, H., Nakatani, Y., Miyatsuka, T., Matsuoka, T. -a., Matsuhisa, M., Hori, M., and Yamasaki, Y. (2005). PDX-1/VP16 Fusion Protein, Together With NeuroD or Ngn3, Markedly Induces Insulin Gene Transcription and Ameliorates Glucose Tolerance. Diabetes *54*, 1009–1022.

Karamanakos, S.N., Vagenas, K., Kalfarentzos, F., and Alexandrides, T.K. (2008). Weight Loss, Appetite Suppression, and Changes in Fasting and Postprandial Ghrelin and Peptide-YY Levels After Roux-en-Y Gastric Bypass and Sleeve Gastrectomy: A Prospective, Double Blind Study. Annals of Surgery *247*, 401–407.

Kassem, S.A., Ariel, I., Thornton, P.S., Scheimberg, I., and Glaser, B. (2000). Beta-cell proliferation and apoptosis in the developing normal human pancreas and in hyperinsulinism of infancy. Diabetes *49*, 1325–1333.

Katsuta, H., Akashi, T., Katsuta, R., Nagaya, M., Kim, D., Arinobu, Y., Hara, M., Bonner-Weir, S., Sharma, A.J., Akashi, K., et al. (2010). Single pancreatic beta cells co-express multiple islet hormone genes in mice. Diabetologia *53*, 128–138.

Kaye, S.M., Pietiläinen, K.H., Kotronen, A., Joutsi-Korhonen, L., Kaprio, J., Yki-Järvinen, H., Silveira, A., Hamsten, A., Lassila, R., and Rissanen, A. (2012). Obesity-Related Derangements of Coagulation and Fibrinolysis: A Study of Obesity-Discordant Monozygotic Twin Pairs. Obesity *20*, 88–94.

Keenan, H.A., Sun, J.K., Levine, J., Doria, A., Aiello, L.P., Eisenbarth, G., Bonner-Weir, S., and King, G.L. (2010). Residual Insulin Production and Pancreatic -Cell Turnover After 50 Years of Diabetes: Joslin Medalist Study. Diabetes *59*, 2846–2853.

Kim-Muller, J.Y., Fan, J., Kim, Y.J.R., Lee, S.-A., Ishida, E., Blaner, W.S., and Accili, D. (2016). Aldehyde dehydrogenase 1a3 defines a subset of failing pancreatic β cells in diabetic mice. Nature Communications *7*, 12631.

Klein, D., Álvarez-Cubela, S., Lanzoni, G., Vargas, N., Prabakar, K.R., Boulina, M., Ricordi, C., Inverardi, L., Pastori, R.L., and Domínguez-Bendala, J. (2015). BMP-7 Induces Adult Human Pancreatic Exocrine-to-Endocrine Conversion. Diabetes *64*, 4123–4134.

Köhler, C.U., Olewinski, M., Tannapfel, A., Schmidt, W.E., Fritsch, H., and Meier, J.J. (2011). Cell cycle control of β-cell replication in the prenatal and postnatal human pancreas. American Journal of Physiology-Endocrinology and Metabolism *300*, E221–E230.

Kotimaa, J., Klar-Mohammad, N., Gueler, F., Schilders, G., Jansen, A., Rutjes, H., Daha, M.R., and van Kooten, C. (2016). Sex matters: Systemic complement activity of female C57BL/6J and BALB/cJ mice is limited by serum terminal pathway components. Molecular Immunology *76*, 13–21.

Kotronen, A., Peltonen, M., Hakkarainen, A., Sevastianova, K., Bergholm, R., Johansson, L.M., Lundbom, N., Rissanen, A., Ridderstråle, M., Groop, L., et al. (2009). Prediction of Non-Alcoholic Fatty Liver Disease and Liver Fat Using Metabolic and Genetic Factors. Gastroenterology *137*, 865–872.

Kowalczyk, M.S., Tirosh, I., Heckl, D., Rao, T.N., Dixit, A., Haas, B.J., Schneider, R.K., Wagers, A.J., Ebert, B.L., and Regev, A. (2015). Single-cell RNA-seq reveals changes in cell cycle and differentiation programs upon aging of hematopoietic stem cells. Genome Research *25*, 1860–1872.

Kramer, C.K., Zinman, B., and Retnakaran, R. (2013). Short-term intensive insulin therapy in type 2 diabetes mellitus: a systematic review and meta-analysis. The Lancet Diabetes & Endocrinology *1*, 28–34.

Kreymann, B., Ghatei, M.A., Williams, G., and Bloom, S.R. (1987). GLUCAGON-LIKE PEPTIDE-1 7-36: A PHYSIOLOGICAL INCRETIN IN MAN. The Lancet *330*, 1300–1304.

Kroon, E., Martinson, L.A., Kadoya, K., Bang, A.G., Kelly, O.G., Eliazer, S., Young, H., Richardson, M., Smart, N.G., Cunningham, J., et al. (2008). Pancreatic endoderm derived from human embryonic stem cells generates glucose-responsive insulin-secreting cells in vivo. Nature Biotechnology *26*, 443–452.

Kubota, N., Tobe, K., Terauchi, Y., Eto, K., Yamauchi, T., Suzuki, R., Tsubamoto, Y., Komeda, K., Nakano, R., Miki, H., et al. (2000). Disruption of insulin receptor substrate 2 causes type 2 diabetes because of liver insulin resistance and lack of compensatory beta-cell hyperplasia. Diabetes *49*, 1880–1889.

Kuleshov, M.V., Jones, M.R., Rouillard, A.D., Fernandez, N.F., Duan, Q., Wang, Z., Koplev, S., Jenkins, S.L., Jagodnik, K.M., Lachmann, A., et al. (2016). Enrichr: a comprehensive gene set enrichment analysis web server 2016 update. Nucleic Acids Research *44*, W90–W97.

Kulkarni, R.N., Winnay, J.N., Daniels, M., Brüning, J.C., Flier, S.N., Hanahan, D., and Kahn, C.R. (1999a). Altered function of insulin receptor substrate-1–deficient mouse islets and cultured β-cell lines. Journal of Clinical Investigation *104*, R69–R75.

Kulkarni, R.N., Brüning, J.C., Winnay, J.N., Postic, C., Magnuson, M.A., and Kahn, C.R. (1999b). Tissue-specific knockout of the insulin receptor in pancreatic beta cells creates an insulin secretory defect similar to that in type 2 diabetes. Cell *96*, 329–339.

Kulkarni, R.N., Holzenberger, M., Shih, D.Q., Ozcan, U., Stoffel, M., Magnuson, M.A., and Kahn, C.R. (2002). β-cell–specific deletion of the Igf1 receptor leads to hyperinsulinemia and glucose intolerance but does not alter β-cell mass. Nature Genetics *31*, 111–115.

La Manno, G., Soldatov, R., Zeisel, A., Braun, E., Hochgerner, H., Petukhov, V., Lidschreiber, K., Kastriti, M.E., Lönnerberg, P., Furlan, A., et al. (2018). RNA velocity of single cells. Nature *560*, 494–498.

Lam, C.J., Chatterjee, A., Shen, E., Cox, A.R., and Kushner, J.A. (2018). Low Level Insulin Content Within Abundant Non-Beta Islet Endocrine Cells in Long-Standing Type 1 Diabetes. Diabetes db180305.

Lardinois, C.K., Starich, G.H., and Mazzaferri, E.L. (1988). The postprandial response of gastric inhibitory polypeptide to various dietary fats in man. Journal of the American College of Nutrition *7*, 241–247.

Lau, J., Bloch, P., Schäffer, L., Pettersson, I., Spetzler, J., Kofoed, J., Madsen, K., Knudsen, L.B., McGuire, J., Steensgaard, D.B., et al. (2015). Discovery of the Once-Weekly Glucagon-Like Peptide-1 (GLP-1) Analogue Semaglutide. Journal of Medicinal Chemistry *58*, 7370–7380.

Law, C.W., Chen, Y., Shi, W., and Smyth, G.K. (2014). voom: precision weights unlock linear model analysis tools for RNA-seq read counts. Genome Biology *15*, R29.

Laybutt, D.R., Sharma, A., Sgroi, D.C., Gaudet, J., Bonner-Weir, S., and Weir, G.C. (2002). Genetic Regulation of Metabolic Pathways in β-Cells Disrupted by Hyperglycemia. Journal of Biological Chemistry *277*, 10912–10921.

Laybutt, D.R., Glandt, M., Xu, G., Ahn, Y.B., Trivedi, N., Bonner-Weir, S., and Weir, G.C. (2003). Critical Reduction in β-Cell Mass Results in Two Distinct Outcomes over Time: ADAPTATION WITH IMPAIRED GLUCOSE TOLERANCE OR DECOMPENSATED DIABETES. Journal of Biological Chemistry *278*, 2997–3005.

Le May, C., Chu, K., Hu, M., Ortega, C.S., Simpson, E.R., Korach, K.S., Tsai, M.-J., and Mauvais-Jarvis, F. (2006). Estrogens protect pancreatic beta-cells from apoptosis and prevent insulin-deficient diabetes mellitus in mice. Proc. Natl. Acad. Sci. U.S.A. *103*, 9232–9237.

Lee, C.S., De León, D.D., Kaestner, K.H., and Stoffers, D.A. (2006). Regeneration of pancreatic islets after partial pancreatectomy in mice does not involve the reactivation of neurogenin-3. Diabetes *55*, 269–272.

Leibiger, I.B., Leibiger, B., and Berggren, P.-O. (2008). Insulin Signaling in the Pancreatic β-Cell. Annual Review of Nutrition *28*, 233–251.

Li, J., Casteels, T., Frogne, T., Ingvorsen, C., Honoré, C., Courtney, M., Huber, K.V.M., Schmitner, N., Kimmel, R.A., Romanov, R.A., et al. (2017). Artemisinins Target GABA A Receptor Signaling and Impair α Cell Identity. Cell *168*, 86-100.e15.

Li, W., Cavelti-Weder, C., Zhang, Y., Clement, K., Donovan, S., Gonzalez, G., Zhu, J., Stemann, M., Xu, K., Hashimoto, T., et al. (2014). Long-term persistence and development of induced pancreatic beta cells generated by lineage conversion of acinar cells. Nature Biotechnology *32*, 1223–1230.

Li, Y., Hansotia, T., Yusta, B., Ris, F., Halban, P.A., and Drucker, D.J. (2003). Glucagon-like Peptide-1 Receptor Signaling Modulates β Cell Apoptosis. Journal of Biological Chemistry *278*, 471–478.

Li, Y., Cao, X., Li, L.-X., Brubaker, P.L., Edlund, H., and Drucker, D.J. (2005). beta-Cell Pdx1 expression is essential for the glucoregulatory, proliferative, and cytoprotective actions of glucagon-like peptide-1. Diabetes *54*, 482–491.

Lipska, K.J., Yao, X., Herrin, J., McCoy, R.G., Ross, J.S., Steinman, M.A., Inzucchi, S.E., Gill, T.M., Krumholz, H.M., and Shah, N.D. (2017). Trends in Drug Utilization, Glycemic Control, and Rates of Severe Hypoglycemia, 2006–2013. Diabetes Care *40*, 468–475.

Liu, G. (2001). Cholecystokinin expression in the developing and regenerating pancreas and intestine. Journal of Endocrinology *169*, 233–240.

Liu, R., Holik, A.Z., Su, S., Jansz, N., Chen, K., Leong, H.S., Blewitt, M.E., Asselin-Labat, M.-L., Smyth, G.K., and Ritchie, M.E. (2015). Why weight? Modelling sample and observational level variability improves power in RNA-seq analyses. Nucleic Acids Research *43*, e97–e97.

Luo, Y., Duan, H., Qian, Y., Feng, L., Wu, Z., Wang, F., Feng, J., Yang, D., Qin, Z., and Yan, X. (2017). Macrophagic CD146 promotes foam cell formation and retention during atherosclerosis. Cell Research *27*, 352–372.

Marselli, L., Suleiman, M., Masini, M., Campani, D., Bugliani, M., Syed, F., Martino, L., Focosi, D., Scatena, F., Olimpico, F., et al. (2014). Are we overestimating the loss of beta cells in type 2 diabetes? Diabetologia *57*, 362–365.

Martínez de Morentin, P.B., González-García, I., Martins, L., Lage, R., Fernández-Mallo, D., Martínez-Sánchez, N., Ruíz-Pino, F., Liu, J., Morgan, D.A., Pinilla, L., et al. (2014). Estradiol Regulates Brown Adipose Tissue Thermogenesis via Hypothalamic AMPK. Cell Metabolism *20*, 41–53.

Matthews, D.R., Cull, C.A., Stratton, I.M., Holman, R.R., and Turner, R.C. (1998). UKPDS 26: Sulphonylurea failure in non-insulin-dependent diabetic patients over six years. UK Prospective Diabetes Study (UKPDS) Group. Diabet. Med. *15*, 297–303.

Mauvais-Jarvis, F. (2016). Role of Sex Steroids in β Cell Function, Growth, and Survival. Trends in Endocrinology & Metabolism *27*, 844–855.

Mauvais-Jarvis, F., Manson, J.E., Stevenson, J.C., and Fonseca, V.A. (2017). Menopausal Hormone Therapy and Type 2 Diabetes Prevention: Evidence, Mechanisms, and Clinical Implications. Endocrine Reviews *38*, 173–188.

Md Moin, A.S., Dhawan, S., Cory, M., Butler, P.C., Rizza, R.A., and Butler, A.E. (2016). Increased Frequency of Hormone Negative and Polyhormonal Endocrine Cells in Lean Individuals With Type 2 Diabetes. J. Clin. Endocrinol. Metab. *101*, 3628–3636.

Meier, J.J., Butler, A.E., Saisho, Y., Monchamp, T., Galasso, R., Bhushan, A., Rizza, R.A., and Butler, P.C. (2008). -Cell Replication Is the Primary Mechanism Subserving the Postnatal Expansion of -Cell Mass in Humans. Diabetes *57*, 1584–1594.

Menge, B.A., Tannapfel, A., Belyaev, O., Drescher, R., Muller, C., Uhl, W., Schmidt, W.E., and Meier, J.J. (2008). Partial Pancreatectomy in Adult Humans Does Not Provoke -Cell Regeneration. Diabetes *57*, 142–149.

Mertens, I., and Van Gaal, L.F. (2002). Obesity, haemostasis and the fibrinolytic system. Obes Rev *3*, 85–101.

van der Meulen, T., Lee, S., Noordeloos, E., Donaldson, C.J., Adams, M.W., Noguchi, G.M., Mawla, A.M., and Huising, M.O. (2018). Artemether Does Not Turn α Cells into β Cells. Cell Metabolism *27*, 218-225.e4.

Mezza, T., Muscogiuri, G., Sorice, G.P., Clemente, G., Hu, J., Pontecorvi, A., Holst, J.J., Giaccari, A., and Kulkarni, R.N. (2014). Insulin Resistance Alters Islet Morphology in Nondiabetic Humans. Diabetes *63*, 994–1007.

Middleton, K.R., Anton, S.D., and Perri, M.G. (2013). Long-Term Adherence to Health Behavior Change. American Journal of Lifestyle Medicine *7*, 395–404.

Mingrone, G., Panunzi, S., De Gaetano, A., Guidone, C., Iaconelli, A., Nanni, G., Castagneto, M., Bornstein, S., and Rubino, F. (2015). Bariatric–metabolic surgery versus conventional medical treatment in obese patients with type 2 diabetes: 5 year follow-up of an open-label, single-centre, randomised controlled trial. The Lancet *386*, 964–973.

Miras, A.D., and le Roux, C.W. (2013). Mechanisms underlying weight loss after bariatric surgery. Nature Reviews Gastroenterology & Hepatology *10*, 575–584.

Mullally, J.A., Febres, G.J., Bessler, M., and Korner, J. (2019). Sleeve Gastrectomy and Roux-en-Y Gastric Bypass Achieve Similar Early Improvements in Beta-cell Function in Obese Patients with Type 2 Diabetes. Scientific Reports *9*.

Müller, T.D., Finan, B., Bloom, S.R., D'Alessio, D., Drucker, D.J., Flatt, P.R., Fritsche, A., Gribble, F., Grill, H.J., Habener, J.F., et al. (2019). Glucagon-like peptide 1 (GLP-1). Molecular Metabolism *30*, 72–130.

Nauck, M.A., and Meier, J.J. (2016). The incretin effect in healthy individuals and those with type 2 diabetes: physiology, pathophysiology, and response to therapeutic interventions. The Lancet Diabetes & Endocrinology *4*, 525–536.

Nauck, M.A., Heimesaat, M.M., Orskov, C., Holst, J.J., Ebert, R., and Creutzfeldt, W. (1993). Preserved incretin activity of glucagon-like peptide 1 [7-36 amide] but not of synthetic human gastric inhibitory polypeptide in patients with type-2 diabetes mellitus. Journal of Clinical Investigation *91*, 301–307.

Nishimura, W., Kondo, T., Salameh, T., El Khattabi, I., Dodge, R., Bonner-Weir, S., and Sharma, A. (2006). A switch from MafB to MafA expression accompanies differentiation to pancreatic beta-cells. Dev. Biol. *293*, 526–539.

Niu, L., Geyer, P.E., Wewer Albrechtsen, N.J., Gluud, L.L., Santos, A., Doll, S., Treit, P.V., Holst, J.J., Knop, F.K., Vilsbøll, T., et al. (2019). Plasma proteome profiling discovers novel proteins associated with non-alcoholic fatty liver disease. Molecular Systems Biology *15*.

O'Brien, B.A., Harmon, B.V., Cameron, D.P., and Allan, D.J. (1996). Beta-cell apoptosis is responsible for the development of IDDM in the multiple low-dose streptozotocin model. J. Pathol. *178*, 176–181.

O'Brien, P., McPhail, T., Chaston, T., and Dixon, J. (2006). Systematic Review of Medium-Term Weight Loss after Bariatric Operations. Obesity Surgery *16*, 1032–1040.

O'Neil, P.M., Birkenfeld, A.L., McGowan, B., Mosenzon, O., Pedersen, S.D., Wharton, S., Carson, C.G., Jepsen, C.H., Kabisch, M., and Wilding, J.P.H. (2018). Efficacy and safety of semaglutide compared with liraglutide and placebo for weight loss in patients with obesity: a randomised, double-blind, placebo and active controlled, dose-ranging, phase 2 trial. The Lancet *392*, 637–649.

Pagliuca, F.W., Millman, J.R., Gürtler, M., Segel, M., Van Dervort, A., Ryu, J.H., Peterson, Q.P., Greiner, D., and Melton, D.A. (2014). Generation of Functional Human Pancreatic β Cells In Vitro. Cell *159*, 428–439.

Palsson-McDermott, E.M., Curtis, A.M., Goel, G., Lauterbach, M.A.R., Sheedy, F.J., Gleeson, L.E., van den Bosch, M.W.M., Quinn, S.R., Domingo-Fernandez, R., Johnston, D.G.W., et al. (2015). Pyruvate Kinase M2 Regulates Hif-1α Activity and IL-1β Induction and Is a Critical Determinant of the Warburg Effect in LPS-Activated Macrophages. Cell Metabolism *21*, 65–80.

Pan, F.C., and Wright, C. (2011). Pancreas organogenesis: From bud to plexus to gland. Developmental Dynamics *240*, 530–565.

Parsons, J.A., Brelje, T.C., and Sorenson, R.L. (1992). Adaptation of islets of Langerhans to pregnancy: increased islet cell proliferation and insulin secretion correlates with the onset of placental lactogen secretion. Endocrinology *130*, 1459–1466.

Pearson, J.A., Wong, F.S., and Wen, L. (2016). The importance of the Non Obese Diabetic (NOD) mouse model in autoimmune diabetes. Journal of Autoimmunity *66*, 76–88.

Pek, S.L.T., Cheng, A.K.S., Lin, M.X., Wong, M.S., Chan, E.Z.L., Moh, A.M.C., Sum, C.F., Lim, S.C., and Tavintharan, S. (2018). Association of circulating proinflammatory marker, leucine-rich-α2-glycoprotein (LRG1), following metabolic/bariatric surgery. Diabetes/Metabolism Research and Reviews *34*, e3029.

Peng, S., Zhu, L., Chen, M., Zhang, M., Li, D., Fu, Y., Chen, S., and Wei, C. (2009). Heterogeneity in Mitotic Activity and Telomere Length Implies an Important Role of Young Islets in the Maintenance of Islet Mass in the Adult Pancreas. Endocrinology *150*, 3058–3066.

Peshavaria, M., Larmie, B.L., Lausier, J., Satish, B., Habibovic, A., Roskens, V., LaRock, K., Everill, B., Leahy, J.L., and Jetton, T.L. (2006). Regulation of Pancreatic -Cell Regeneration in the Normoglycemic 60% Partial-Pancreatectomy Mouse. Diabetes *55*, 3289–3298.

Polyzogopoulou, E.V., Kalfarentzos, F., Vagenakis, A.G., and Alexandrides, T.K. (2003). Restoration of Euglycemia and Normal Acute Insulin Response to Glucose in Obese Subjects With Type 2 Diabetes Following Bariatric Surgery. Diabetes *52*, 1098–1103.

Potter, K.J., Westwell-Roper, C.Y., Klimek-Abercrombie, A.M., Warnock, G.L., and Verchere, C.B. (2014). Death and dysfunction of transplanted β-cells: lessons learned from type 2 diabetes? Diabetes *63*, 12–19.

Prentki, M. (2006). Islet cell failure in type 2 diabetes. Journal of Clinical Investigation *116*, 1802–1812.

Puah, J., and Bailey, C. (1985). Insulinotropic Effect of Ovarian Steroid Hormones in Streptozotocin Diabetic Female Mice. Hormone and Metabolic Research *17*, 216–218.

Puig, O., Yuan, J., Stepaniants, S., Zieba, R., Zycband, E., Morris, M., Coulter, S., Yu, X., Menke, J., Woods, J., et al. (2011). A Gene Expression Signature That Classifies Human Atherosclerotic Plaque by Relative Inflammation Status. Circulation: Cardiovascular Genetics *4*, 595–604.

Qadir, M.M.F., Álvarez-Cubela, S., Klein, D., Lanzoni, G., García-Santana, C., Montalvo, A., Pláceres-Uray, F., Mazza, E.M.C., Ricordi, C., Inverardi, L.A., et al. (2018). P2RY1/ALK3-Expressing Cells within the Adult Human Exocrine Pancreas Are BMP-7 Expandable and Exhibit Progenitor-like Characteristics. Cell Reports *22*, 2408–2420.

Qi, L., Tsai, B., and Arvan, P. (2017). New Insights into the Physiological Role of Endoplasmic Reticulum-Associated Degradation. Trends in Cell Biology *27*, 430–440.

Quarta, C., Clemmensen, C., Zhu, Z., Yang, B., Joseph, S.S., Lutter, D., Yi, C.-X., Graf, E., García-Cáceres, C., Legutko, B., et al. (2017). Molecular Integration of Incretin and Glucocorticoid Action Reverses Immunometabolic Dysfunction and Obesity. Cell Metabolism *26*, 620-632.e6.

Rakieten, N., Rakieten, M.L., and Nadkarni, M.V. (1963). Studies on the diabetogenic action of streptozotocin (NSC-37917). Cancer Chemother Rep *29*, 91–98.

Rankin, M.M., Wilbur, C.J., Rak, K., Shields, E.J., Granger, A., and Kushner, J.A. (2013). -Cells Are Not Generated in Pancreatic Duct Ligation-Induced Injury in Adult Mice. Diabetes *62*, 1634–1645.

Ratner, R.E., Maggs, D., Nielsen, L.L., Stonehouse, A.H., Poon, T., Zhang, B., Bicsak, T.A., Brodows, R.G., and Kim, D.D. (2006). Long-term effects of exenatide therapy over 82 weeks on glycaemic control and weight in over-weight metformin-treated patients with type 2 diabetes mellitus. Diabetes, Obesity and Metabolism *8*, 419–428.

Reers, C., Erbel, S., Esposito, I., Schmied, B., Büchler, M.W., Nawroth, P.P., and Ritzel, R.A. (2009). Impaired islet turnover in human donor pancreata with aging. European Journal of Endocrinology *160*, 185–191.

Rezania, A., Bruin, J.E., Arora, P., Rubin, A., Batushansky, I., Asadi, A., O'Dwyer, S., Quiskamp, N., Mojibian, M., Albrecht, T., et al. (2014). Reversal of diabetes with insulin-producing cells derived in vitro from human pluripotent stem cells. Nature Biotechnology *32*, 1121–1133.

Rhodes, C.J., White, M.F., Leahy, J.L., and Kahn, S.E. (2013). Direct Autocrine Action of Insulin on -Cells: Does It Make Physiological Sense? Diabetes *62*, 2157–2163.

Rieck, S., and Kaestner, K.H. (2010). Expansion of β-cell mass in response to pregnancy. Trends in Endocrinology & Metabolism *21*, 151–158.

Ritchie, M.E., Phipson, B., Wu, D., Hu, Y., Law, C.W., Shi, W., and Smyth, G.K. (2015). limma powers differential expression analyses for RNA-sequencing and microarray studies. Nucleic Acids Research *43*, e47–e47.

Roux, C.W. le, Aylwin, S.J.B., Batterham, R.L., Borg, C.M., Coyle, F., Prasad, V., Shurey, S., Ghatei, M.A., Patel, A.G., and Bloom, S.R. (2006). Gut Hormone Profiles Following Bariatric Surgery Favor an Anorectic State, Facilitate Weight Loss, and Improve Metabolic Parameters: Annals of Surgery *243*, 108–114.

Rui, J., Deng, S., Arazi, A., Perdigoto, A.L., Liu, Z., and Herold, K.C. (2017). β Cells that Resist Immunological Attack Develop during Progression of Autoimmune Diabetes in NOD Mice. Cell Metabolism *25*, 727–738.

Sachs S, Bastidas-Ponce A, Tritschler S, Bakhti M, Böttcher A, Sánchez-Garrido MA, Tarquis-Medina M, Kleinert M, Fischer K, Jall S, Harger A, Bader E, Roscioni S, Ussar S, Feuchtinger A, Yesildag B, Neelakandhan A, Jensen CB, Cornu M, Yang B, Finan B, DiMarchi RD, Tschöp MH, Theis FJ, Hofmann SM, Müller TD, Lickert H. (2020a). Targeted pharmacological therapy restores β-cell function for diabetes remission. Nat Metab (2):192-209.

Sachs S, Niu L, Geyer P, Jall S, Kleinert M, Feuchtinger A, Stemmer K, Brielmeier M, Finan B, DiMarchi RD, Tschöp MH, Albrechtsen NW, Mann M, Müller TD, Hofmann SM. (2020b). Plasma proteome profiles treatment efficacy of incretin dual agonism in diet-induced obese female and male mice. Diabetes Obes Metab. Oct 1.

Saisho, Y., Butler, A.E., Manesso, E., Elashoff, D., Rizza, R.A., and Butler, P.C. (2013). -Cell Mass and Turnover in Humans: Effects of obesity and aging. Diabetes Care *36*, 111–117.

Sanjurjo, L., Aran, G., Roher, N., Valledor, A.F., and Sarrias, M.-R. (2015). AIM/CD5L: a key protein in the control of immune homeostasis and inflammatory disease. Journal of Leukocyte Biology *98*, 173–184.

Satija, R., Farrell, J.A., Gennert, D., Schier, A.F., and Regev, A. (2015). Spatial reconstruction of single-cell gene expression data. Nature Biotechnology *33*, 495–502.

Schauer, P.R., Bhatt, D.L., Kirwan, J.P., Wolski, K., Aminian, A., Brethauer, S.A., Navaneethan, S.D., Singh, R.P., Pothier, C.E., Nissen, S.E., et al. (2017). Bariatric Surgery versus Intensive Medical Therapy for Diabetes — 5-Year Outcomes. New England Journal of Medicine *376*, 641–651.

Schellenberg, E.S., Dryden, D.M., Vandermeer, B., Ha, C., and Korownyk, C. (2013). Lifestyle Interventions for Patients With and at Risk for Type 2 Diabetes: A Systematic Review and Meta-analysis. Annals of Internal Medicine *159*, 543.

Schmitt, C., Portron, A., Jadidi, S., Sarkar, N., and DiMarchi, R. (2017). Pharmacodynamics, pharmacokinetics and safety of multiple ascending doses of the novel dual glucose-dependent insulinotropic polypeptide/glucagon-like peptide-1 agonist RG7697 in people with type 2 diabetes mellitus. Diabetes, Obesity and Metabolism *19*, 1436–1445.

Scholtz, S., Miras, A.D., Chhina, N., Prechtl, C.G., Sleeth, M.L., Daud, N.M., Ismail, N.A., Durighel, G., Ahmed, A.R., Olbers, T., et al. (2014). Obese patients after gastric bypass surgery have lower brain-hedonic responses to food than after gastric banding. Gut *63*, 891–902.

Schwenk, R.W., Baumeier, C., Finan, B., Kluth, O., Brauer, C., Joost, H.-G., DiMarchi, R.D., Tschöp, M.H., and Schürmann, A. (2015). GLP-1–oestrogen attenuates hyperphagia and protects from beta cell failure in diabetes-prone New Zealand obese (NZO) mice. Diabetologia *58*, 604–614.

Seeley, R.J., Chambers, A.P., and Sandoval, D.A. (2015). The Role of Gut Adaptation in the Potent Effects of Multiple Bariatric Surgeries on Obesity and Diabetes. Cell Metabolism *21*, 369–378.

Seghieri, M., Christensen, A.S., Andersen, A., Solini, A., Knop, F.K., and Vilsbøll, T. (2018). Future Perspectives on GLP-1 Receptor Agonists and GLP-1/glucagon Receptor Co-agonists in the Treatment of NAFLD. Frontiers in Endocrinology *9*.

Seiron, P., Wiberg, A., Kuric, E., Krogvold, L., Jahnsen, F.L., Dahl-Jørgensen, K., Skog, O., and Korsgren, O. (2019). Characterisation of the endocrine pancreas in type 1 diabetes: islet size is maintained but islet number is markedly reduced. The Journal of Pathology: Clinical Research *5*, 248–255.

Shapiro, A.M.J., Lakey, J.R.T., Ryan, E.A., Korbutt, G.S., Toth, E., Warnock, G.L., Kneteman, N.M., and Rajotte, R.V. (2000). Islet Transplantation in Seven Patients with Type 1 Diabetes Mellitus Using a Glucocorticoid-Free Immunosuppressive Regimen. New England Journal of Medicine *343*, 230–238.

Shapiro, A.M.J., Ricordi, C., Hering, B.J., Auchincloss, H., Lindblad, R., Robertson, R.P., Secchi, A., Brendel, M.D., Berney, T., Brennan, D.C., et al. (2006). International Trial of the Edmonton Protocol for Islet Transplantation. New England Journal of Medicine *355*, 1318–1330.

Shen, W., Taylor, B., Jin, Q., Nguyen-Tran, V., Meeusen, S., Zhang, Y.-Q., Kamireddy, A., Swafford, A., Powers, A.F., Walker, J., et al. (2015). Inhibition of DYRK1A and GSK3B induces human β-cell proliferation. Nature Communications *6*.

Smukler, S.R., Arntfield, M.E., Razavi, R., Bikopoulos, G., Karpowicz, P., Seaberg, R., Dai, F., Lee, S., Ahrens, R., Fraser, P.E., et al. (2011). The Adult Mouse and Human Pancreas Contain Rare Multipotent Stem Cells that Express Insulin. Cell Stem Cell *8*, 281–293.

Solimena, M., Schulte, A.M., Marselli, L., Ehehalt, F., Richter, D., Kleeberg, M., Mziaut, H., Knoch, K.-P., Parnis, J., Bugliani, M., et al. (2018). Systems biology of the IMIDIA biobank from organ donors and pancreatectomised patients defines a novel transcriptomic signature of islets from individuals with type 2 diabetes. Diabetologia *61*, 641–657.

Soneson, C., and Robinson, M.D. (2018). Bias, robustness and scalability in single-cell differential expression analysis. Nature Methods *15*, 255–261.

Sorenson, R., and Brelje, T. (1997). Adaptation of Islets of Langerhans to Pregnancy: β-Cell Growth, Enhanced Insulin Secretion and the Role of Lactogenic Hormones. Hormone and Metabolic Research *29*, 301–307.

Spivia, W., Magno, P.S., Le, P., and Fraser, D.A. (2014). Complement protein C1q promotes macrophage anti-inflammatory M2-like polarization during the clearance of atherogenic lipoproteins. Inflammation Research *63*, 885–893.

Stark Casagrande, S., Fradkin, J.E., Saydah, S.H., Rust, K.F., and Cowie, C.C. (2013). The Prevalence of Meeting A1C, Blood Pressure, and LDL Goals Among People With Diabetes, 1988-2010. Diabetes Care *36*, 2271–2279.

Stopková, R., Stopka, P., Janotová, K., and Jedelský, P.L. (2007). Species-specific Expression of Major Urinary Proteins in the House Mice (Mus musculus musculus and Mus musculus domesticus). Journal of Chemical Ecology *33*, 861–869.

Suissa, Y., Magenheim, J., Stolovich-Rain, M., Hija, A., Collombat, P., Mansouri, A., Sussel, L., Sosa-Pineda, B., McCracken, K., Wells, J.M., et al. (2013). Gastrin: A Distinct Fate of Neurogenin3 Positive Progenitor Cells in the Embryonic Pancreas. PLoS ONE *8*, e70397.

Sumithran, P., Prendergast, L.A., Delbridge, E., Purcell, K., Shulkes, A., Kriketos, A., and Proietto, J. (2011). Long-Term Persistence of Hormonal Adaptations to Weight Loss. New England Journal of Medicine *365*, 1597–1604.

Swisa, A., Avrahami, D., Eden, N., Zhang, J., Feleke, E., Dahan, T., Cohen-Tayar, Y., Stolovich-Rain, M., Kaestner, K.H., Glaser, B., et al. (2016). PAX6 maintains β cell identity by repressing genes of alternative islet cell types. Journal of Clinical Investigation *127*, 230–243.

Takahashi, K., Tanabe, K., Ohnuki, M., Narita, M., Ichisaka, T., Tomoda, K., and Yamanaka, S. (2007). Induction of Pluripotent Stem Cells from Adult Human Fibroblasts by Defined Factors. Cell *131*, 861–872.

Takeda, J., Seino, Y., Tanaka, K., Fukumoto, H., Kayano, T., Takahashi, H., Mitani, T., Kurono, M., Suzuki, T., and Tobe, T. (1987). Sequence of an intestinal cDNA encoding human gastric inhibitory polypeptide precursor. Proceedings of the National Academy of Sciences *84*, 7005–7008.

Talchai, C., Xuan, S., Lin, H.V., Sussel, L., and Accili, D. (2012). Pancreatic β Cell Dedifferentiation as a Mechanism of Diabetic β Cell Failure. Cell *150*, 1223–1234.

Taylor, B.L., Liu, F.-F., and Sander, M. (2013). Nkx6.1 Is Essential for Maintaining the Functional State of Pancreatic Beta Cells. Cell Reports *4*, 1262–1275.

Téllez, N., Vilaseca, M., Martí, Y., Pla, A., and Montanya, E. (2016). β-Cell dedifferentiation, reduced duct cell plasticity, and impaired β-cell mass regeneration in middle-aged rats. American Journal of Physiology-Endocrinology and Metabolism *311*, E554–E563.

Teta, M., Long, S.Y., Wartschow, L.M., Rankin, M.M., and Kushner, J.A. (2005). Very Slow Turnover of -Cells in Aged Adult Mice. Diabetes *54*, 2557–2567.

Teta, M., Rankin, M.M., Long, S.Y., Stein, G.M., and Kushner, J.A. (2007). Growth and regeneration of adult beta cells does not involve specialized progenitors. Dev. Cell *12*, 817–826.

The Emerging Risk Factors Collaboration (2011). Separate and combined associations of body-mass index and abdominal adiposity with cardiovascular disease: collaborative analysis of 58 prospective studies. The Lancet *377*, 1085–1095.

The GBD 2015 Obesity Collaborators (2017). Health Effects of Overweight and Obesity in 195 Countries over 25 Years. New England Journal of Medicine *377*, 13–27.

The RISE Consortium (2019). Lack of Durable Improvements in β-Cell Function Following Withdrawal of Pharmacological Interventions in Adults With Impaired Glucose Tolerance or Recently Diagnosed Type 2 Diabetes. Diabetes Care *42*, 1742–1751.

Thomson, J.A. (1998). Embryonic Stem Cell Lines Derived from Human Blastocysts. Science *282*, 1145–1147.

Thorel, F., Népote, V., Avril, I., Kohno, K., Desgraz, R., Chera, S., and Herrera, P.L. (2010). Conversion of adult pancreatic α-cells to β-cells after extreme β-cell loss. Nature *464*, 1149–1154.

Tiano, J.P., and Mauvais-Jarvis, F. (2012). Importance of oestrogen receptors to preserve functional β-cell mass in diabetes. Nature Reviews Endocrinology *8*, 342–351.

Tiano, J.P., Delghingaro-Augusto, V., Le May, C., Liu, S., Kaw, M.K., Khuder, S.S., Latour, M.G., Bhatt, S.A., Korach, K.S., Najjar, S.M., et al. (2011). Estrogen receptor activation reduces lipid synthesis in pancreatic islets and prevents β cell failure in rodent models of type 2 diabetes. Journal of Clinical Investigation *121*, 3331–3342.

Tikka, A., and Jauhiainen, M. (2016). The role of ANGPTL3 in controlling lipoprotein metabolism. Endocrine *52*, 187–193.

Tilg, H., Moschen, A.R., and Roden, M. (2017). NAFLD and diabetes mellitus. Nature Reviews Gastroenterology & Hepatology *14*, 32–42.

Tirosh, I., Izar, B., Prakadan, S.M., Wadsworth, M.H., Treacy, D., Trombetta, J.J., Rotem, A., Rodman, C., Lian, C., Murphy, G., et al. (2016). Dissecting the multicellular ecosystem of metastatic melanoma by single-cell RNA-seq. Science *352*, 189–196.

Toft-Nielsen, M.B., Madsbad, S., and Holst, J.J. (1999). Continuous subcutaneous infusion of glucagon-like peptide 1 lowers plasma glucose and reduces appetite in type 2 diabetic patients. Diabetes Care *22*, 1137–1143.

Torrent, M., Chalancon, G., de Groot, N.S., Wuster, A., and Madan Babu, M. (2018). Cells alter their tRNA abundance to selectively regulate protein synthesis during stress conditions. Science Signaling *11*, eaat6409.

Tourrel, C., Bailbé, D., Meile, M.J., Kergoat, M., and Portha, B. (2001). Glucagon-like peptide-1 and exendin-4 stimulate beta-cell neogenesis in streptozotocin-treated newborn rats resulting in persistently improved glucose homeostasis at adult age. Diabetes *50*, 1562–1570.

Tritschler, S., Theis, F.J., Lickert, H., and Böttcher, A. (2017). Systematic single-cell analysis provides new insights into heterogeneity and plasticity of the pancreas. Molecular Metabolism *6*, 974–990.

Tritschler, S., Büttner, M., Fischer, D.S., Lange, M., Bergen, V., Lickert, H., and Theis, F.J. (2019). Concepts and limitations for learning developmental trajectories from single cell genomics. Development *146*, dev170506.

Tschen, S.-I., Dhawan, S., Gurlo, T., and Bhushan, A. (2009). Age-Dependent Decline in -Cell Proliferation Restricts the Capacity of -Cell Regeneration in Mice. Diabetes *58*, 1312–1320.

Tyanova, S., Temu, T., Sinitcyn, P., Carlson, A., Hein, M.Y., Geiger, T., Mann, M., and Cox, J. (2016). The Perseus computational platform for comprehensive analysis of (prote)omics data. Nature Methods *13*, 731–740.

Ueki, K., Okada, T., Hu, J., Liew, C.W., Assmann, A., Dahlgren, G.M., Peters, J.L., Shackman, J.G., Zhang, M., Artner, I., et al. (2006). Total insulin and IGF-I resistance in pancreatic β cells causes overt diabetes. Nature Genetics *38*, 583–588.

Unick, J.L., Beavers, D., Bond, D.S., Clark, J.M., Jakicic, J.M., Kitabchi, A.E., Knowler, W.C., Wadden, T.A., Wagenknecht, L.E., and Wing, R.R. (2013). The Long-term Effectiveness of a Lifestyle Intervention in Severely Obese Individuals. The American Journal of Medicine *126*, 236-242.e2.

Wang, P., Alvarez-Perez, J.-C., Felsenfeld, D.P., Liu, H., Sivendran, S., Bender, A., Kumar, A., Sanchez, R., Scott, D.K., Garcia-Ocaña, A., et al. (2015). A high-throughput chemical screen reveals that harmine-mediated inhibition of DYRK1A increases human pancreatic beta cell replication. Nature Medicine *21*, 383–388.

Wang, P., Karakose, E., Liu, H., Swartz, E., Ackeifi, C., Zlatanic, V., Wilson, J., González, B.J., Bender, A., Takane, K.K., et al. (2019). Combined Inhibition of DYRK1A, SMAD, and Trithorax Pathways Synergizes to Induce Robust Replication in Adult Human Beta Cells. Cell Metabolism *29*, 638-652.e5.

Wang, R.N., Kl□ppel, G., and Bouwens, L. (1995). Duct- to islet-cell differentiation and islet growth in the pancreas of duct-ligated adult rats. Diabetologia *38*, 1405–1411.

Wang, W., Liu, H., Xiao, S., Liu, S., Li, X., and Yu, P. (2017). Effects of Insulin Plus Glucagon-Like Peptide-1 Receptor Agonists (GLP-1RAs) in Treating Type 1 Diabetes Mellitus: A Systematic Review and Meta-Analysis. Diabetes Therapy *8*, 727–738.

Wang, Z., York, N.W., Nichols, C.G., and Remedi, M.S. (2014). Pancreatic β Cell Dedifferentiation in Diabetes and Redifferentiation following Insulin Therapy. Cell Metabolism *19*, 872–882.

Watanabe, H., Saito, H., Rychahou, P.G., Uchida, T., and Evers, B.M. (2005). Aging Is Associated With Decreased Pancreatic Acinar Cell Regeneration and Phosphatidylinositol 3-Kinase/Akt Activation. Gastroenterology *128*, 1391–1404.

Watanabe, J., Chou, K.J., Liao, J.C., Miao, Y., Meng, H.-H., Ge, H., Grijalva, V., Hama, S., Kozak, K., Buga, G., et al. (2007). Differential Association of Hemoglobin with Proinflammatory High Density Lipoproteins in Atherogenic/Hyperlipidemic Mice: *A NOVEL BIOMARKER OF ATHEROSCLEROSIS*. Journal of Biological Chemistry *282*, 23698–23707.

Weir, G.C., and Bonner-Weir, S. (2013). Islet β cell mass in diabetes and how it relates to function, birth, and death: Islet β cell mass in diabetes. Annals of the New York Academy of Sciences *1281*, 92–105.

Weng, J., Li, Y., Xu, W., Shi, L., Zhang, Q., Zhu, D., Hu, Y., Zhou, Z., Yan, X., Tian, H., et al. (2008). Effect of intensive insulin therapy on β-cell function and glycaemic control in patients with newly diagnosed type 2 diabetes: a multicentre randomised parallel-group trial. The Lancet *371*, 1753–1760.

Wewer Albrechtsen, N.J., Geyer, P.E., Doll, S., Treit, P.V., Bojsen-Møller, K.N., Martinussen, C., Jørgensen, N.B., Torekov, S.S., Meier, F., Niu, L., et al. (2018). Plasma Proteome Profiling Reveals Dynamics of Inflammatory and Lipid Homeostasis Markers after Roux-En-Y Gastric Bypass Surgery. Cell Systems *7*, 601-612.e3.

Withers, D.J., Gutierrez, J.S., Towery, H., Burks, D.J., Ren, J.-M., Previs, S., Zhang, Y., Bernal, D., Pons, S., Shulman, G.I., et al. (1998). Disruption of IRS-2 causes type 2 diabetes in mice. Nature *391*, 900–904.

Wolf, F.A., Angerer, P., and Theis, F.J. (2018). SCANPY: large-scale single-cell gene expression data analysis. Genome Biology *19*.

Wolf, F.A., Hamey, F.K., Plass, M., Solana, J., Dahlin, J.S., Göttgens, B., Rajewsky, N., Simon, L., and Theis, F.J. (2019). PAGA: graph abstraction reconciles clustering with trajectory inference through a topology preserving map of single cells. Genome Biology *20*.

Wolock, S.L., Lopez, R., and Klein, A.M. (2019). Scrublet: Computational Identification of Cell Doublets in Single-Cell Transcriptomic Data. Cell Systems *8*, 281-291.e9.

Wong, W.P.S., Tiano, J.P., Liu, S., Hewitt, S.C., Le May, C., Dalle, S., Katzenellenbogen, J.A., Katzenellenbogen, B.S., Korach, K.S., and Mauvais-Jarvis, F. (2010). Extranuclear estrogen receptor-stimulates NeuroD1 binding to the insulin promoter and favors insulin synthesis. Proceedings of the National Academy of Sciences *107*, 13057–13062.

Xu, B., Allard, C., Alvarez-Mercado, A.I., Fuselier, T., Kim, J.H., Coons, L.A., Hewitt, S.C., Urano, F., Korach, K.S., Levin, E.R., et al. (2018). Estrogens Promote Misfolded Proinsulin Degradation to Protect Insulin Production and Delay Diabetes. Cell Reports *24*, 181–196.

Xu, G., Stoffers, D.A., Habener, J.F., and Bonner-Weir, S. (1999). Exendin-4 stimulates both beta-cell replication and neogenesis, resulting in increased beta-cell mass and improved glucose tolerance in diabetic rats. Diabetes *48*, 2270–2276.

Xu, G., Kaneto, H., Laybutt, D.R., Duvivier-Kali, V.F., Trivedi, N., Suzuma, K., King, G.L., Weir, G.C., and Bonner-Weir, S. (2007). Downregulation of GLP-1 and GIP Receptor Expression by Hyperglycemia: Possible Contribution to Impaired Incretin Effects in Diabetes. Diabetes *56*, 1551–1558.

Yang, Y., Smith, D.L., Keating, K.D., Allison, D.B., and Nagy, T.R. (2014). Variations in body weight, food intake and body composition after long-term high-fat diet feeding in C57BL/6J mice: Variations in Diet-Induced Obese C57BL/6J Mice. Obesity *22*, 2147–2155.

Yin, X., Subramanian, S., Hwang, S.-J., O'Donnell, C.J., Fox, C.S., Courchesne, P., Muntendam, P., Gordon, N., Adourian, A., Juhasz, P., et al. (2014). Protein Biomarkers of New-Onset Cardiovascular Disease: Prospective Study From the Systems Approach to Biomarker Research in Cardiovascular Disease Initiative. Arteriosclerosis, Thrombosis, and Vascular Biology *34*, 939–945.

Yoneda, S., Uno, S., Iwahashi, H., Fujita, Y., Yoshikawa, A., Kozawa, J., Okita, K., Takiuchi, D., Eguchi, H., Nagano, H., et al. (2013). Predominance of β-Cell Neogenesis Rather Than Replication in Humans With an Impaired Glucose Tolerance and Newly Diagnosed Diabetes. The Journal of Clinical Endocrinology & Metabolism *98*, 2053–2061.

Younossi, Z.M., Koenig, A.B., Abdelatif, D., Fazel, Y., Henry, L., and Wymer, M. (2016). Global epidemiology of nonalcoholic fatty liver disease-Meta-analytic assessment of prevalence, incidence, and outcomes: HEPATOLOGY, Vol. XX, No. X 2016. Hepatology *64*, 73–84.

Zaykov, A.N., Mayer, J.P., and DiMarchi, R.D. (2016). Pursuit of a perfect insulin. Nature Reviews Drug Discovery *15*, 425–439.

Zheng, G.X.Y., Terry, J.M., Belgrader, P., Ryvkin, P., Bent, Z.W., Wilson, R., Ziraldo, S.B., Wheeler, T.D., McDermott, G.P., Zhu, J., et al. (2017). Massively parallel digital transcriptional profiling of single cells. Nature Communications *8*, 14049.

Zheng, Y., Ley, S.H., and Hu, F.B. (2018). Global aetiology and epidemiology of type 2 diabetes mellitus and its complications. Nature Reviews Endocrinology *14*, 88–98.

Zhou, Q., and Melton, D.A. (2018). Pancreas regeneration. Nature *557*, 351–358.

Zhou, Q., Brown, J., Kanarek, A., Rajagopal, J., and Melton, D.A. (2008). In vivo reprogramming of adult pancreatic exocrine cells to β-cells. Nature *455*, 627–632.

Zhu, D., Zhao, Z., Cui, G., Chang, S., Hu, L., See, Y.X., Lim, M.G.L., Guo, D., Chen, X., Poudel, B., et al. (2018). Single-Cell Transcriptome Analysis Reveals Estrogen Signaling Coordinately Augments One-Carbon, Polyamine, and Purine Synthesis in Breast Cancer. Cell Reports *25*, 2285-2298.e4.

(1998). Effect of Intensive Therapy on Residual β-Cell Function in Patients with Type 1 Diabetes in the Diabetes Control and Complications Trial: A Randomized, Controlled Trial. Annals of Internal Medicine *128*, 517.

Acknowledgements

Throughout my time as a PhD student I have received a great deal of support from a lot of people and I would like to express my gratitude.

First, I would like to thank Prof. Dr. Matthias Tschöp and Prof. Dr. Heiko Lickert for giving me the opportunity to perform my PhD at an outstanding research institute. This first-class environment supported me in all aspects of my projects. I would like to extend my greatest thanks to Prof. Dr. Heiko Lickert. Your direct supervision, scientific support, ideas, enthusiasm and motivation has allowed me to grow as a scientist. I thoroughly enjoy working with you.

I extend my deepest gratitude to Prof. Dr. Susanna Hofmann for being my supervisor and mentor for the last five years. I think that there could not have been a better guidance through all these years and scientific challenges. You let me develop and pursuit my scientific interests. I hope that the end of my PhD is not the end of your mentorship.

Similarly, I want to thank Dr. Timo Müller for his great supervision during the whole time as graduate student. The scientific discussions with you put projects to a high impact gate. Besides my direct supervisors, I would like to thank Prof. Dr. Johannes Beckers for mentorship in my thesis committee, your time and your scientific guidance and discussions.

This PhD thesis was based on many collaborations within the institute (IDO, IDR, ICB) and outside. My deepest gratitude to Marc, Sonja, Robby, Sebastian, Cynthia, Mostafa, Laura, Emilija, Brian, Christoffer, Max, Christine, Burcak, Sigrid, Katrin, Aaron, and many more. A special thanks goes to Aimée and Sophie. Without your work and help, this would not have been possible. Thank you for all the scientific and emotional support, making the time in the lab a very enjoyable one.

Finally, I am eternally grateful to my family and friends for unfailing support, their continuous encouragement throughout my life. This achievement would not have been possible without them.

To Luisa, for her endless patience, support, and love.